FINAL REPORT

# Development of Deep Foundations Test Site


Submitted by
F.C. Townsend
J. Brian Anderson
Evelio Horta
Julian Sandoval


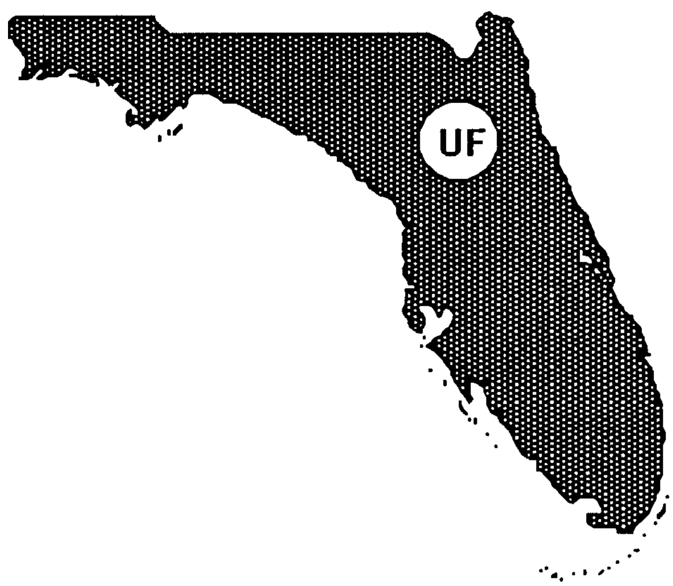


Submitted to: **The University of Central Florida** and **Florida Department of Transportation**


FDOT # BC 354, RPWO 93

UF Contract No. 4910 4504 987

September 2003

Technical Report Documentation Page

| 1. Report No. | 2. Government Accession No. | 3. Recipient's Catalog No. |
|---|---|---|
| | | |

| 4. Title and Subtitle | 5. Report Date |
|---|---|
| Development of Deep Foundations Test Site | September 2003 |
| | 6. Performing Organization Code |
| 7. Author(s)<br>F.C. Townsend, J. Brian Anderson, Evelio Horta, Julian Sandoval | 8. Performing Organization Report No.<br>4910-4504-987-12 |
| 9. Performing Organization Name and Address<br>University of Florida<br>Department of Civil & Coastal Engineering<br>345 Weil / P.O. Box 116580<br>Gainesville, FL 32611-6580 | 10. Work Unit No. (TRAIS)<br><br>11. Contract or Grant No.<br>BC-354 |
| 12. Sponsoring Agency Name and Address<br>Florida Department of Transportation<br>Research Management Center<br>605 Suwannee Street, MS 30<br>Tallahassee, FL 32301-8064 | 13. Type of Report and Period Covered<br>Final Report<br>January 2003-September 2003<br><br>14. Sponsoring Agency Code |

15. Supplementary Notes

Prepared in cooperation with the Federal Highway Administration

16. Abstract


Previously, a report, "*Site Preparation for a Deep Foundation Test Site at the University of Central Florida,"* was submitted (September 2002) to FDOT. This supplemental research project complimented this previous report, and had the objectives of; (1) Providing laboratory testing on recovered Shelby tube samples and evaluating insitu test correlations for engineering parameters, (2) Evaluating PMT test discrepancies, and (3) Comparing geophysical ER and GRP measurements with those from SPT and CPT.

A comparison of SPT estimated $\phi$ or cohesion values with laboratory triaxial tests suggests the SPT estimates used in FB-PIER are comfortably conservative. However, SPT $E_{50}$ FB-Pier estimates were poor. CPT and DMT estimated $\phi$ values agreed well with triaxial data.

A testing program implemented to investigate PMT differences at the FDOT-UCF revealed: (A) A comparison of two different probes (ring and no-ring on tip) for cohesive soils shows no apparent differences. However, for cohesionless soils a significant difference occurred. (B) Interagency (FDOT-SMO, UF, UNCC, and FIT) PMT tests had total disagreement at the cohesive Lake Alice site. Although site variability may explain some of the disagreement, other unknown factors are occurring. However, excellent agreement was obtained between FDOT-SMO and UF at the cohesionless Archer Landfill site.

A comparison of the geophysical data with the traditional insitu test data shows excellent agreement. However, the SPT and CPT compliment and assist geophysical interpretation.


| 17. Key Words | 18. Distribution Statement |
|---|---|
| Insitu Testing, SPT, CPT, DMT, Pressuremeter, Geophysical Tests | No restrictions. This document is available to the public through the National Technical Information Service, Springfield, VA, 22161 |

| 19. Security Classif. (of this report) | 20. Security Classif. (of this page) | 21. No. of Pages | 22. Price |
|---|---|---|---|
| Unclassified | Unclassified | | |

Form DOT F 1700.7 (8-72)
Reproduction of completed page authorized

## TABLE of CONTENTS

## LIST of TABLES

# LIST of FIGURES

# CHAPTER 1

# INTRODUCTION, PURPOSE AND SCOPE

## INTRODUCTION

An experimental deep foundations test site is being developed by FDOT at the University of Central Florida campus, Orlando, FL. The test site is about 300 feet by 300 feet, has been cleared of trees and bushes, and is protected with a fence. Topographically, the lot is flat and there are no significant differences in elevation through the site.

Previously, a report, "*Site Preparation for a Deep Foundation Test Site at the University of Central Florida,*" was submitted (September 2002) to FDOT. This report documented the results of: five SPT, seventeen CPT, four DMT, and two PMT soundings. Inasmuch as the SPT is the most common insitu test, comparisons were made between; (1) drilling operators, (2) hammer type (safety vs. automatic), and (3) cased vs. drilling mudded holes. Energy measurements were also conducted to compare the SPT data.

The generalized soil profile from SPT borings was found to be: (1) 0-5 ft medium sand, (2) 5-33 ft sand–silty sand, (3) 33-52 ft silty clay – clay, (4) 52-60 ft medium cemented sand. From the center eastward a hard pan sand layer exists from about 10 to 15 ft.

Comparisons between SPT borings using a hollow stem auger vs. a cased hole using an automatic trip hammer revealed little difference in N values. SPT energy measurements gave energy measurements of 82% for an automatic hammer, and only 65% for a safety hammer.

Comparisons between DMT borings using three different agencies revealed consistent results with little variation between agencies.

However, PMT measurements between two different agencies revealed substantial differences. These differences speculatively were attributed primarily to an oversized friction reducer on the tip, which caused an oversized hole and subsequent near hole disturbance leading to a softer response.

A copy of "*Site Preparation for a Deep Foundation Test Site at the University of Central Florida*" in included in the CD attached to this report for completeness.

## STATEMENT OF THE PROBLEM

Based upon the findings of the previous insitu testing program, several issues requiring additional research evolved; specifically:

1. The SPT borings only went to 60 ft. and did not penetrate or encounter bedrock. Consequently, District 5 (Deland) "volunteered" to perform 2 additional SPT borings to bedrock and also to obtain Shelby tube samples for laboratory testing.

2. Laboratory tests (triaxial and oedometer) on selected samples are needed to develop and verify current insitu test – engineering parameter correlations ($\phi$, $\gamma$, $S_u$, E, etc.). Consequently, a laboratory-testing program is needed.

3. Considerable differences in PMT results were obtained between UF and SMO tests. This difference is speculatively attributed to the small friction reducer ring placed on the cone tip, which disturbs the soil upon insertion. Additionally, PMT calibration procedures need refinement and documentation. Accordingly, these testing differences need to be resolved and calibration methods crystallized.

4. Electrical Resistivity (ER) and Ground Penetrating Radar (GPR) testing were performed at the FDOT-UCF site. However, these data were unreported and not interpreted.

## SCOPE OF WORK

To address these aforementioned problems, the following Tasks were performed, and constitute the information contained in this supplemental report.

***Task 1*** **–** Laboratory Testing and Correlations: The objective of this Task was to verify existing insitu test correlations for engineering parameters. Both SMO and UF conducted triaxial and oedometer tests on selected Shelby tube samples obtained from the two additional District 5 SPT borings. The laboratory results were compared with correlations in the FLPIER, the manual and others.

***Task 2*** **–** PMT Testing and Calibration**:** The objective of this Task was to resolve SMO and UF PMT testing differences. The work performed for this Task was:

1. Friction ring evaluation. Companion tests here in Gainesville using UF's PMT were performed using PMT cone tips with and without various sized friction-reducing rings on the tip. Two sites were tested (cohesionless- Archer Landfill, and cohesive- Lake Alice).

2. PMT testing and training workshop. A 2-day PMT workshop was held June 12-13 in Gainesville, which evaluated calibration methods, and performed PMT tests with UF and SMO equipment. Profs. Paul Constantino (FIT) and Brian Anderson (UNCC) participated in calibration and testing.

3. Prof. Anderson's calibration spreadsheet was verified via hand calibrations.

***Task 3*** **–** Electrical Resistivity and GPR Documentation**:** The objective and scope of this task was to evaluate and compare ER and GRP data with other insitu tests at the FDOT-UCF site.

# CHAPTER 2

# LITERATURE REVIEW

The FDOT-UCF site is to be used for evaluating deep foundations, so the objective of the site characterization program was to provide a comprehensive suite of insitu testing for future evaluation of axial and lateral capacities of deep foundations.

The scope of work to accomplish this program was to perform conventional insitu tests, i.e., SPT, CPT, DMT, and PMT. Laboratory testing was implemented as well as the use of geophysical methods of exploration i.e., GPR and Electro-Resistivity.

The following is an explanation of the history and characteristics of the equipment used. For the case of the PMT, new recommendations are given. Figure 2.1 presents the “accuracy” of insitu testing method for perspective.

## STANDARD PENETRATION TEST (SPT)

### The Standard Penetration Test

This test is probably the most widely used field test in the United States. It has the advantages of simplicity, the availability of a wide variety of correlations for its data, and the fact that a sample is obtainable with each test.

#### *Test History*

- 1902 C.R Gow, used a 1” diameter sampling tube driven with a 110 lb weight. Prior to this time samples were recovered from wash water.
- 1927 L. Hart and G.A. Fletcher devised the 2” diameter split-spoon sampler. At the same time Fletcher and H.A Mohr standardized the test using the split spoon sampler, a hammer with a mass of 140 lb drop from 30” height.
- Terzaghi and Peck incorporated the test and correlations in their book, “Theory and Practice in Soil Mechanics” in 1948.
- Use of the test grew rapidly; today it is the common tool for the soils engineer.

#### *Test Concept*

A standard split barrel sampler is advanced into the soil by dropping a 140-pound (63.5-kilogram) safety or automatic hammer on the drill rod from a height of 30 inches (760 mm). The sampler is advanced a total of 18 inches (450 mm). The number of blows required to advance the sampler for each of three 6-inch (150 mm) increments is recorded. The sum of the number of blows for the second and third increments is called the Standard Penetration Value, or more commonly, N-value (blows per foot [300 mm]). Tests shall be performed in accordance with ASTM

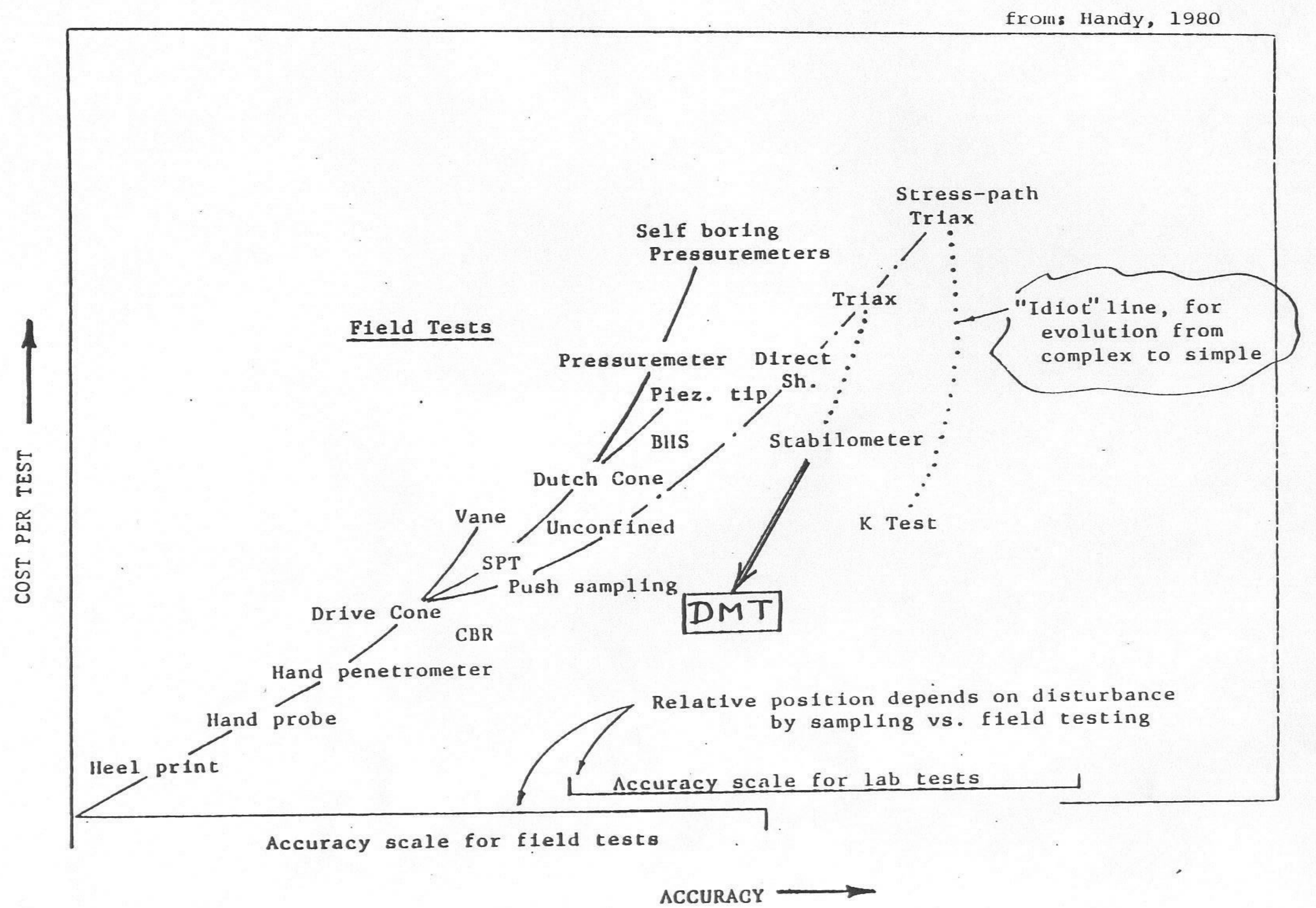


Figure 2.1 Accuracy or reliability scale for field insitu testing. (Handy, 1980)

D 1586. The Figure 2.2 shows a cross-section of the split-spoon or sampler used in the standard penetration test.

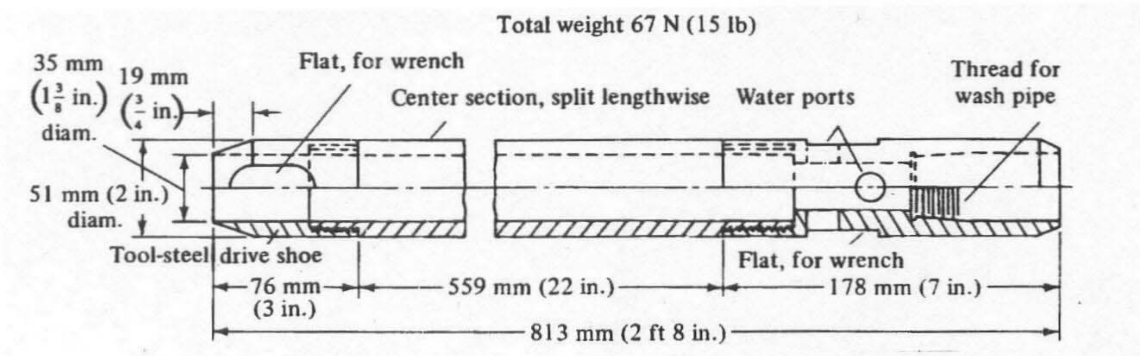


Figure 2.2 Split-spoon sampler used in standard penetration test.

During design, the N-values may need to be corrected for overburden pressure. Many correlations exist relating the corrected N-values to relative density, angle of internal friction, shear strength, and other parameters. Due to the popularity of the SPT a great number of design methods are available for using N-values in the design of driven piles, embankments, spread footings, and drilled shafts.

But the SPT values should not be used indiscriminately. They are sensitive to the fluctuations in individual drilling practices and equipment. Studies have also indicated that the results are more reliable in sands than clays. Although extensive use of this test in subsurface exploration is recommended, it should always be augmented by other field and laboratory tests, particularly when dealing with clays. The type of hammer (safety or automatic) should be noted on the boring logs, since this will affect the actual input driving energy. Peck et al. (1974) suggested the following correction in order to approach this phenomena, when dealing with safety hammers:

$$N_{60} = \eta * C_N * N$$

where: $\eta$is the energy ratio and $C_N$ is defined by Peck as:

$$C_N = 0.77 \log \frac{20}{\sigma_v'}$$

There are several approaches and equations developed by various authors, based on their criteria and experience, which relate to this energy correction problem. Other examples of corrections of the N value due to energy variations are presented in Chapter 3 Presentation of Data: SPT and Laboratory Tests.

*Energy Measurements*

The FDOT uses the two most common systems – the safety hammer with cathead and rope mechanism and the automatic trip hammer system. Therefore, only these two systems were tested under the scope of this project and are discussed in the FDOT-UCF Site Characterization report.

***Safety Hammer***

The safety hammer, shown in Figure 2.3, is one of the two most common hammers used in the United States because of its internal striking ram that greatly reduces the risk of injuries. When the hammer is lifted to the prescribed height, the outer barrel and the enclosed hammer move together as one piece. When released, the hammer falls, striking the internal anvil and creating an energy wave. The kinetic energy of the system, in the form of the wave, is transmitted through the anvil to the center rod. Because the center rod is threaded into the drill rod string, the wave is then transmitted through the drill rod string and into the split-spoon sampler.

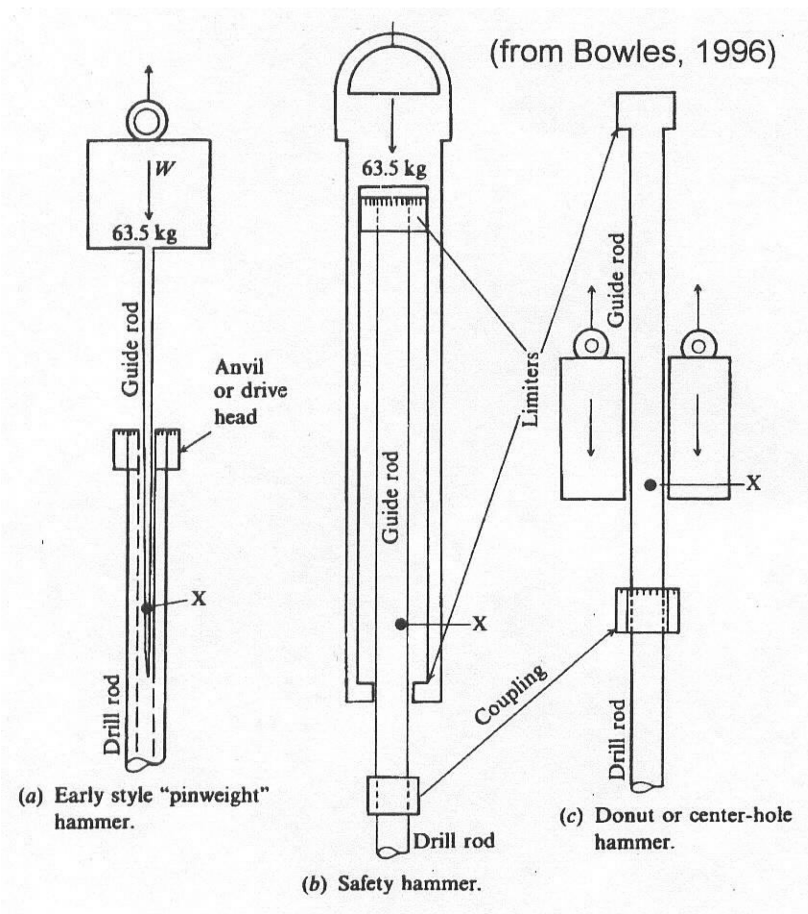


Figure 2.3 Evolution of the SPT hammer to the safety hammer, or standardized hammer.

The mechanism used to lift the safety hammer is the cathead and rope system. A rope is tied to the outer barrel of the safety hammer and strung through a pulley, or crown sheave, where it is wrapped around a rotating cathead. The free end of the rope is held by the operator. To conduct the test, the operator pulls the rope to raise the hammer and then "throws" the rope quickly to release the tension holding the hammer at the 30-inch drop height thereby causing the hammer to fall. The raising and dropping of the hammer is conducted repeatedly until the sampler penetrates the required depth of 18 inches.

### *Problem Statement*

Unfortunately the ASTM standard (ASTM D1586) allows a wide diversity of equipment for performing standard penetration testing. As a consequence there are a variety of hammer types in use, ranging from donut and safety hammers using cathead and rope systems to the latest in automatic trip hammers. Different hammers introduce different amounts of energy per blow into the rods and different N-values result. The difference in energy between the best automatic trip hammer and a cathead system in which the winch is spooled by the weight of the hammer can be a factor of 4 to 5.

### *Approach to the Energy Measurement*

In the early studies of the SPT energy, Kovacs (1981) used a light scanner and reflection technique to measure the height of hammer fall and the velocity just before impact. These measurements allowed them to calculate the potential energy of the hammer drop and the kinetic energy of the hammer just before impact. They found that the hammer energy just before impact was always less than the potential energy of the hammer drop due to energy loss in the hammer system. They found a linear relationship between SPT N-value and hammer energy impact, and proposed that a "standard energy" be established in order to calibrate or adjusting the hammer fall height to deliver that "standard energy."

Schmertmann and Palacios (1979), incorporated the hollow-center, strain gauge load cells near the top and bottom of the drill rods to measure the force-time histories of the stress waves. The force data were used to calculate energy transfer in the rods and energy loss on the sampling process. They found out that the longer the drill rods, the longer the hammer rod contact time and the more hammer energy that enters the rods.

Based on these investigations, in order to reduce significant variability, it is recommended that the SPT N-value be standardized to a particular energy level, e.g., 60% of the theoretically available energy of 4200 in-lbs. The corrected N-value would be equal to the N-value obtained, multiplied by the ratio of that rig's energy input to the standard 60% energy of 2520 in-lbs.

### *Energy Measurement at FDOT-UCF Site*

For this test site, equipment for performing the energy calibration was supplied by GRL-Pile Dynamics Inc.

Because non uniformity of cross-section causes force/velocity disproportionality, it is imperative to conduct the test using an instrumented rod of the same size as the drill string.

Two type of sensors are used for the rod instrumentation:

- Foil strain gages (350 ohm) glued directly onto the rod in a full Wheatstone bridge configuration to measure strain, which is converted to force using the cross-sectional area, and modulus of elasticity of the rod.
- Piezoresistive accelerometers, which are bolted to the instrumented rod. The acceleration measured by these sensors is instantly integrated to obtain velocity, which is used in the Fv computations.

### *Data Control Unit*

The data control unit, has an LCD touch-screen for entering rod area and length, descriptions and names, and user comments. The programmed screens allow for easy data control and review. The force and velocity traces are continuously displayed during testing. The data are saved for a user-selected blow frequency in the memory of the unit. The memory holds the data from approximately 175 blows. The raw data and energy-related quantities are stored in the memory until downloaded into a computer using the SPTPC software. After analyzing the data using SPTPC, data plots can be made using PDIPLOT Version 1.1.

## CONE PENETROMETER TEST (CPT)

### The Cone Penetrometer Test

The Cone Penetrometer Test is a quasi-static penetration test in which a cylindrical rod with a conical point is advanced through the soil at a constant rate and the resistance to penetration is measured. A series of tests performed at varying depths at one location is commonly called a sounding.

Several types of penetrometers are in use, including mechanical (mantle) cone, mechanical friction-cone, electric cone, electric friction-cone, and piezocone penetrometers. Cone penetrometers measure the resistance to penetration at the tip of the penetrometer, or the end-bearing component of resistance. Friction-cone penetrometers are equipped with a friction sleeve, which provides the added capability of measuring the side friction component of resistance. Mechanical penetrometers have telescoping tips allowing measurements to be taken incrementally, generally at intervals of 8 inches (200 mm) or less. Electric or electronic penetrometers, as the one shown in Figure 2.4, use electric force transducers, to obtain continuous measurements with depth. Piezocone penetrometers are electric penetrometers, which are also capable of measuring pore water pressures during penetration.

For all types of penetrometers, cone dimensions of a 60-degree tip angle and a 1.55 $in^2$ (10 $cm^2$) projected end area are standard. The friction sleeve's outside diameter is the same as the base of the cone. Figure 2.5 shows a cone penetrometer. Penetration rates should be between 0.4 to 0.8 in/sec (10 and 20 mm/sec). Tests shall be performed in accordance with ASTM D 3441 (which includes mechanical cones) and ASTM D 5778 (which includes piezocones).

Figure 2.4 Electric force transducers located at the sleeve of the electrical cone probe.

Figure 2.5 Fully assembled (ready for testing) electrical cone penetrometer.

The penetrometer data is plotted showing the end-bearing resistance, the friction resistance, and the friction ratio (friction resistance divided by end bearing resistance) as functions of depth. Pore pressures, if measured, can also be plotted with depth. The results should also be presented in tabular form indicating the interpreted results of the raw data. The friction ratio plot can be analyzed to determine soil type. Many correlations of the cone test results to other soil parameters have been made, and design methods are available for spread footings and piles. The penetrometer can be used in sands or clays, but not in rock or other extremely dense soils. Generally, soil samples are not obtained with soundings, so penetrometer exploration should always be augmented by SPT borings or other borings with soil samples taken.

**CPT Correlations**

***Cohesionless Soil***

Relative Density Dr: (Jamiolkowski et al. 1985)

$$Dr = -98 + 66 \log_{10} \frac{q_c}{\left[\sigma'_{vo}\right]^{0.5}}$$

Friction angle $\phi$ (Figure 2.6): (Design using CPT, by Campanella, 1995)

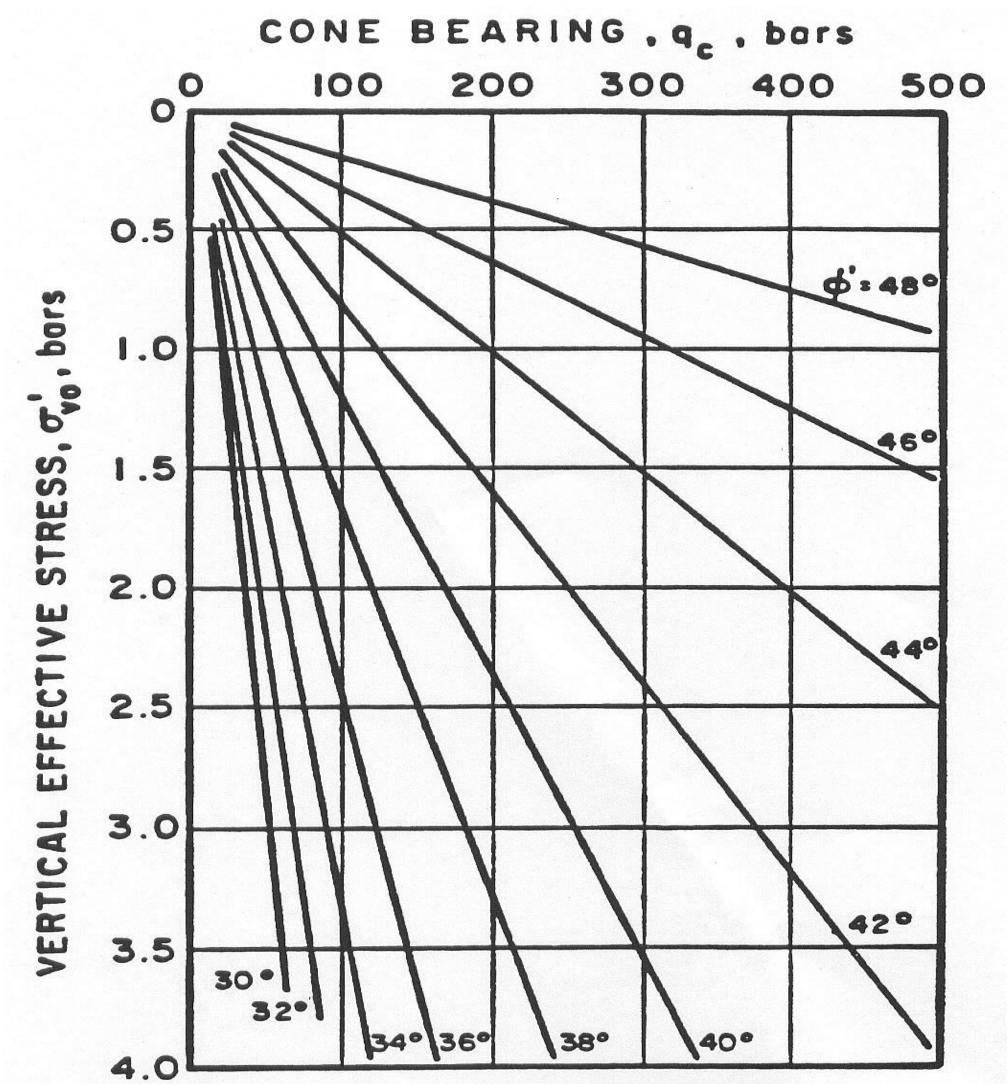


Figure 2.6 Proposed correlation between Cone Bearing and Peak Friction Angle for uncemented quartz sands. (Robertson and Campanella, 1983)

Tangent modulus $M_t$ : (Baldi et al., reported in Guidelines for geotechnical design using CPT, by Campanella, 1995)

$$M_t = \frac{1}{m_v} = \alpha q_c, \ \alpha = 3 - 11$$

Secant modulus: (Baldi et al., Reported in Guidelines for geotechnical design using CPT, by Campanella, 1995)

$$E_{25} = \alpha q_c, \ \alpha = 1.5 - 3$$

Dynamic shear modulus $G_{max}$ : (Imai and Tomouchi, 1982)

$$G_{max} = 125 N^{0.611}, \ \frac{qc}{N} = 4.5$$

***Cohesive Soil***

Undrained shear strength, Su:

$$S_u = \frac{q_c - \sigma_0}{N_k}, \ N_k = 15$$

Sensitivity, $S_t$ : (Campanella, 1995)

$$S_t = \frac{N_s}{R_f\,(\%)}, \ Ns = 6$$

Stress history OCR; using Campanella procedure (section 4.5.5, Guidelines for Geotechnical design using CPT, by Campanella, 1995.)

Estimate $s_u$ from $q_c$ or $\Delta u$

Estimate vertical effective stress, $\sigma'_{vo}$ from soil profile.

Compute $Su/\sigma'_{vo}$

Estimate the average normally consolidated $(Su/\sigma'_{vo})$ NC for the soil using Figure 2.7. A knowledge of the plasticity index (PI) is required.

Estimate OCR from correlations by Ladd and Foote (1974) and normalized by Schmertmann (1978) and reproduced in Figure 2.8.

If the PI of the deposit is not available, Schmertmann (1978) suggests assuming an average $(Su/\sigma'_{vo})$ NC ratio of 0.33 for most post-pleistocene clays.

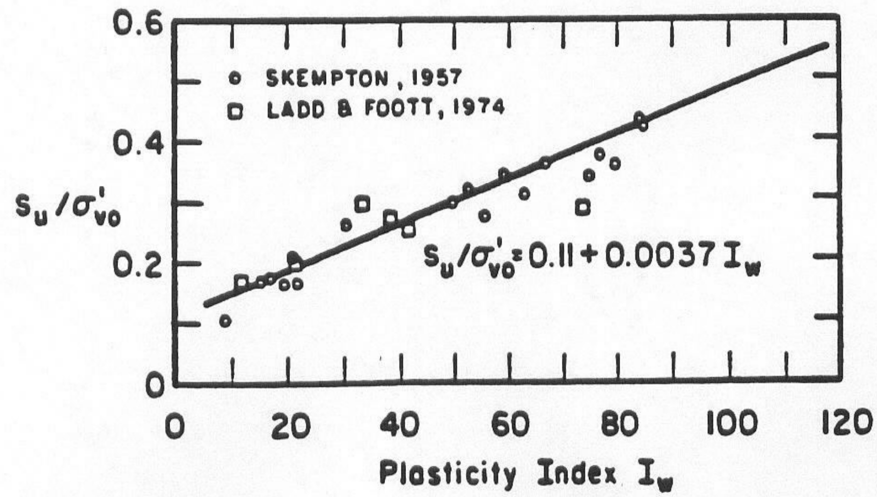


Figure 2.7 Statistical relation between Su/σ'$_{vo}$ ratio and Plasticity Index, for Normally consolidated clays.

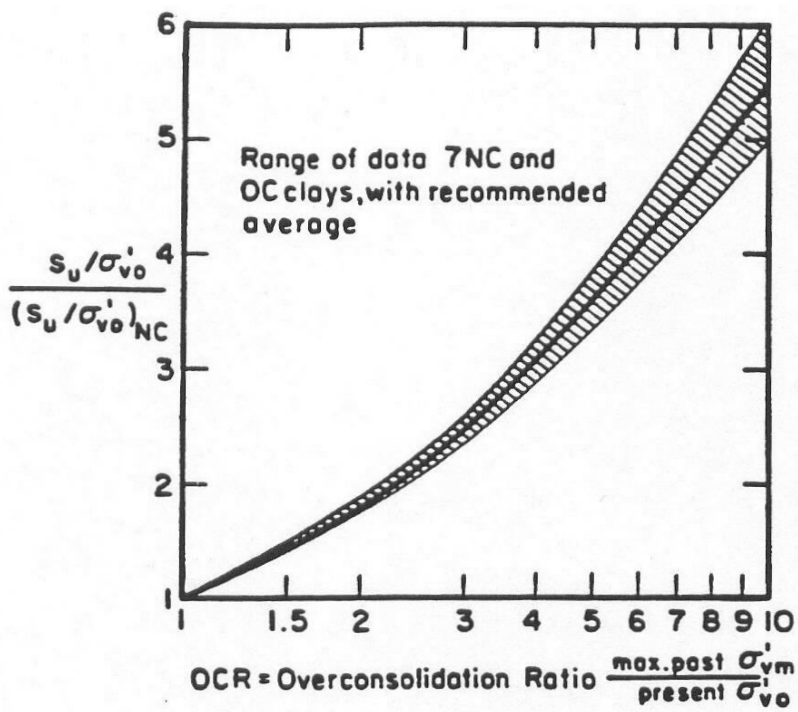


Figure 2.8 Normalized Su/σ'$_{vo}$ ratio and plasticity Index, for Normally consolidated clays.

### *The Piezocone Penetrometer*

The piezocone penetrometer can also be used to measure the dissipation rate of the excessive pore water pressure. This type of test is useful for sub-soils, such as fibrous peat or muck, which are very sensitive to sampling techniques. The cone should be equipped with a pressure transducer that is capable of measuring the induced water pressure. To perform this test, the cone will be advanced into the subsoil at a standard rate of 0.8 inch/sec (20 mm/sec). Pore water pressures will be measured immediately and at several time intervals thereafter. The recorded data is then used to plot a pore pressure versus log-time graph. Using this graph one can directly calculate the pore water pressure dissipation rate or rate of consolidation of the soil.

## DILATOMETER TEST (DMT)

### The Flat Dilatometer Test

The flat Dilatometer Test (DMT) shown at Figure 2.9, was developed in Italy by Marchetti in the late 70's. The Dilatometer probe consists of a stainless steel blade with a thin flat circular expandable steel membrane on one side. To minimize disturbance, the thickness of the blade (15 mm) was chosen as small as possible consistent with the requirement that it must not be easily damaged or bent. The specified deflection, $s_0$ , was chosen as small as possible (1 mm) in order to keep soil strains in the expansion stage as small as possible. When at rest, the external surface of the membrane is flush with the surrounding flat surface of the blade. The blade is jacked into the ground using a penetrometer rig or a ballasted drilling rig. The blade is connected to a control unit on the surface by a nylon tube containing an electrical wire. The tube runs through the penetrometer rods. At 20 cm depth intervals jacking is stopped and, without delay, the membrane is inflated by means of pressurized gas. Readings are taken of the *A* pressure required to just begin to move the membrane and of the *B* pressure required to move its center 1.00 mm into the soil. The rate of pressure increase is set so that the expansion occurs in 15 sec – 30 sec.

Figure 2.9 Dissembled dilatometer blade (probe), showing expandable membrane mechanism.

The DMT is best used in soils which are finer than gravelly sands. It is not recommended in soils which have penetration obstructions such as rock layers, cobbles, cemented zones, large shells (bouldery glacial sediments or gravelly deposits). The previous soils resist penetration and may damage the blade and the membrane.

**Penetration Stage**

The penetration of the dilatometer can be regarded as a complex loading test on the soil. A possible way of analyzing the penetration process is to model it as the expansion of a flat cavity, where the measured horizontal total soil pressure against the blade increases with the horizontal insitu stress, soil strength parameters, and soil stiffness.

The penetration of the dilatometer causes a horizontal displacement of the soil elements originally on the vertical axis of 7 mm (half thickness of the dilatometer). This displacement is considerably lower than that induced by currently used conical tips [18 mm for cone penetration test (CPT)] which, according to a theoretical solution by Baligh (Research Report, MIT No517), shows the different strains caused by wedges having an apex angle of 16° (angle of the dilatometer) and 60° (angle of many conical tips) may give an idea of the different magnitudes of the strains induced by DMT and CPT. Figure 2.10 gives a graphical explanation to the previous statement.

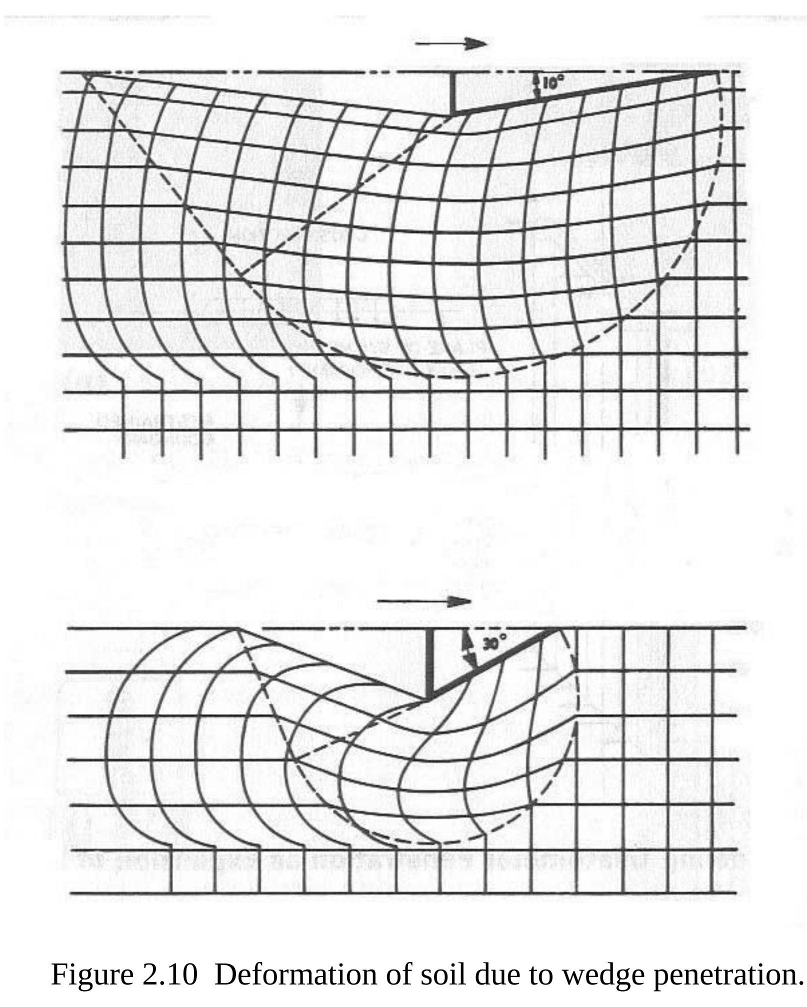


Figure 2.10 Deformation of soil due to wedge penetration.

During the penetration of the dilatometer there is a concentration of shear strain near the edges of the blade, so that the volume of soil facing the membrane undergoes a shear strain lower than the average.

**Expansion Stage**

In this stage the increments of strain in the soil are relatively small. The theory of elasticity may be used to infer a modulus. This modulus relates primarily to the volume of soil facing the membrane; however, this soil has been prestrained during the penetration. As already noted, shear strains in this volume are low (compared with the strains induced by other presently used penetrating devices, as the cone penetrometer). However, soil stiffness is sensitive to prestrains. Thus correction factors are necessary for evaluating the stiffness of the original soil.

The pressure readings of A and B, (taken from the dilatometer control unit), are corrected by the values $\Delta A$ and $\Delta B$, determined by taking into account the membrane stiffness and converting into $P_0$, $P_1$. The fundamentals of the proceedings and calibrations needed in order to obtain these corrections are shown at the Chapter 3 "Presentation OF Data: SPT and Laboratory Tests."

**Intermediate and Common Soil Parameters**

The corrected pressures $P_o$ and $P_l$ are key values used in the interpretation of "intermediate" DMT parameters. The original correlations (Marchetti, 1980) were obtained by calibrating DMT results versus high quality parameters. The interpretation evolved by first identifying the three "intermediate" DMT parameters - the material index $I_D$, the horizontal stress index $K_D$, and the dilatometer modulus $E_D$. The values of insitu equilibrium pore pressure $u_o$ and of the vertical effective stress $\sigma'_{vo}$, prior to the insertion of the probe, must be known in order to be introduced into the formulae.

Table 2.1 shows the reduction formulae needed to determine the common soil parameters for which the DMT provides an interpretation. The constrained modulus M and the undrained shear strength Cu are believed to be the most reliable and useful parameters obtained by DMT (Marchetti et al. 2001).

**P-Y Predictions from DMT**

Most of the existing methods for obtaining *P-y* curves are highly empirical. Often little account is taken of the method of pile installation and the influence that this may have on the soil behavior. But several methods (Townsend et al. 1999) have recently been proposed for the design of laterally loaded piles using DMT and pressuremeter data.

For driven displacement piles, both the DMT and pressuremeter can be pushed into the soil in a full displacement manner. For cast-in-place or bored piles, a pre-bored or self-bored pressuremeter test can model the disturbance caused during pile installation. The method by Robertson et al. (for the ASTM, 1984) uses the results from a pressuremeter pushed into the soil to model the installation of a driven displacement pile. Although the pressuremeter methods have been shown to usually provide adequate results, several problems still exist.

Table 2.1 Basic DMT data reduction formulae, for determining soil parameters. (Marchetti et al. 2001)

| SYM-BOL | DESCRIPTION | BASIC DMT REDUCTION FORMULAE | |
|---|---|---|---|
| $\rho_0$ | Corrected First Reading | $\rho_0 = 1.05(A - Z_u + \Delta A) - 0.05(B - Z_M - \Delta B)$ | $Z_M$ = Gage reading when vented to atm. If $\Delta A$ & $\Delta B$ are measured with the same gage used for current readings A & B, set $Z_M = 0$ ($Z_M$ is compensated) |
| $\rho_1$ | Corrected Second Reading | $\rho \quad = B - Z_M - \Delta B$ | |
| $I_D$ | Material Index | $I_D = (p_1 - p_0)/(p_0 - u_0)$ | $u_0$ = pre-insertion pore pressure |
| $K_D$ | Horizontal Stress Index | $K_D = (p_0 - u_0)/\sigma'_{v0}$ | $\sigma'_{v0}$ = pre-insertion overburden stress |
| $E_D$ | Dilatometer Modulus | $E_D = 34.7\ (p_1 - p_0)$ | $E_D$ is NOT a Young's modulus E $E_D$ should be used only AFTER combining it with $K_D$ (Stress History) First obtain $M_{DMT} = R_m E_D$, then e.g., $E \approx 0.8\ M_{DMT}$ |
| $K_0$ | Coeff. Earth Pressure In Situ | $K_{0,DMT} = (K_D/1.5)^{0.47} - 0.6$ | for $I_D < 1.2$ |
| OCR | Overconsolidation Ratio | $OCR_{DMT} = (0.5\ K_D)^{1.56}$ | for $I_D < 1.2$ |
| $c_u$ | Undrained Shear Strength | $c_{u,DMT} = 0.22\ \sigma'_{v0}\ (0.5\ K_D)^{1.25}$ | for $I_D < 1.2$ |
| $\Phi$ | Friction Angle | $\Phi_{safe,DMT} = 28° + 14.6° \log K_D = 2.1° \log^2 K_D$ | for $I_D > 1.8$ |
| $c_h$ | Coefficient of Consolidation | $c_{h,DMTA} \approx 7\ cm^2/t_{max}$ | $t_{max}$ from A-log t DMT-A decay curve |
| $k_h$ | Coefficient of Permeability | $k_h = c_h \gamma_w / M_h\ (M_h \approx K_0 M_{DMT})$ | |
| M | Vertical Drained Constrained Modulus | $M_{DMT} = R_m E_D$<br>if $I_D \le 0\ 6$ $\quad R_M = 0.14 + 2.36 \log K_D$<br>if $I_D \ge 3$ $\quad R_M = 0.5 + 2 \log K_D$<br>if $0\ 6 < I_D < 3$ $\quad R_M = R_{mo} + (2.5 - R_{mo}) \log K_D$<br>with $R_{mo} = 0.14 + 0.15\ (I_D - 0\ 6)$<br>if $K_D > 10$ $\quad R_M = 0.32 + 2.18 \log K_D$<br>if $R_M < 0.85$ $\quad$ set $R_M = 0.85$ | |
| $u_0$ | Equilibrium Pore Pressure | $u_0 = p_2 = C - Z_M + \Delta A$ | in free-draining soils |

### *DMT Approach to the $P_u$-$y_c$ Curves*

The flat dilatometer test (DMT) is a simple, repeatable and economic insitu penetration test. The small size of the dilatometer blade enables data to be collected close to the foundation surface where the lateral response of piles is most influenced. Also, since the dilatometer blade is pushed into the soil it can be considered a model of a driven pile.

In contrast, pressuremeter methods, however, have the advantage that the cylindrical expansion can be considered a reasonable model of the lateral movement of the soil during lateral loading of piles. Any method that uses the DMT must rely on empirical correlations that relate DMT data to the required geotechnical parameters.

### *Cohesive Soil*

In cohesive soil deflection $y_c$ is a function of the undrained strength of the soil, the insitu effective stress level, and the soil stiffness. The value of the pile deflection $y_c$ is based on the concept proposed by Skempton (1951) that combines elasticity theory, ultimate strength method, and laboratory soil properties. Based on his work and the experience gained by University of British Columbia and different authors $y_c$ is determine by the following equation.

$$y_c = \frac{23.67 \cdot Su \cdot D^{0.5}}{F_C \cdot E_D}$$

where:

Su and $E_D$ are calculated with the empirical correlations (Table 2.1).

D = diameter of the pile in cm

$F_C$ = 10 (as first approximation for cohesive soil).

For clays, the evaluation of the ultimate static lateral resistance $P_u$ is given by Matlock (1960) as:

$$P_u = N_p \cdot Su \cdot D$$

where:

Su is calculated with the empirical correlations (Table 2.1).

D = diameter of the pile

$N_p$ = Non dimensional ultimate resistance coefficient ≤ 9

Near the surface, because of the lower confining stress level, the value of $N_p$ is calculated by:

$$N_p = 3 + \frac{\sigma'_{vo}}{Su} + \left( J \frac{x}{D} \right)$$

where:

$\sigma'_{vo}$ = effective vertical stress at x

x = depth

J = empirical coefficient 0.25 – 0.5

***Cohesionless Soils***

The ultimate lateral soil resistance $P_u$ is determined from the lesser value given by the following two equations:

$$P_u = \sigma'_{vo} \left[ D\left(k_p - k_a\right) + x \cdot k_p \tan\phi' \cdot \tan\beta \right]$$

$$P_u = \sigma'_{vo}\, D\left[k_p^3 + 2\,k_o\,k_p^2 \tan\phi' + \tan\phi' - k_a\right]$$

where:

| | | |
|---|---|---|
| $\phi'$ | = | Angle of internal friction |
| $k_a$ | = | Rankine active coefficient |
| $k_p$ | = | Rankine passive coefficient |
| $k_o$ | = | Coefficient of earth at rest |
| $\beta$ | = | $45° + \phi/2$ |

For the prediction of lateral pile response on sands, $y_c$ is calculated as:

$$y_c = \frac{4.17 \sin\phi'\, \sigma'_{vo}}{E_D \cdot F_S\,(1 - \sin\phi')}\, D$$

The method outlined above does not address the effect of pile group or the effect of cycling loadings. Respective corrections must be applied for these effects.

## THE PRESSUREMETER TEST (PMT)

### History of the Pressuremeter

Kögler, a German, developed the first pressuremeter and used it to determine soil properties somewhere around 1930. His pressuremeter was a single cell, long, and hollow device, which he inflated with gas. The results of this early pressuremeter were often difficult to interpret, and its development was hampered by technological difficulties (Baguelin et al., 1978). Figure 2.11 shows Kögler's pressuremeter.

Louis Ménard, developed the modern soil pressuremeter in 1954 working on his university final year project. This apparatus was a tri-cell design with two gas-filled guard cells and a central water-filled measuring cell. Ménard continued his work under Peck at the University of Illinois for his Masters degree, "An Apparatus for Measuring the Strength of Soils in Place." By 1957, Ménard had opened the Center d'Etudes Ménard where he produced pressuremeters for practicing engineers. Figure 2.12 shows a modern Ménard Pressuremeter marketed by Roctest, Inc.

Although the pressuremeter seemed a radical departure from traditional geotechnical tests, there were inherent problems with the device. Many believed that the stresses induced or reduced by drilling the borehole were significant. These stresses were further complicated by the general quality of drilling. If the hole were too large, the pressuremeter would possibly not inflate enough to develop a full pressuremeter curve. On the other hand, if the hole were too small, the insertion of the probe would disturb the borehole and therefore diminish the quality of the test data.

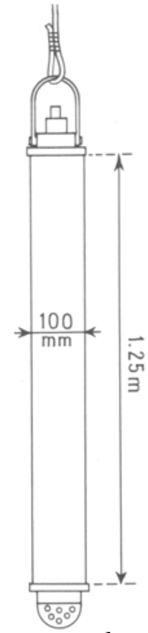


Figure 2.11  Kögler's sausage-shaped pressuremeter. (Baguelin, 1978)

Figure 2.12  A modern version of the Ménard Pressuremeter. (http://www.roctest.com/
roctelemac/product/product/g-am_menard.html)

In an attempt to rectify these drilling issues, engineers at the Saint Brieuc Laboratory of the Ponts et Chaussées (LPC) in France developed the first self-boring pressuremeter. As the name implies, this pressuremeter inserts itself into the borehole as the borehole is being drilled. The premise behind the new device was to prevent movement of the borehole wall after drilling, and therefore prevent any changes in stress. A similar device was developed at Cambridge and is sold by Cambridge Insitu called the Camkometer (Figure 2.13). Data from this pressuremeter proved to be radically different than that of the Ménard. While the self-boring pressuremeter may have seemed to be the panacea to PMT problems, it suffered from more of its own. These new probes were extremely complex and required a great deal of experience and maintenance to operate.

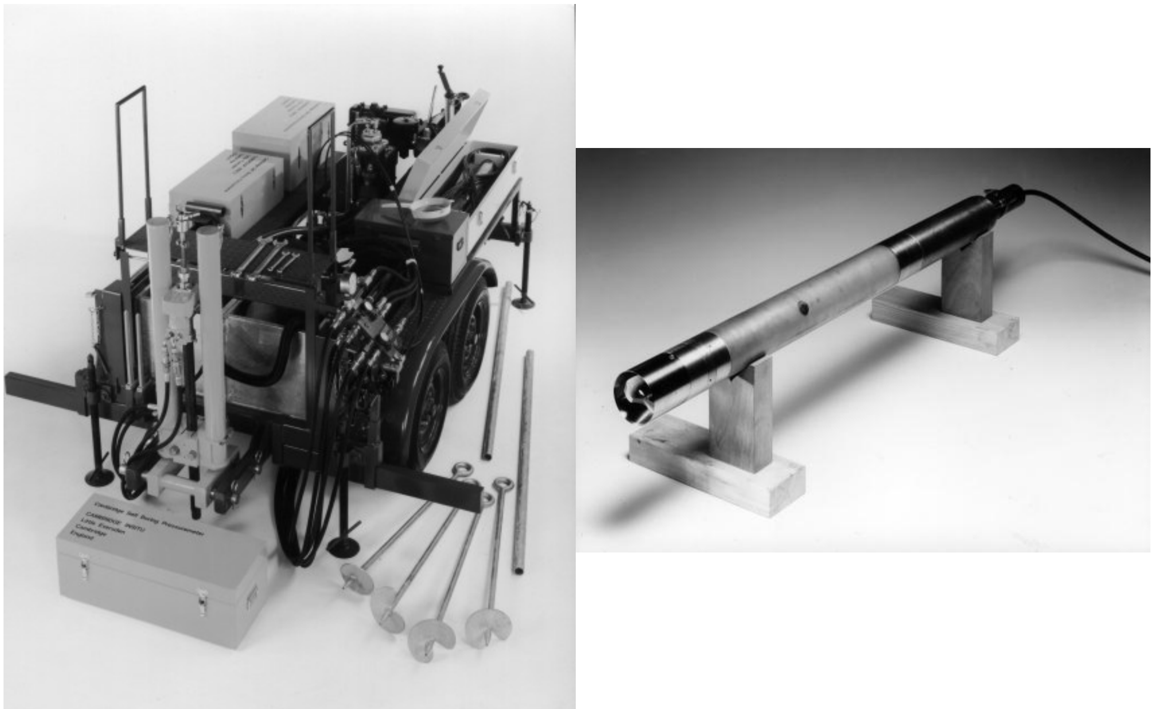

Figure 2.13 Self-boring pressuremeter sold by Cambridge Insitu. (http://www .cambridge-insitu.com/csbp_leaflet2.htm)

Also to address the problems with drilled pressuremeters, Reid et al. (1982) and Fyffe et al. (1985) developed a push-in type of pressuremeter. This new probe was developed primarily for use in the characterization of soils for offshore drilling structures. This new pressuremeter is hollow much like a Shelby tube. Soil is displaced into the probe during pushing, thus eliminating the cutting system. Unfortunately, the probe has to be extracted after every test to clean out the displaced soil.

A more recent development in pressuremeter technology is the full displacement or cone pressuremeter. This probe is pushed, as a cone penetration test, and then inflated as a traditional pressuremeter. This method eliminates the problems associated with drilling and the complexity of the self-boring equipment. Full displacement probes have been researched at the University of British Columbia, the University of Ottawa, and Oxford University. A commercially available full displacement type of pressuremeter is shown in Figure 2.14.

The first intent to develop such a probe was done by Briaud and Shields (1979). Their pressuremeter was developed primarily for the pavement industry to test the granular base and subbase layers, and cohesive and granular subgrades.

The pavement pressuremeter was developed as a rugged, inexpensive, portable apparatus for the direct evaluation of the deformation characteristics of the pavement and subgrade layers. A traditional Ménard type of probe could not be used in the case of pavement design. The magnitude of the loads and depths of influence due to traffic loading are very different to that of a shallow foundation. Since the depth of influence was much smaller, a cone penetration test tip sized monocellular probe with a singular hydraulic tubing was used. The shortened length of the probe facilitated a reasonable amount of measurements within the relatively shallow zone of influence. Strain control was chosen to allow for better definition of the elastic portion of the curve since stiffness is the important measurement. Additionally, strain control also simplified the equipment and facilitated cyclic testing.

**The Pencel Pressuremeter**

The testing device used in this study was the PENCEL model pressuremeter. This is more or less the commercial version of the pavement pressurememeter (Figure 2.15) developed by Biraud and Shields (1979). Roctest, Inc. manufactures the unit in Canada and markets it worldwide.

As with other pressuremeters, the parameters determined are the Limit Pressure and Pressuremeter Modulus. The PENCEL limit pressure is defined as the pressure required to double the probe volume, or more simply the maximum pressure during the test. On the other hand, the modulus could come from many portions of the pressuremeter curve. Due to probe insertion, the initial modulus, $E_i$, may not be that reliable. Other portions of the PENCEL curve that could be used for calculating stiffness are an unload-reload loop, if available, and the final unload portion of the test. These moduli are referred to as $E_{UR}$ and $E_{UL}$, respectively. Figure 2.16 shows these moduli and the limit pressure on an arbitrary pressuremeter test.

Calculation of the PENCEL Pressuremeter modulus is identical to the Ménard method:

$$E_{PMT} = 2(1+\mu)\left[V_c + \frac{V_o + V_f}{2}\right]\left[\frac{p_f - p_o}{V_f - V_o}\right]$$

where:

$\mu$ is Poisson's Ratio

$V_c$ is the initial volume of the pressuremeter

$V_o$ and $p_o$ are the first point on the linear portion of the pressuremeter curve

$V_f$ and $p_f$ are the final points on the linear portion of the pressuremeter curve.

Practice has shown that the standard pressuremeter test could give good estimates of bearing capacity and settlement of shallow foundation. Comparisons of predictions with actual performances have shown that measured, long-term settlements are in most cases within ± 50% of the predicted values, and often within ± 30% (Baguelin, Jézéquel, Shields, 1978).

The design of bearing capacity of piles under axial loading based on the pressuremeter method (Menard, 1963 reported in Briaud, 1989) requires the knowledge of an end-bearing factor $K_p$ and the unit limit frictions $q_{si}$ in all layers. Then the limit load $Q_L$ is:

$$Q_L = Q_{PL} + Q_{SL}$$

Figure 2.14  Full displacement pressuremeter, very similar to the CPT probe.

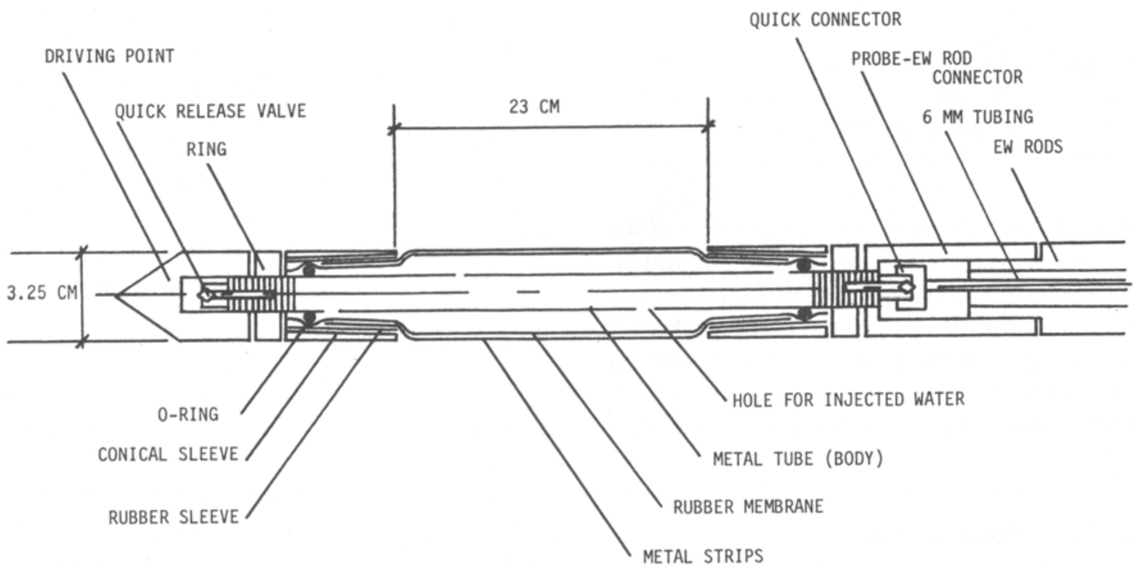


Figure 2.15  The pavement pressuremeter probe. (Briaud and Shields, 1979)

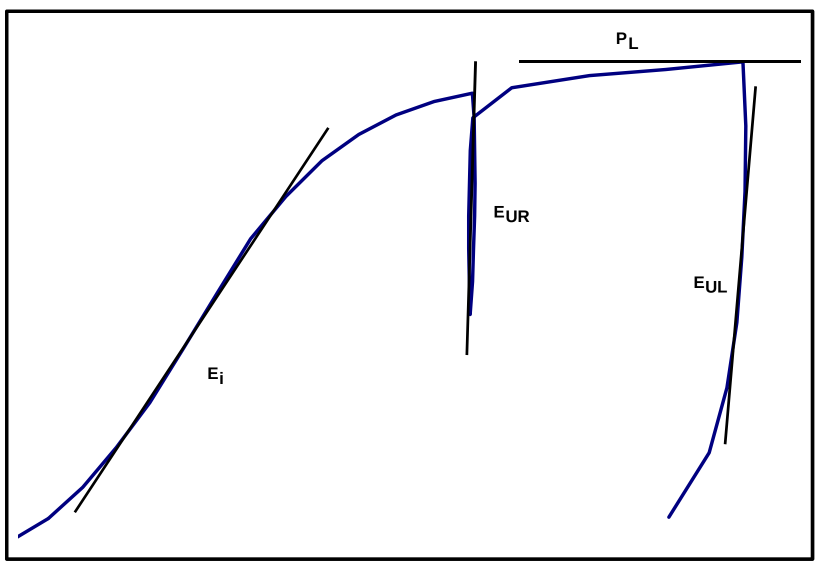


Figure 2.16  Pressuremeter curve with limit pressure and moduli denoted.

with:

$Q_{PL} = A_p \left[ K_P \left( p_l - p_o \right) + q_o \right]$ the limit tip load

$Q_{SL} = \sum_i A_{si} \times q_{si}$ the limit shaft friction load were:

$P_l$ = the limit pressure from the pressuremeter test

$P_o$ = the horizontal ground pressure, before the test (roughly estimated from at rest coefficient $k_o$)

$Q_o$ = the initial vertical pressure at the foundation level.

Readjusted design factors $k_p$ and $q_s$ have been proposed for isolated piles by Bustamante and Gianeselli (1981, reported by Briaud, 1989) from the examination of numerous full-scale static loading test results, and are presented in Table 2.2 and Figure 2.17.

Table 2.2 Values of end bearing factor $k_p$ for driven or bored piles. (after Bustamante and Gianeselli, 1981)

| Type of Soil | Type of Pile | |
|---|---|---|
| | Bored | Driven |
| Clay or silt | 1.2 - 1.4 | 1.8 - 2.2 |
| Sand or gravel | 1.0 - 1.2 | 3.2 - 4.2 |
| Chalk, marl or calcareous marl | 1.8 | 2.4 - 2.8 |
| Weathered rock | 1.0 - 1.8 | 1.8 - 2.8 |

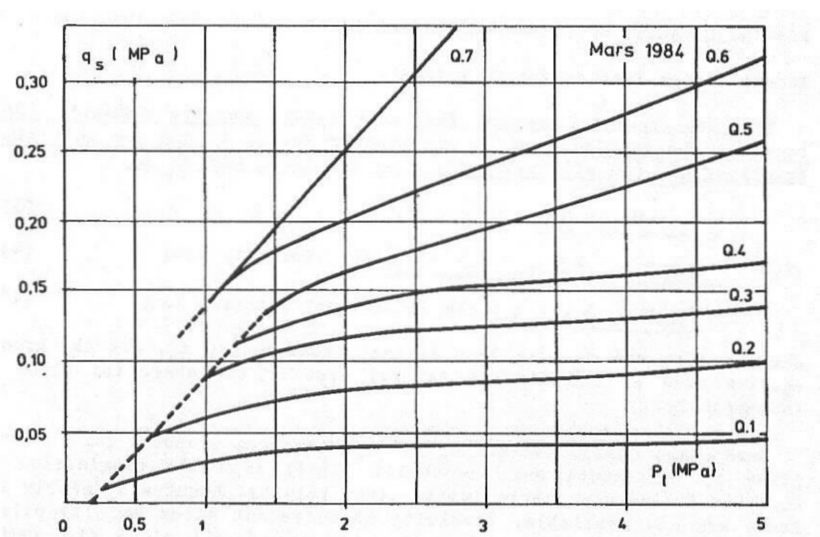


Figure 2.17 Curves for the assessment of unit limit friction $q_s$ .
(after Bustamante and Gianeselli, 1981)

## GEOPHYSICAL METHODS

### Ground Penetrating Radar

#### *Introduction*

Ground-penetrating radar (GPR) uses a high-frequency (80 to 1,000 MHz) EM pulse transmitted from a radar antenna to probe the earth. The transmitted radar pulses are reflected from various interfaces within the ground and this return is detected by the radar receiver analogous to seismic refraction. A trace of the reflected wave vs. time (nanoseconds) is obtained. The relative magnitude of the reflected energy indicates changes in the media penetrated (soil, rock, air, water). These reflecting interfaces may be soil horizons, the groundwater surface, soil/rock interfaces, man-made objects, or any other interface possessing a contrast in dielectric properties.

GPR methodology consists of imparting a radar signal to the ground by an antenna that is in close proximity to the ground surface. The reflected signals are then detected by the transmitting antenna or by a second, separate receiving antenna. The received signals are processed and displayed on a graphic recorder. As the antenna (or antenna pair) is moved along the surface, the graphic recorder displays results in a cross-section record or radar image of the earth. The two reflection methods used in seismic reflection (common offset and common midpoint) are also used in GPR. The typical mode of operation is the common-offset mode where the receiver and transmitter are maintained at a fixed distance and moved along a line to produce a profile. Figure 2.18 illustrates the procedure.

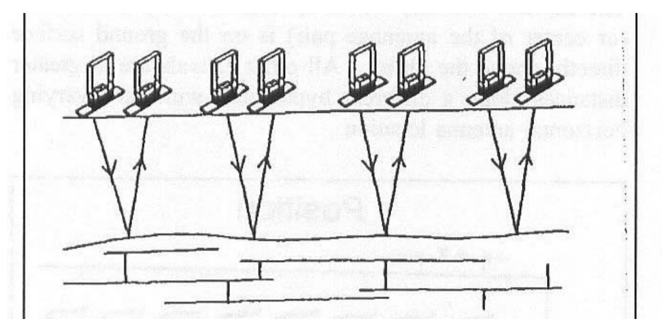

Figure 2.18 GPR Reflection method, using Common Offset Mode. (Annan, 1992)

As GPR has short wavelengths in most earth materials, resolution of interfaces and discrete objects is very good. However, the attenuation of the signals in earth materials is high and depths of penetration seldom exceed 10 m. Water and clay soils increase the attenuation, decreasing penetration. Note that as in seismic reflection, the energy does not necessarily propagate only downwards and a reflection will be received from objects off to the side. An added complication with GPR is the fact that some of the energy is radiated into the air and if reflected off nearby objects like buildings or support vehicles, will appear on the record as arrivals (illustrated in Figure 2.19).

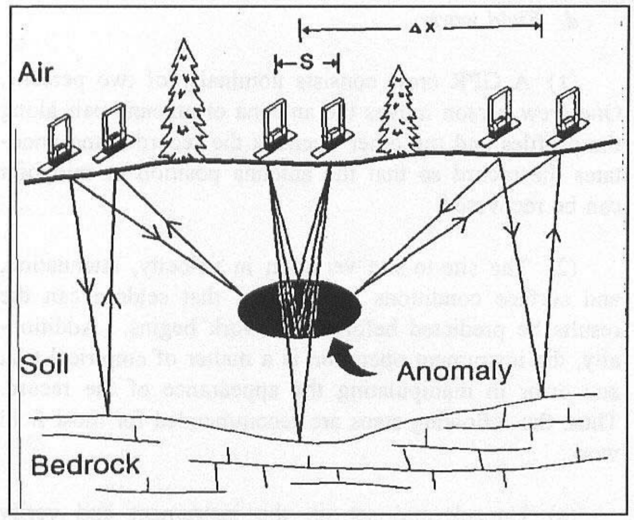


Figure 2.19 Schematic illustration of common offset single fold profiling.

*The GPR Surveys Focus*

1. To map near-surface interfaces.
2. For many surveys, the location of objects such as tanks or pipes in the subsurface is the objective.
3. Groundwater location.
4. Identification of subsurface anomalies.

Dielectric properties of materials are not measured directly. The method is most useful for detecting changes in the geometry of subsurface interfaces.

The following questions are important considerations in advance of a GPR survey.

1. What is the target depth? Though target detection has been reported under unusually favorable circumstances at depths of 100 m or more, a careful feasibility evaluation is necessary if the investigation depths need to exceed 10 m.
2. What is the target geometry? Size, orientation, and composition are important.
3. What are the electrical properties of the target? As with all geophysical methods, a contrast in physical properties must be present. Dielectric constant and electrical conductivity are the important parameters. Conductivity is most likely to be known or easily estimated.
4. What are the electrical properties of the host material? Both the electrical properties and homogeneity of the host must be evaluated. Attenuation of the signal is dependent on the electrical properties and on the number of minor interfaces which will scatter the signal.

5. Are there any possible interfering effects? Radio frequency transmitters, extensive metal structures (including cars) and power poles are probable interfering effects for GPR.

6. Electromagnetic wave propagation. There are two physical parameters of materials which are important in wave propagation at GPR frequencies.

- One property is conductivity (σ), the inverse of electrical resistivity (ρ). The relationships of earth material properties to conductivity, measured in mS/rn (1/1,000 Qm), are given in Table 2.3.

- The other physical property of importance at GPR frequencies is the dielectric constant (ε), which is dimensionless. Materials made up of polar molecules, such as water, have a high ε. Physically, a great deal of the energy in an EM field is consumed in interaction with the molecules of water or other polarizable materials. Thus waves propagating through such a material both go slower and are subject to more attenuation. To complicate matters, water, of course, plays a large role in determining the conductivity (resistivity) of earth materials.

### *Earth Material Properties*

The roles of two earth materials, which cause important variations in the EM response in a GPR survey, need to be appreciated. The ubiquitous component of earth materials is water; the other material is clay. At GPR frequencies, the polar nature of the water molecule causes it to

Table 2.3 Electromagnetic properties of Earth materials.

| Material | ε | Conductivity (mS/m) | Velocity (m/ns) | Attenuation (db/m) |
|---|---|---|---|---|
| Air | 1 | 0 | .3 | 0 |
| Distilled Water | 80 | .01 | .033 | .002 |
| Fresh Water | 80 | .5 | .033 | .1 |
| Sea Water | 80 | 3,000 | .01 | 1,000 |
| Dry Sand | 3-5 | .01 | .15 | .01 |
| Wet Sand | 20-30 | .1-1 | .06 | .03-.3 |
| Limestone | 4-8 | .5-2 | .12 | .4-1 |
| Shales | 5-15 | 1-100 | .09 | 1-100 |
| Silts | 5-30 | 1-100 | .07 | 1-100 |
| Clays | 5-40 | 2-1,000 | .06 | 1-300 |
| Granite | 4-6 | .01-1 | .13 | .01-1 |
| Dry Salt | 5-6 | .01-1 | .13 | .01-1 |
| Ice | 3-4 | .01 | .16 | .01 |
| Metals | | ∞ | | ∞ |

contribute disproportionately to the displacement currents which dominate the current flow at GPR frequencies. Thus, if significant amounts of water are present, the ε will be high and the velocity of propagation of the electromagnetic wave will be lowered. Clay materials with their trapped ions behave similarly. Additionally, many clay minerals also retain water.

The physical parameters in Table 2.3 are typical for the characterization of earth materials. The range for each parameter is large; thus the application of these parameters for field use is not elementary.

Simplified equations for attenuation and velocity (at low loss) are:

$$V = \frac{3 \times 10^8}{\varepsilon^{1/2}}$$

$$a = \frac{1.69\sigma}{\varepsilon^{1/2}}$$

where:

| | | |
|---|---|---|
| V | = | velocity in m/s |
| ε | = | dielectric constant (dimensionless) |
| a | = | attenuation in decibels/m (db/m) |
| σ | = | electrical conductivity in mS/m |

The large variations in velocity and especially attenuation, are the causes of success (target detection) and failure (insufficient penetration) for surveys in apparently similar geologic settings. As exhaustive catalogs of the properties of specific earth materials are not readily available, most GPR work is based on trial and error and empirical findings.

**Electro-Resistivity**

The use of an Earth Resistivity Meter is one of the options in the study of shallow depth earth exploration, pollution monitoring, and archaeological problems. The test consists on setting several electrodes over a straight measured line on the field, spaced to a desire length. A current is passed through the electrodes and the voltage drop is measured between electrodes. A value of resistivity is calculated knowing the current, the voltage difference, and the electrode spacing. The electricity is conducted through the ground by the electrolytic conductivity of the soil or rock pore fluid and to a lesser degree by electronic conductivity of metallic solid particles. For the present study performed at FDOT-UCF site an Electrical Resistivity Imaging (ERI) geophysical method was used.

***Description of the ERI Technique***

Electrical resistivity imaging (ERI) is an advanced geophysical method and is a much more powerful way of documenting the lateral extent of subsurface layers than old-fashioned resistivity soundings or profiling. In an ERI survey, typically, 28 or 56 electrodes are placed in the ground in a straight line and are connected by a switching cable. The electrodes are spaced evenly, usually at distances of 5 to 20 feet, which corresponds, approximately, to the resolution.

A computer is used to switch power on and off, usually to groups of four electrodes so that every geometrically possible combination of electrodes is used to collect measurements. Typically, 138 to 281 data points are measured per transect depending on the type of electrode array. The depth of testing is about one-half of the length of the line, but the depth of reliable modeling is about 15-25% of the transect length. Depth of scanning is commonly greater than 100 feet. Usually about four or five ERI transects can be measured per day.

Measured apparent resistivity values represent weighted averages for the ground around each group of electrodes. By themselves, they do not show a cross-section of the ground. To get a useful image, the measured values are downloaded to a personal computer and processed using a program called RES2DINV. This program estimates the true resistivity values at points along a finite-element grid, beneath the survey line, using a least-squares method. The true resistivity values are modeled through an iterative process that approaches a unique solution for the subsurface resistivity. There is NO guessing about layer thickness, number of layers or average resistivity of the layers. The model's gridded values are contoured to produce a cross section of the subsurface resistivity. Goodness of fit for the model is automatically calculated as root mean square error.

### *Electrical Concepts*

Resistivity of a material is a measure of how difficult it is to make an electrical current flow through the material, and is measured in Ohm-meters.

Apparent resistivity is a weighted average of the measured resistivity. If the ground is homogeneous, the apparent resistivity theoretically equals the true resistivity.

Conductivity of a material is a measure of how easy it is to make an electrical current flow through the material and is measured in Siemens or mho and usually expressed in milliS/meter or millimhos/meter. Conductivity is the reciprocal of resistivity in terms of propagation of an electrical signal through a medium or material.

Properties which affect the resistivity of soils and rocks:

- Porosity; shape, size, and connection of pore spaces.
- Moisture content.
- Dissolved electrolytes, minerals, or contaminants/pollutants.
- Temperature of pore water. Conductivity of minerals.

### *Electrical Resistivities of Selected Earth Materials*

The resistivity of earth materials varies widely for any one material and between different materials. Various ranges are cited in the geological literature (Table 2.4). The variation is due largely to differences in moisture content and the salinity of the ground water (pour fluid) than to the minerals themselves. Subsurface Evaluations, Inc., recommends using the resistivity values presented by Vogelsang (1995), as they seem to represent more accurately the conditions commonly encountered in Florida.

Table 2.4 Electrical resistivities of selected Earth materials.

| | Resistivity (Ohm-Meters) According to Various Sources | | | |
|---|---|---|---|---|
| Material | Guegen & Palciauskas 1994 (p. 185) | Lowrie 1997 (p. 208) | Advanced Geo-sciences, Inc. 1998 (p. 72) | Vogelsang 1995 (p. 12) |
| Clay | 3-100 | 1-100 | 10-100 | 3-30 |
| Clay, sandy | -- | -- | -- | 25-150 |
| Sand, clayey | -- | -- | -- | 50-300 |
| Sand | 500-10,000 | 100-10,000 | 600-10,000 | 800-5,000 |
| Sand, wet | -- | -- | -- | 200-400 |
| Limestone | 1,000-100,000 | 10-10,000 | 100-10,000 | 500-3,500 |

## LABORATORY TESTING

### The Triaxial Test

In the triaxial test a cylindrical specimen of soil is sealed in a watertight rubber membrane and enclosed in a cell which is subjected to a fluid pressure. A load applied axially, through ram acting on the top cap, is used to control the deviator stress. Under these conditions the axial stress is the major principal stress $\sigma_1$; the intermediate and minor principal stresses ($\sigma_2$ and $\sigma_3$) are both equal to the cell pressure.

Connections to the ends of the sample permit either the drainage of water and air from the voids of the soil or, alternatively, the measurement of pore pressure under the conditions of no drainage.

Generally the application of the all-round pressure and of the deviatoric stress form two separate stages of the test; tests are therefore classified according to the condition of drainage obtained during each stage as:

1. Undrained Test (U/U or Q): No drainage and hence no dissipation of pore pressure, is permitted during the application of the all-round stress. No drainage is allowed during the application of deviator stress. It is used during the end of construction phase of testing.

2. Consolidated-Undrained Test (C/U or R): This method combines a CD test with a UU test. Drainage is permitted during the application of the all-round stress, so that the sample is fully consolidated under the pressure. No drainage is allowed during the application of deviator stress. It is used primarily to obtain effective stress parameters of impermeable soils. It is used for rapid draw down analyses or means to determine the effective conditions via measured pore water pressure.

3. Drained Test (C/D or S): Drainage is permitted throughout the test, so that the full consolidation occurs under the all round stress and no excess pore pressure is set up during the application of the deviator stress. It is used for sands or partially saturated soils.

Fundamental to performing a laboratory triaxial test is understanding the calculations required for data reduction in determining the pore water pressure during undrained loading (undrained strength), deformations during drained loading (including volume change), c and $\phi$ values of the soil sample and the effect of stress path leading to the failure on these values.

# CHAPTER 3

## PRESENTATION OF DATA: SPT and Laboratory Tests

### INTRODUCTION

Two 200-ft SPT borings were made by GEC and Amdrill, with Shelby tubes recovered for laboratory testing. Borings, SPT GEC -1 and -2 were located on the Eastside (hard) and Westside (soft) areas of the site, respectively, as shown in Figure 3.1. Shelby tubes were recovered at depths ranging from 2 to 55-ft.

### SPT RESULTS

The SPT logs for borings GEC-1 and -2 are tabulated in Table 3.1 and summarized in Figure 3.2. Figures 3.3 and 3.4 present the boring logs. A CME-55 rig using a safety hammer was used to perform the borings.

Appendix C contains the SPT data. (file: Gecboring1UCF.xls)

Energy measurements were performed by FDOT's SMO (Brian Bixler), with the results tabulated in Table 3.2. (file: Gecboring1UCF.xls) The energy levels are quite good for a safety hammer; i.e., above 60%.

### LABORATORY TESTING – CLASSIFICATION TESTS

Tables 3.3 and 3.4 present the classification tests performed by the FDOT-SMO on the split spoon samples from GEC-1 and GEC-2.(file:updated classification.xls)

### LABORATORY TESTS – ROCK CORE UNCONFINED COMPRESSION TESTS

Tables 3.5 and 3.6 summarize, respectively, the Unconfined Compression and Split Tensile tests on rock cores from GEC-1 and 2. (file:AmdrillUCF.xls)

### LABORATORY TESTS – TRIAXIAL COMPRESSION TESTS

Five triaxial tests with single confining pressures on single Shelby tube samples resulting in a single Mohr's circle per tube were conducted by UF. The FDOT-SMO lab used 3 different confining pressures for samples from a single Shelby tube resulting in a failure envelope tangent to the Mohr's circles. These tests resulted in 7 shear strength estimates.

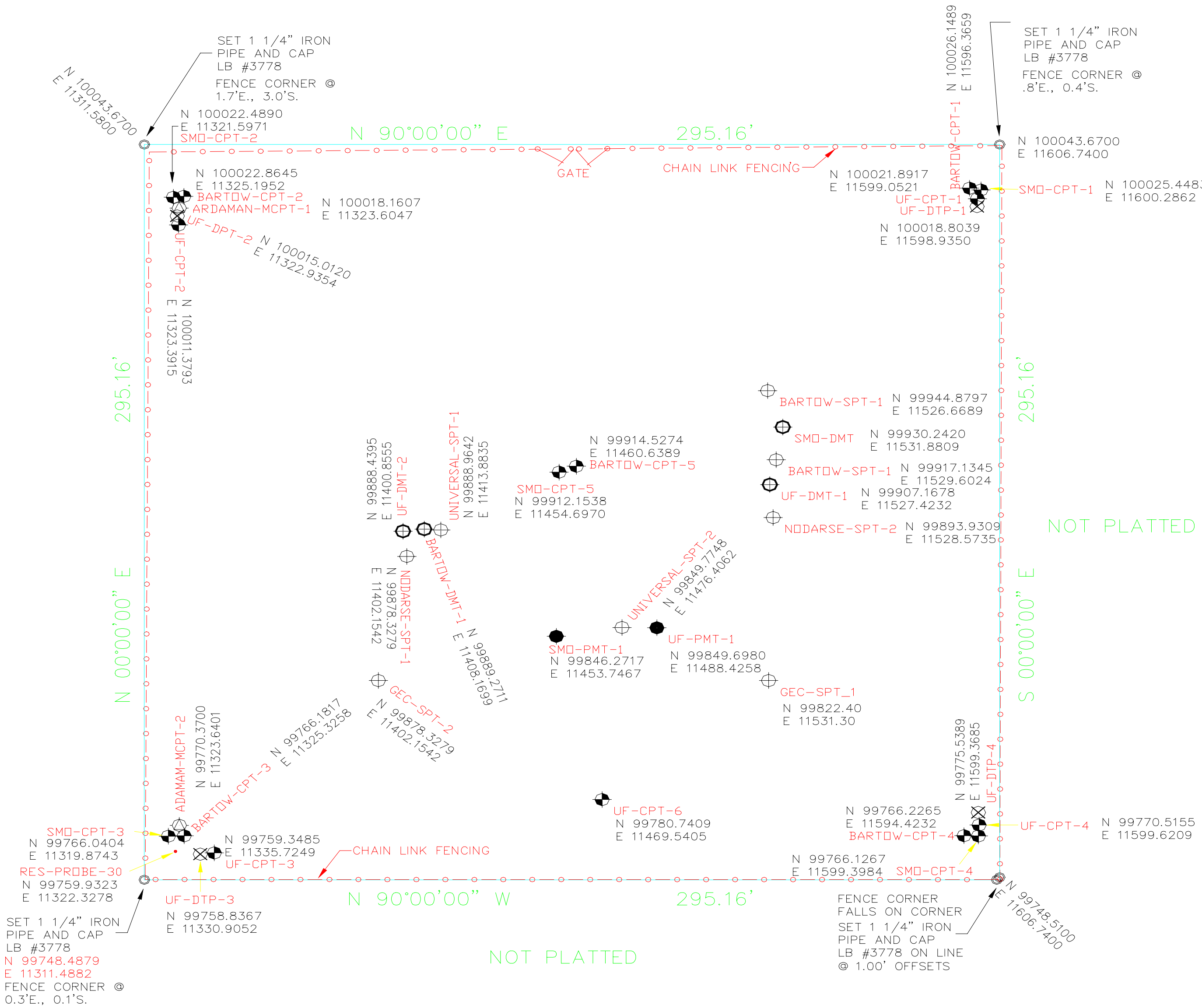


Figure 3.1 Location of SPT testing for extraction of Shelby tubes.

Table 3.1 SPT Borings GEC-1 and GEC-2.

| Depth (ft) | BORING GEC-1 | | | BORING GEC-2 | | |
|---|---|---|---|---|---|---|
| | N (blows/ft) | AASHTO | USCS | N (blows/ft) | AASHTO | USCS |
| 2.0 | 7 | A-3 | SP | 8 | A-3 | SP-SM |
| 4.0 | | | | 4 | A-2-4 | SM |
| 6.0 | 18 | A-2-4 | SM | 14 | | |
| 8.0 | | | | 7 | A-2-4 | SM |
| 10.0 | 10 | A-2-4 | SM | 7 | A-2-4 | SM |
| 13.0 | 7 | A-3 | SP-SM | 11 | A-2-4 | SM |
| 15.5 | 7 | A-2-4 | SM | 5 | | |
| 18.0 | 15 | A-3 | SP-SM | 6 | A-2-4 | SM |
| 20.5 | 10 | A-2-4 | SM | 11 | A-3 | SP-SM |
| 23.0 | 6 | A-2-4 | SM | 8 | A-2-4 | SP-SM |
| 25.5 | 13 | A-3 | SP-SM | 1 | A-2-4 | SM |
| 28.5 | 8 | A-2-4 | SP-SM | | | |
| 29.0 | | | | 0 | A-4 | SM |
| 30.5 | 5 | A-2-4 | SM | 0 | A-2-4 | SC-SM |
| 33.0 | 4 | A-2-4 | SM | 5 | A-2-6 | SC |
| 35.5 | 6 | A-4 | SC-SM | 11 | A-6 | sandy CL |
| 39.0 | 4 | A-3 | SP-SM | 4 | | |
| 40.5 | 5 | A-4 | SC-SM | 4 | A-7-6 | sandy MH |
| 43.0 | 6 | A-4 | SC | 2 | A-7-5 | sandy CL |
| 45.5 | 6 | A-4 | SM | | | |
| 46.5 | | | | 7 | | |
| 48.0 | | | | 8 | A-4 | SC-SM |
| 49.0 | 5 | A-6 | sandy (CL) | | | |
| 50.0 | 7 | A-4 | sandy (SC) | | | |
| 50.5 | | | | 9 | A-4 | SC |
| 53.0 | 9 | A-7-6 | sandy (CL) | 12 | A-3 | SP-SM |
| 55.0 | 19 | A-1-b | SW-SM | | | |
| 55.5 | | | | 16 | A-3 | SP |
| 58.0 | 14 | A-1-a | (SW) w/gravel | | | |
| 58.5 | | | | 12 | A-1-b | SW-SM w/gravel |
| 60.5 | 11 | A-1-a | (SW-SM) w/gravel | 21 | A-1-b | SW-SM |
| 63.0 | 16 | A-1-a | (SW) w/gravel | 50+ | A-1-b | SW-SM |
| 65.5 | 14 | A-1-b | (SW-SM) w/gravel | 14 | | |
| 68.0 | 19 | A-1-a | (SW-SM) w/gravel | 17 | A-1-b | SC |
| 70.5 | 20 | A-1-b | SM | 16 | A-7-5 | sandy MH |
| 73.0 | 72 | A-1-b | (SW-SM) w/gravel | 50+ | A-1-b | SM w/gravel |
| 75.5 | 36 | A-1-b | SW-SM | 23 | A-1-b | SM |
| 78.0 | 10 | A-4 | SM | 17 | A-5 | sandy ML |
| 80.5 | 16 | A-4 | SM | 9 | A-7-5 | SM |
| 83.0 | 17 | A-1-b | SM | 10 | A-2-7 | SC |
| 85.5 | 75 | A-4 | SM | 10 | A-1-b | SM |
| 88.0 | 75 | A-2-4 | SM | 56 | A-4 | SM |
| 90.5 | | | | 17 | A-2-6 | SC |
| 93.0 | | | | 14 | A-2-7 | SC |
| 95.5 | | | | 54 | A-2-4 | SM w/gravel |

| Depth (ft) | BORING GEC-1 | | | BORING GEC-2 | | |
|---|---|---|---|---|---|---|
| | N (blows/ft) | AASHTO | USCS | N (blows/ft) | AASHTO | USCS |
| 98.0 | 30 | A-7-5 | SC | | | |
| 100.5 | 90 | A-1-b | (SM) w/gravel | 90 | A-2-7 | SC |
| 103.0 | | | | 50+ | A-1-b | SW-SM w/gravel |
| 108.0 | 62 | A-4 | sandy (ML) | 50+ | A-4 | sandy ML |
| 110.5 | 33 | A-4 | ML | 78 | A-4 | sandy ML |
| 113.0 | 13 | A-1-b | SM | 53 | A-2-4 | SM |
| 115.5 | 20 | A-1-b | SM | 14 | A-1-b | SM |
| 118.0 | 15 | A-1-b | (SM) w/gravel | 19 | A-1-b | SM |
| 120.5 | 27 | A-1-b | (SM) w/gravel | 14 | A-2-4 | SM |
| 123.0 | 50+ | A-1-b | SM | 49 | A-1-b | SM |
| 125.5 | 63 | A-1-b | (SM) w/gravel | 50+ | A-1-b | SW-SM w/gravel |
| 135.5 | 50+ | A-1-a | (SW-SM) w/gravel | 73 | A-2-4 | SM |
| 138.0 | 59 | A-2-4 | SP-SM | 52 | A-2-4 | SP-SM |
| 140.5 | 50+ | A-1-b | SW-SM w/gravel | 50+ | A-3 | SP-SM |
| 143.0 | 50+ | A-1-b | SW-SM w/gravel | | | |
| 145.5 | 41 | A-2-4 | SP-SM | 78 | A-1-a | SP-SM |
| 148.0 | 50+ | A-1-b | (SW-SM) w/gravel | | | |
| 150.5 | | | | 25 | A-2-4 | SP-SM |
| 153.0 | | | | 19 | A-2-4 | SM |
| 153.5 | 22 | A-2-4 | SM | | | |
| 155.5 | 22 | A-2-4 | SP-SM | 15 | A-2-4 | SM |
| 158.0 | 19 | A-2-4 | SM | 15 | A-2-4 | SM |
| 160.5 | 25 | A-2-4 | SM | 27 | A-2-4 | SM |
| 163.0 | 50+ | A-2-5 | SM | 35 | A-2-4 | SM |
| 165.5 | 33 | A-2-6 | SM | 20 | A-2-4 | SM |
| 168.0 | 25 | A-2-7 | SM | | | |
| 170.5 | 80 | A-1-b | (SW-SM) w/gravel | 12 | A-2-4 | SM |
| 173.0 | 53 | A-2-4 | SP-SM | 31 | A-2-4 | SM |
| 175.5 | 50+ | A-2-5 | SP-SM | 21 | A-2-4 | SM |
| 178.0 | 30 | A-2-4 | SM | 61 | A-2-4 | SM |
| 180.5 | 79 | A-1-b | SW-SM (w/gravel) | 42 | A-2-4 | SM |
| 183.0 | 50+ | A-1-b | SW-SM (w/gravel) | 50+ | A-1-b | SW-SM |
| 188.5 | | | | | | |
| 190.5 | 50+ | A-1-b | SM | 16 | A-4 | sandy ML |
| 193.0 | 9 | A-1-b | SM | 50+ | A-1-b | SM |
| 195.5 | 24 | A-4 | ML | 19 | A-4 | ML with sand |
| 198.0 | 50+ | A-1-b | (SW) w/gravel | 50+ | A-4 | ML w/sand |
| 200.5 | 18 | A-5 | SC-SM | 15 | A-2-4 | SM |

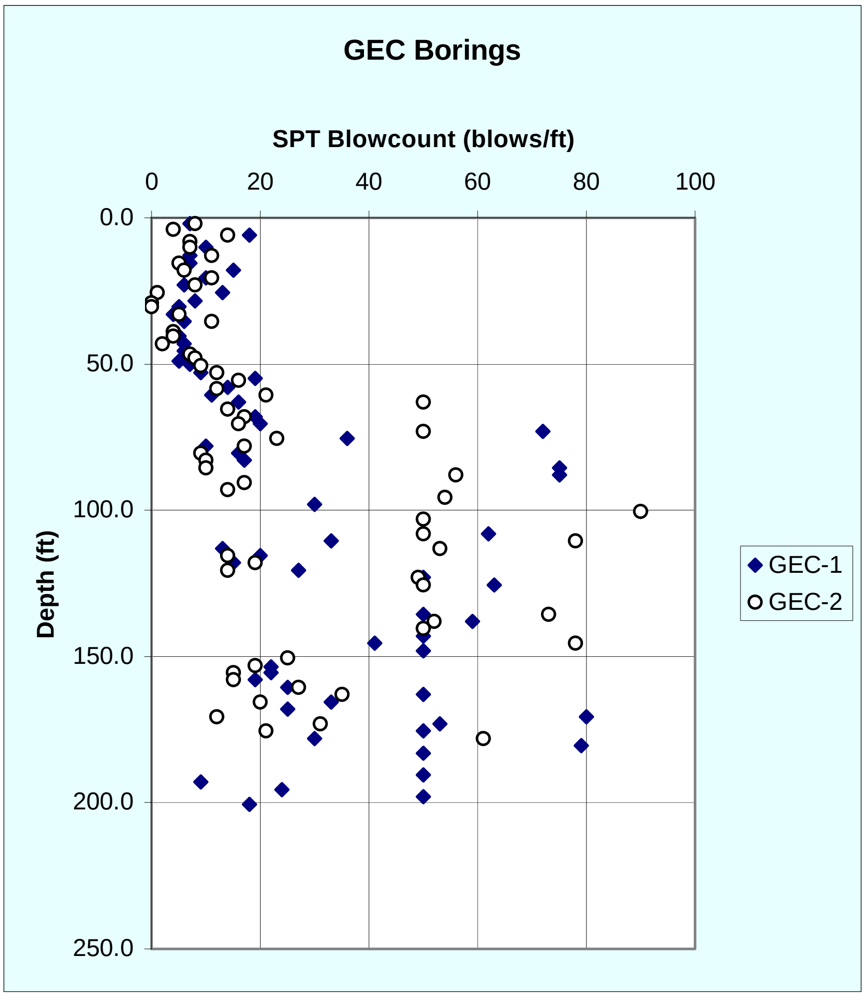


Figure 3.2 SPT N-Values vs. Depth for GEC-1 and GEC-2.
File: JAS-GEC Boring-2.xls

# STANDARD PENETRATION TEST BORING LOG

## BORING GEC-1

PROJECT: UCF Orlando FILE No.:

BORING LOCATION: As per plan DRILL CREW: PJB/TJR

WATER OBSERVED AT DEPTH 1.5 FEET DATE DRILLED: 10-1-02

| FIELD TEST DATA | SOIL DESCRIPTION | SAMPLE No. | N VALUE |
|---|---|---|---|
| 3/6 3/6 4/6 | Loose light gray fine sand | 1 | 7 |
| | Shelby tube from 2 to 4 feet (recovery 6 inch) | | |
| 6/6 9/6 9/6 | Medium dense brown slightly silty fine sand | 2 | 18 |
| | Shelby tube from 6 to 8 feet (recovery 22 inch) | | |
| 1/6 5/6 5/6 | Medium dense light brown slightly silty fine sand | 3 | 10 |
| 2/6 3/6 4/6 | Loose light brown fine sand | 4 | 7 |
| 2/6 3/6 4/6 | | | 7 |
| 5/6 8/6 7/6 | Medium dense sand | 5 | 15 |
| | Shelby tube from 18 to 19 feet (recovery 0 inch) | | |
| 6/6 6/6 4/6 | Medium dense light brown fine sand | 6 | 10 |
| 3/6 3/6 3/6 | Loose light gray silty fine sand | 7 | 6 |
| 4/6 6/6 7/6 | Medium dense light brown fine sand | 8 | 13 |
| | Shelby tube from 25.5 to 27 feet (recovery 0 inch) | | |
| 4/6 4/6 4/6 | | | 8 |
| 3/6 2/6 3/6 | Loose light brown slightly silty fine sand | 10 | 5 |
| 2/6 2/6 2/6 | Loose light brown fine sand | 11 | 4 |
| 1/6 2/6 | | | 6 |

NOTES: Weight of the Hammer 140 lbs Drop of the hammer 30" Using Grout hole and casing at 135 feet.

FIELD TEST DATA ARE "BLOWS"/"INCHES DRIVEN" 140-LB HAMMER, 30-INCH FALL. (ASTM D-1586)

Figure 3.3 GEC Boring 1.

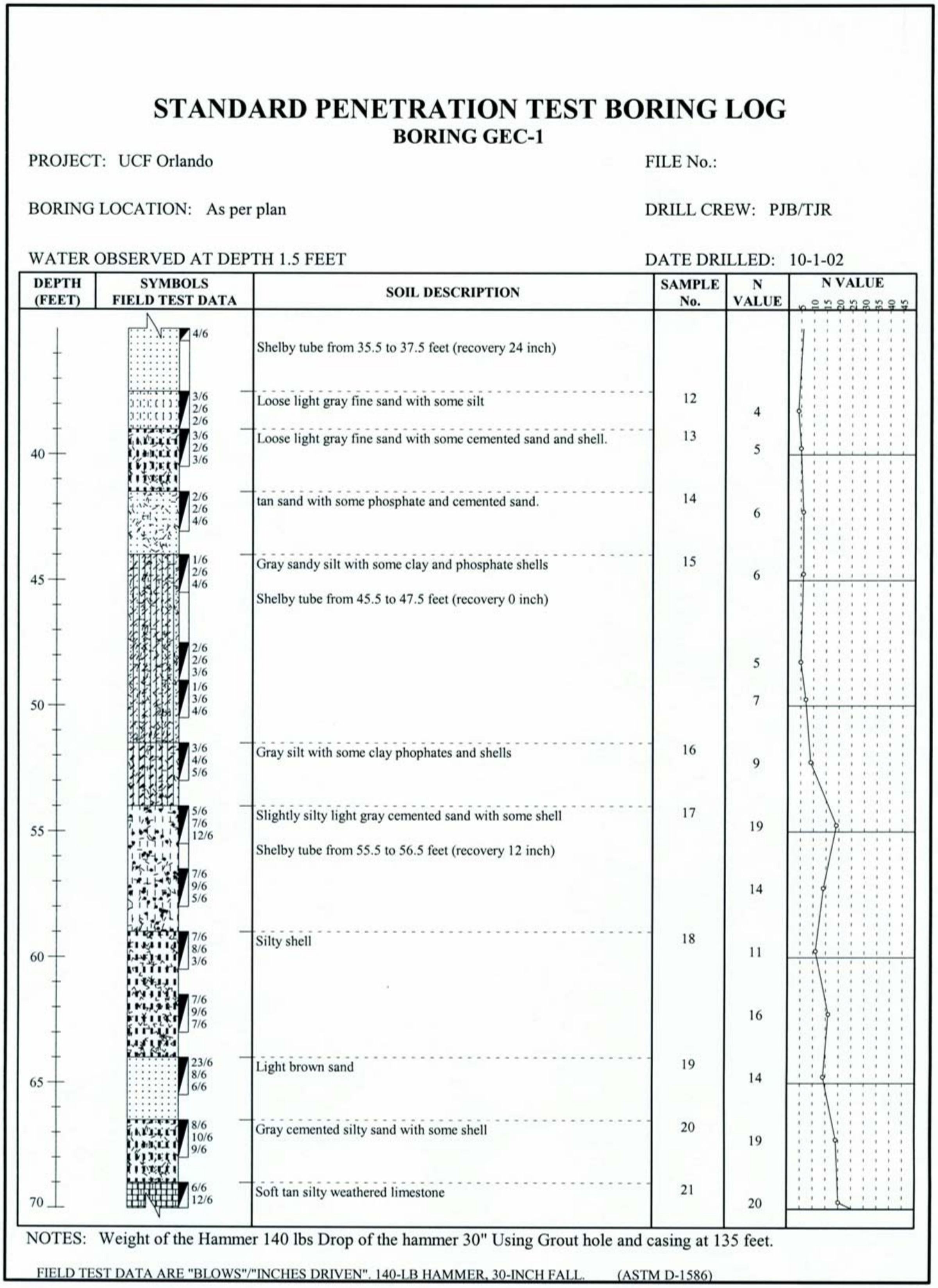

# STANDARD PENETRATION TEST BORING LOG

## BORING GEC-1

PROJECT: UCF Orlando | FILE No.:

BORING LOCATION: As per plan | DRILL CREW: PJB/TJR

WATER OBSERVED AT DEPTH 1.5 FEET | DATE DRILLED: 10-1-02

| DEPTH (FEET) | SYMBOLS FIELD TEST DATA | SOIL DESCRIPTION | SAMPLE No. | N VALUE |
|---|---|---|---|---|
| | 4/6 | Shelby tube from 35.5 to 37.5 feet (recovery 24 inch) | | |
| | 3/6 2/6 2/6 | Loose light gray fine sand with some silt | 12 | 4 |
| 40 | 3/6 2/6 3/6 | Loose light gray fine sand with some cemented sand and shell. | 13 | 5 |
| | 2/6 2/6 4/6 | tan sand with some phosphate and cemented sand. | 14 | 6 |
| 45 | 1/6 2/6 4/6 | Gray sandy silt with some clay and phosphate shells<br>Shelby tube from 45.5 to 47.5 feet (recovery 0 inch) | 15 | 6 |
| | 2/6 2/6 3/6 | | | 5 |
| 50 | 1/6 3/6 4/6 | | | 7 |
| | 3/6 4/6 5/6 | Gray silt with some clay phophates and shells | 16 | 9 |
| 55 | 5/6 7/6 12/6 | Slightly silty light gray cemented sand with some shell<br>Shelby tube from 55.5 to 56.5 feet (recovery 12 inch) | 17 | 19 |
| | 7/6 9/6 5/6 | | | 14 |
| 60 | 7/6 8/6 3/6 | Silty shell | 18 | 11 |
| | 7/6 9/6 7/6 | | | 16 |
| 65 | 23/6 8/6 6/6 | Light brown sand | 19 | 14 |
| | 8/6 10/6 9/6 | Gray cemented silty sand with some shell | 20 | 19 |
| 70 | 6/6 12/6 | Soft tan silty weathered limestone | 21 | 20 |



NOTES: Weight of the Hammer 140 lbs Drop of the hammer 30" Using Grout hole and casing at 135 feet.

FIELD TEST DATA ARE "BLOWS"/"INCHES DRIVEN". 140-LB HAMMER, 30-INCH FALL. (ASTM D-1586)

Figure 3.3 (continued).

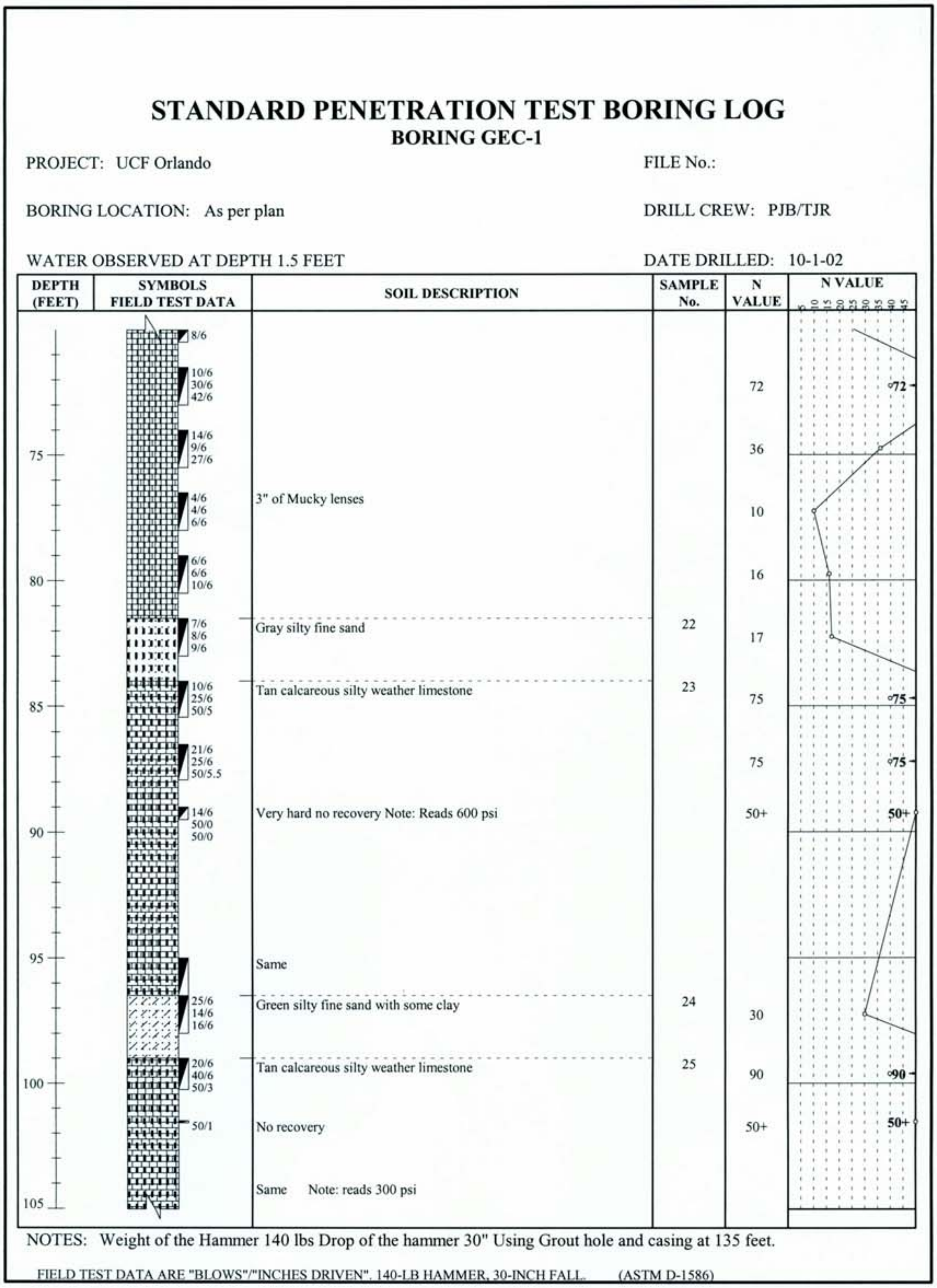

# STANDARD PENETRATION TEST BORING LOG

**BORING GEC-1**

PROJECT: UCF Orlando | FILE No.:

BORING LOCATION: As per plan | DRILL CREW: PJB/TJR

WATER OBSERVED AT DEPTH 1.5 FEET | DATE DRILLED: 10-1-02

| FIELD TEST DATA | SOIL DESCRIPTION | SAMPLE No. | N VALUE |
|---|---|---|---|
| 8/6 | | | |
| 10/6 30/6 42/6 | | | 72 |
| 14/6 9/6 27/6 | | | 36 |
| 4/6 4/6 6/6 | 3" of Mucky lenses | | 10 |
| 6/6 6/6 10/6 | | | 16 |
| 7/6 8/6 9/6 | Gray silty fine sand | 22 | 17 |
| 10/6 25/6 50/5 | Tan calcareous silty weather limestone | 23 | 75 |
| 21/6 25/6 50/5.5 | | | 75 |
| 14/6 50/0 50/0 | Very hard no recovery Note: Reads 600 psi | | 50+ |
| | Same | | |
| 25/6 14/6 16/6 | Green silty fine sand with some clay | 24 | 30 |
| 20/6 40/6 50/3 | Tan calcareous silty weather limestone | 25 | 90 |
| 50/1 | No recovery | | 50+ |
| | Same Note: reads 300 psi | | |

Depth (feet): 75, 80, 85, 90, 95, 100, 105

NOTES: Weight of the Hammer 140 lbs Drop of the hammer 30" Using Grout hole and casing at 135 feet.

FIELD TEST DATA ARE "BLOWS"/"INCHES DRIVEN". 140-LB HAMMER, 30-INCH FALL. (ASTM D-1586)

Figure 3.3 (continued).

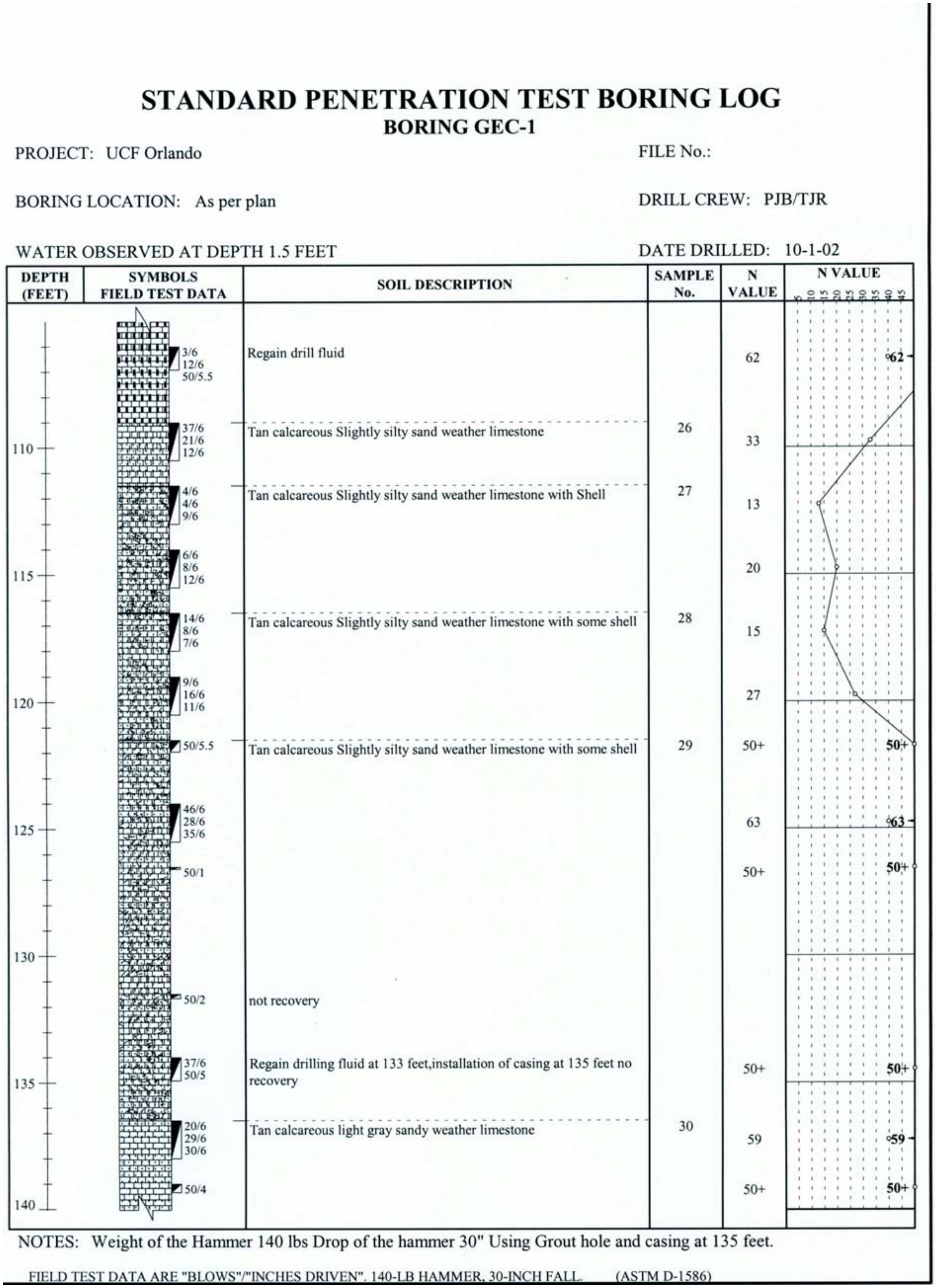

# STANDARD PENETRATION TEST BORING LOG

**BORING GEC-1**

PROJECT: UCF Orlando | FILE No.:

BORING LOCATION: As per plan | DRILL CREW: PJB/TJR

WATER OBSERVED AT DEPTH 1.5 FEET | DATE DRILLED: 10-1-02

| DEPTH (FEET) | SYMBOLS FIELD TEST DATA | SOIL DESCRIPTION | SAMPLE No. | N VALUE |
|---|---|---|---|---|
| | 3/6 12/6 50/5.5 | Regain drill fluid | | 62 |
| 110 | 37/6 21/6 12/6 | Tan calcareous Slightly silty sand weather limestone | 26 | 33 |
| | 4/6 4/6 9/6 | Tan calcareous Slightly silty sand weather limestone with Shell | 27 | 13 |
| 115 | 6/6 8/6 12/6 | | | 20 |
| | 14/6 8/6 7/6 | Tan calcareous Slightly silty sand weather limestone with some shell | 28 | 15 |
| 120 | 9/6 16/6 11/6 | | | 27 |
| | 50/5.5 | Tan calcareous Slightly silty sand weather limestone with some shell | 29 | 50+ |
| 125 | 46/6 28/6 35/6 | | | 63 |
| | 50/1 | | | 50+ |
| 130 | 50/2 | not recovery | | |
| 135 | 37/6 50/5 | Regain drilling fluid at 133 feet,installation of casing at 135 feet no recovery | | 50+ |
| | 20/6 29/6 30/6 | Tan calcareous light gray sandy weather limestone | 30 | 59 |
| 140 | 50/4 | | | 50+ |

NOTES: Weight of the Hammer 140 lbs Drop of the hammer 30" Using Grout hole and casing at 135 feet.

FIELD TEST DATA ARE "BLOWS"/"INCHES DRIVEN". 140-LB HAMMER, 30-INCH FALL. (ASTM D-1586)

Figure 3.3 (continued).

# STANDARD PENETRATION TEST BORING LOG
## BORING GEC-1

PROJECT: UCF Orlando — FILE No.:

BORING LOCATION: As per plan — DRILL CREW: PJB/TJR

WATER OBSERVED AT DEPTH 1.5 FEET — DATE DRILLED: 10-1-02

| FIELD TEST DATA | SOIL DESCRIPTION | SAMPLE No. | N VALUE |
|---|---|---|---|
| 44/6, 50/5 | | | 50+ |
| 48/6, 17/6, 24/6 | | | 41 |
| 31/6, 50/1 | | | 50+ |
| 14/6, 11/6, 11/6 | Sand | | 22 |
| 10/6, 11/6, 11/6 | | | 22 |
| 7/6, 8/6, 11/6 | | | 19 |
| 12/6, 16/6, 9/6 | | | 25 |
| 50/5 | Tan sand | 31 | 50+ |
| 12/6, 13/6, 20/6 | | | 33 |
| 13/6, 11/6, 14/6 | | | 25 |
| 16/6, 39/6, 41/6 | | | 80 |
| 16/6, 31/6, 22/6 | | | 53 |
| 10/6, 50/4 | | | 50+ |

DEPTH (FEET): 145, 150, 155, 160, 165, 170, 175

NOTES: Weight of the Hammer 140 lbs Drop of the hammer 30" Using Grout hole and casing at 135 feet.

FIELD TEST DATA ARE "BLOWS"/"INCHES DRIVEN". 140-LB HAMMER, 30-INCH FALL. (ASTM D-1586)

Figure 3.3 (continued).

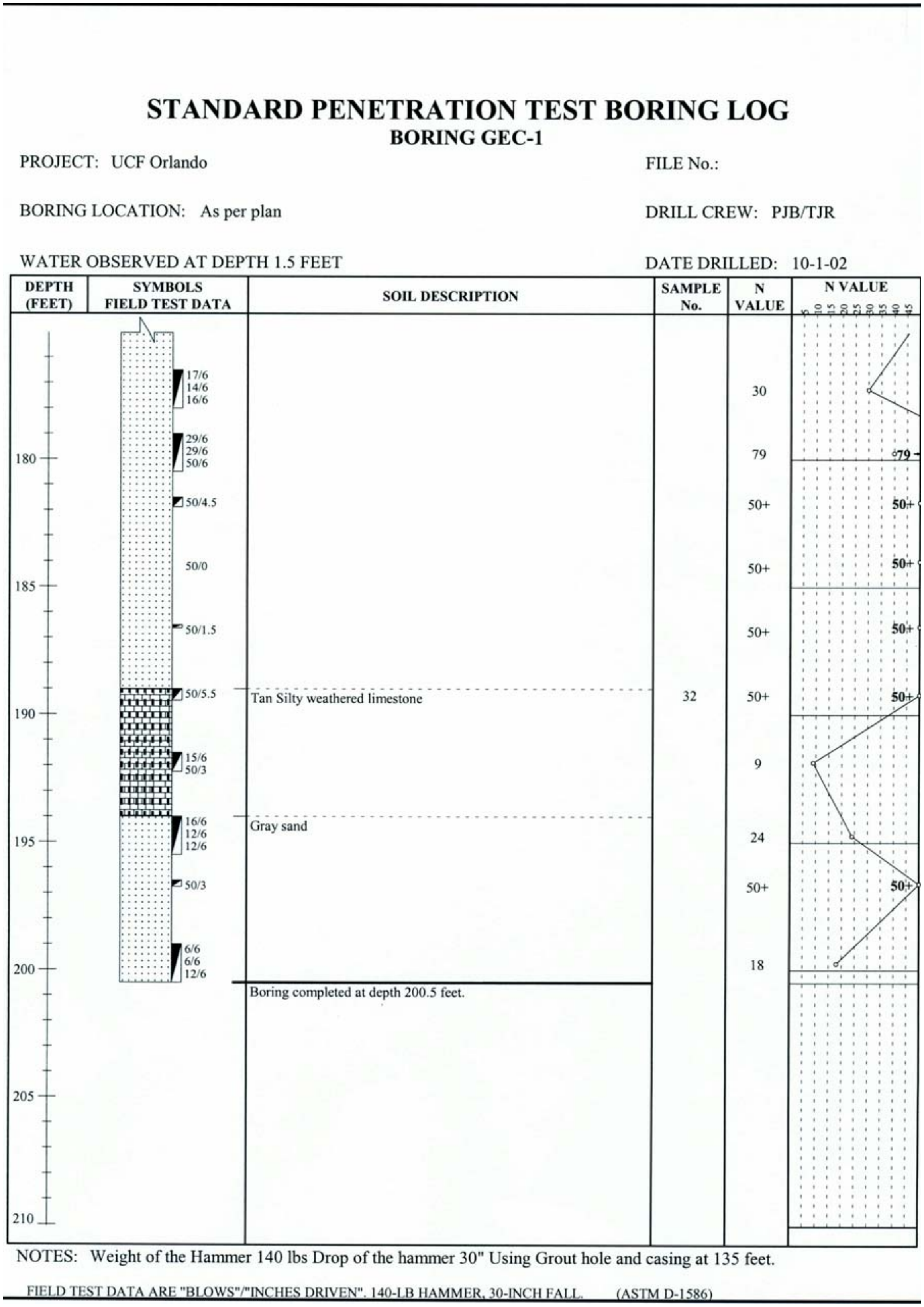


Figure 3.3 (continued).

# STANDARD PENETRATION TEST BORING LOG

## BORING GEC-2

PROJECT: UCF Orlando | FILE No.:

BORING LOCATION: As per plan | DRILL CREW: TJR

WATER OBSERVED AT DEPTH 1.5 FEET | DATE DRILLED: 10-14-02

| FIELD TEST DATA | SOIL DESCRIPTION | SAMPLE No. | N VALUE |
|---|---|---|---|
| 3/6 3/6 5/6 | Loose brown silty fine sand | 1 | 8 |
| 3/6 2/6 2/6 | | 2 | 4 |
| 5/6 5/6 9/6 | Medium dense brown slightly silty fine sand | 3 | 14 |
| 2/6 3/6 4/6 | Brown silty fine sand | 4 | 7 |
| 2/6 2/6 5/6 | | | 7 |
| 3/6 5/6 6/6 | | | 11 |
| 3/6 3/6 2/6 | | | 5 |
| 2/6 2/6 4/6 | Gray silty fine sand | 5 | 6 |
| | Shelby tube from 18 to 19 feet (recovery 0 inch) | | |
| 4/6 5/6 6/6 | loose light gray fine sand | 6 | 11 |
| 4/6 4/6 4/6 | Loose light gray fine sand with silt | 7 | 8 |
| 1/6 1/6 1/6 | | | 1 |
| | Shelby tube from 25.5 to 27.5 feet (recovery 0 inch) | | |
| 0/6 0/6 0/6 | Weight of the hammer | | 0 |
| 1/6 0/6 0/6 | Loose gray silty fine sand | 8 | 0 |
| 2/6 2/6 3/6 | | | 5 |
| 3/6 5/6 | | | 11 |

Depth (feet): 0, 5, 10, 15, 20, 25, 30, 35

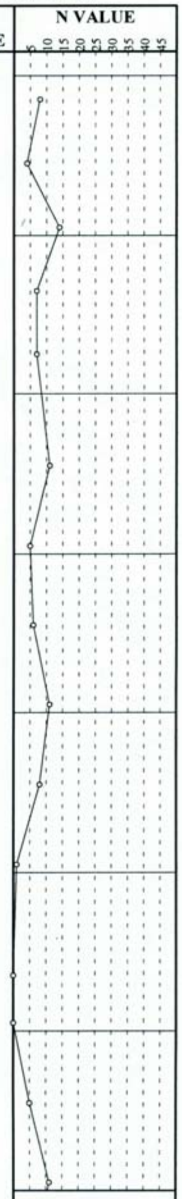


NOTES: Weight of the Hammer 140 lbs Drop of the hammer 30" Grout hole, casing at 80"

**FIELD TEST DATA ARE "BLOWS"/"INCHES DRIVEN" 140-LB HAMMER, 30-INCH FALL. (ASTM D-1586)**

Figure 3.4 GEC Boring 2.

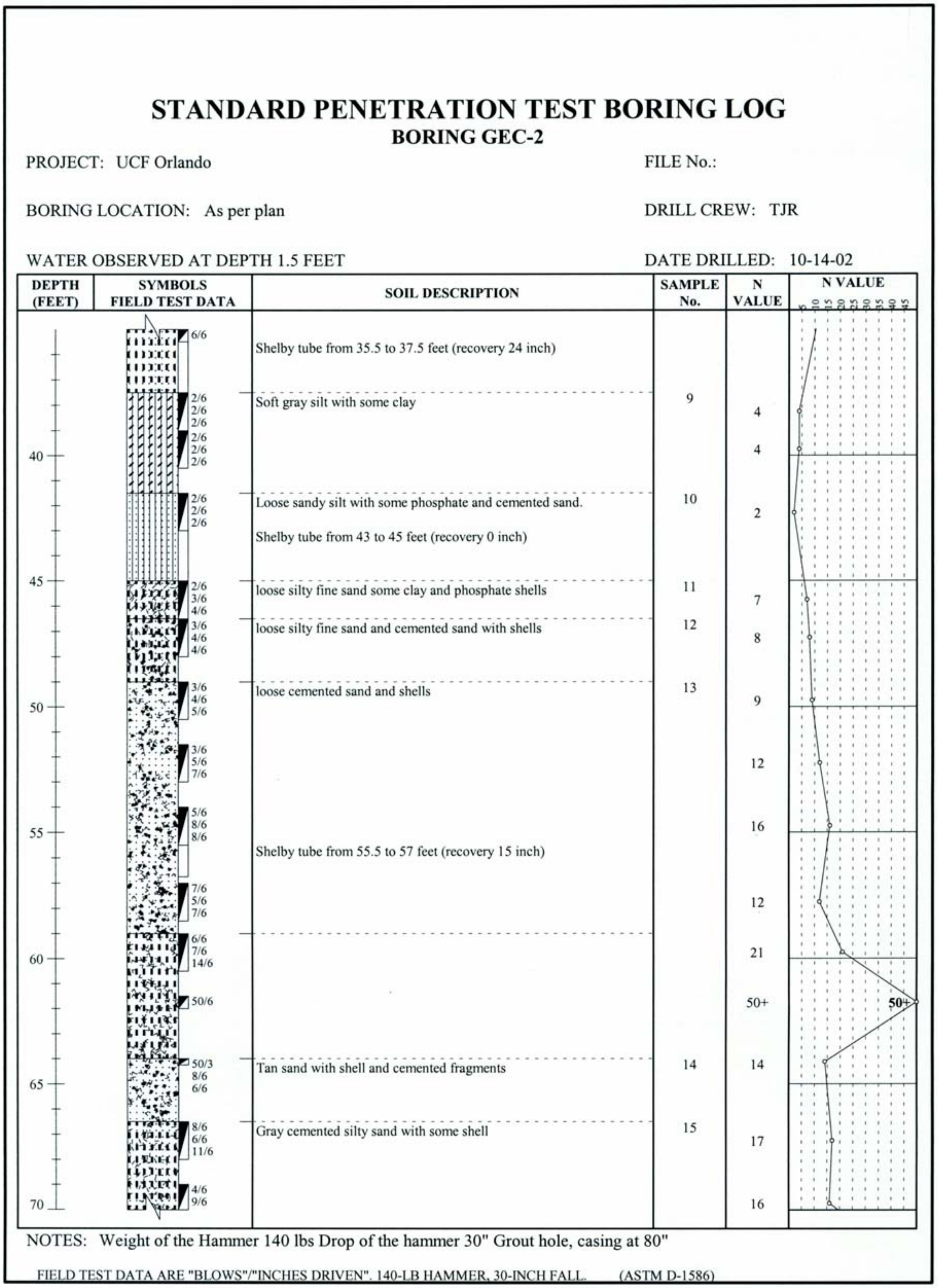

# STANDARD PENETRATION TEST BORING LOG

**BORING GEC-2**

PROJECT: UCF Orlando　　FILE No.:

BORING LOCATION: As per plan　　DRILL CREW: TJR

WATER OBSERVED AT DEPTH 1.5 FEET　　DATE DRILLED: 10-14-02

| DEPTH (FEET) | SYMBOLS FIELD TEST DATA | SOIL DESCRIPTION | SAMPLE No. | N VALUE |
|---|---|---|---|---|
| | 6/6 | Shelby tube from 35.5 to 37.5 feet (recovery 24 inch) | | |
| | 2/6 2/6 2/6 | Soft gray silt with some clay | 9 | 4 |
| 40 | 2/6 2/6 2/6 | | | 4 |
| | 2/6 2/6 2/6 | Loose sandy silt with some phosphate and cemented sand. | 10 | 2 |
| | | Shelby tube from 43 to 45 feet (recovery 0 inch) | | |
| 45 | 2/6 3/6 4/6 | loose silty fine sand some clay and phosphate shells | 11 | 7 |
| | 3/6 4/6 4/6 | loose silty fine sand and cemented sand with shells | 12 | 8 |
| 50 | 3/6 4/6 5/6 | loose cemented sand and shells | 13 | 9 |
| | 3/6 5/6 7/6 | | | 12 |
| 55 | 5/6 8/6 8/6 | | | 16 |
| | | Shelby tube from 55.5 to 57 feet (recovery 15 inch) | | |
| | 7/6 5/6 7/6 | | | 12 |
| 60 | 6/6 7/6 14/6 | | | 21 |
| | 50/6 | | | 50+ |
| 65 | 50/3 8/6 6/6 | Tan sand with shell and cemented fragments | 14 | 14 |
| | 8/6 6/6 11/6 | Gray cemented silty sand with some shell | 15 | 17 |
| 70 | 4/6 9/6 | | | 16 |

N VALUE: 5 10 15 20 25 30 35 40 45; 50+

NOTES: Weight of the Hammer 140 lbs Drop of the hammer 30" Grout hole, casing at 80"

FIELD TEST DATA ARE "BLOWS"/"INCHES DRIVEN". 140-LB HAMMER, 30-INCH FALL. (ASTM D-1586)

Figure 3.4 (continued).

# STANDARD PENETRATION TEST BORING LOG

## BORING GEC-2

PROJECT: UCF Orlando | FILE No.:

BORING LOCATION: As per plan | DRILL CREW: TJR

WATER OBSERVED AT DEPTH 1.5 FEET | DATE DRILLED: 10-14-02

| DEPTH (FEET) | SYMBOLS FIELD TEST DATA | SOIL DESCRIPTION | SAMPLE No. | N VALUE |
|---|---|---|---|---|
| | 10/6 | | | |
| | 19/6, 50/4 | | | 50+ |
| 75 | 9/6, 8/6, 15/6 | | | 23 |
| | 7/6, 8/6, 9/6 | | | 17 |
| 80 | 3/6, 4/6, 5/6 | | | 9 |
| | 4/6, 4/6, 6/6 | Mid dense gray clayey silty fine sand | 16 | 10 |
| 85 | 3/6, 4/6, 6/6 | | | 10 |
| | 32/6, 30/6, 26/6 | Tan calcareous silty weather limestone | 17 | 56 |
| 90 | 5/6, 5/6, 12/6 | Silty fine sand | 18 | 17 |
| | 7/6, 7/6, 7/6 | | | 14 |
| 95 | 9/6, 33/6, 21/6 | | | 54 |
| | 9/6, 3/6, 30/6 | Gray silty cemented sand | 19 | 33 |
| 100 | 20/6, 40/6, 50/3 | Tan calcareous silty weather limestone | 20 | 90 |
| | 50/5 | | | 50+ |
| 105 | 50/3 | | | |

NOTES: Weight of the Hammer 140 lbs Drop of the hammer 30" Grout hole, casing at 80"

FIELD TEST DATA ARE "BLOWS"/"INCHES DRIVEN". 140-LB HAMMER, 30-INCH FALL. (ASTM D-1586)

Figure 3.4 (continued).

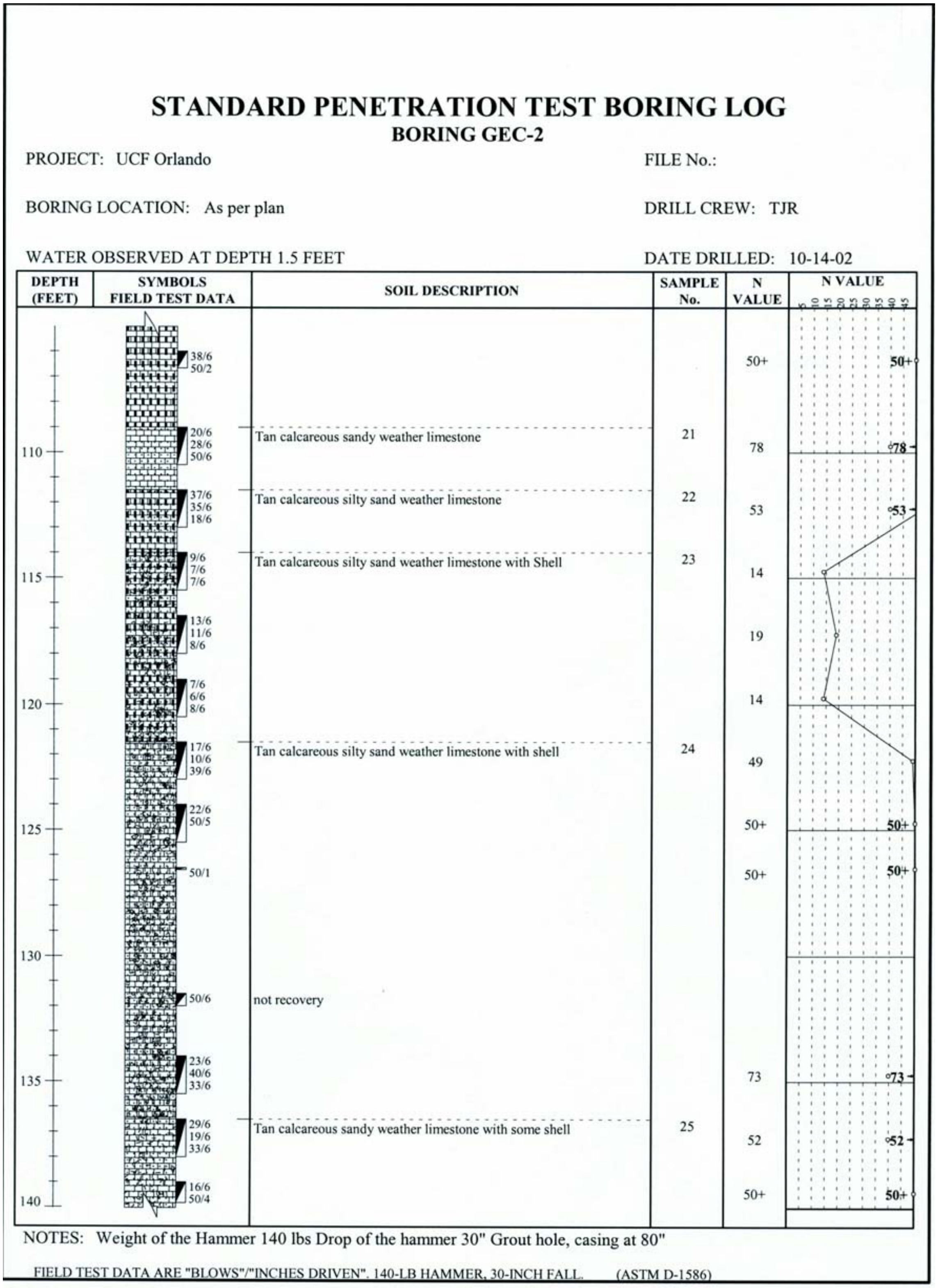


Figure 3.4 (continued).

## STANDARD PENETRATION TEST BORING LOG
### BORING GEC-2

PROJECT: UCF Orlando | FILE No.:

BORING LOCATION: As per plan | DRILL CREW: TJR

WATER OBSERVED AT DEPTH 1.5 FEET | DATE DRILLED: 10-14-02

| DEPTH (FEET) | SYMBOLS FIELD TEST DATA | SOIL DESCRIPTION | SAMPLE No. | N VALUE |
|---|---|---|---|---|
| | 50/3 | | | 50+ |
| 145 | 11/6 28/6 50/4 | | | 78 |
| | 50/5.5 | | | 50+ |
| 150 | 10/6 12/6 13/6 | Tan calcareous sandy weather limestone with some shell | 26 | 25 |
| | 25/6 9/6 10/6 | | | 19 |
| 155 | 11/6 6/6 9/6 | | | 15 |
| | 7/6 8/6 7/6 | | | 15 |
| 160 | 13/6 12/6 15/6 | | | 27 |
| | 14/6 15/6 20/6 | | | 35 |
| 165 | 11/6 9/6 11/6 | | | 20 |
| | 8/6 6/6 6/6 | | | 12 |
| 170 | 5/6 13/6 18/6 | | | 31 |
| | 11/6 10/6 11/6 | | | 21 |
| 175 | 12/6 11/6 | | | 61 |

NOTES: Weight of the Hammer 140 lbs Drop of the hammer 30" Grout hole, casing at 80"

FIELD TEST DATA ARE "BLOWS"/"INCHES DRIVEN". 140-LB HAMMER, 30-INCH FALL. (ASTM D-1586)

Figure 3.4 (continued).

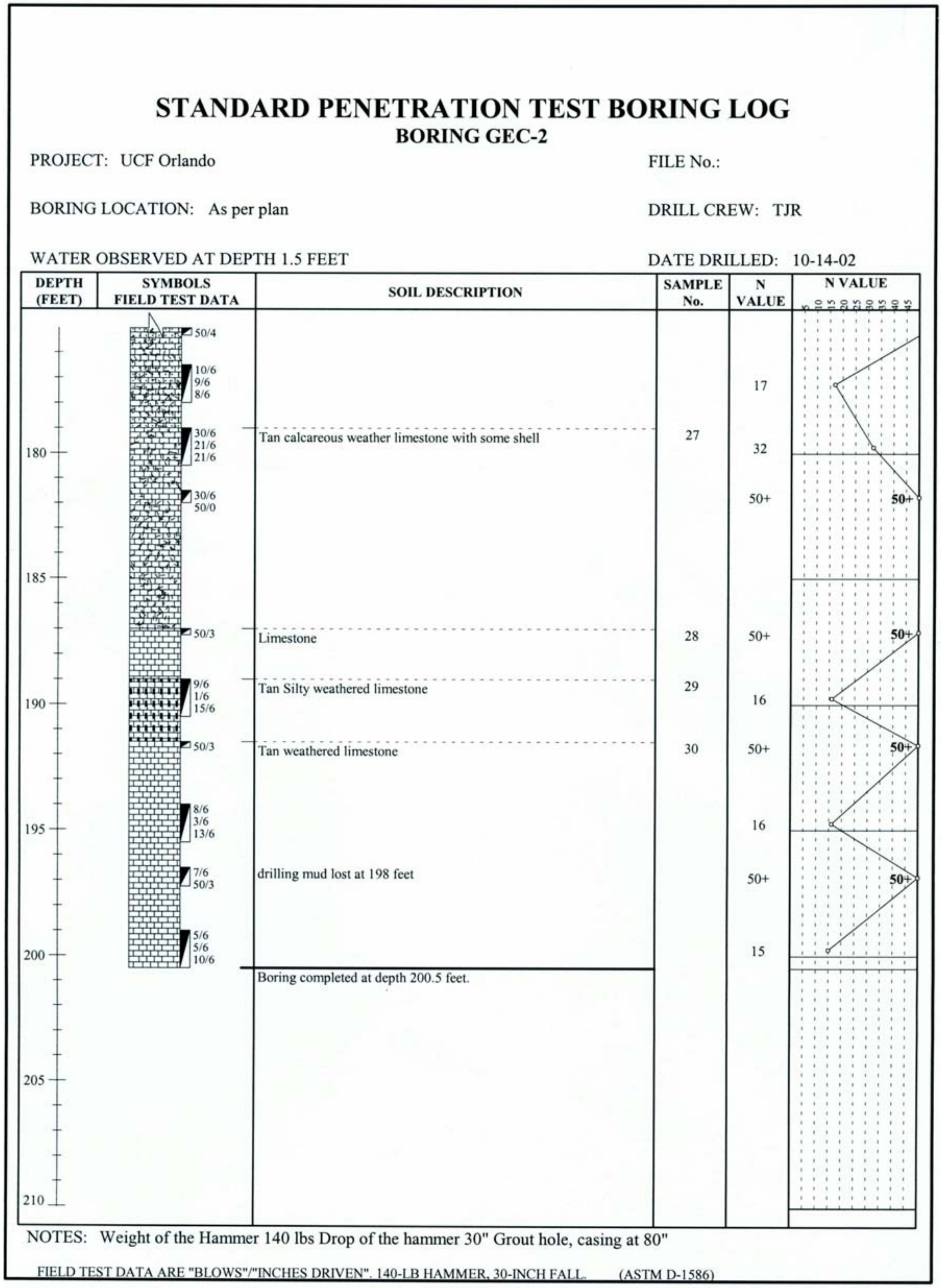
**STANDARD PENETRATION TEST BORING LOG**

**BORING GEC-2**

PROJECT: UCF Orlando — FILE No.:

BORING LOCATION: As per plan — DRILL CREW: TJR

WATER OBSERVED AT DEPTH 1.5 FEET — DATE DRILLED: 10-14-02

| DEPTH (FEET) | SYMBOLS FIELD TEST DATA | SOIL DESCRIPTION | SAMPLE No. | N VALUE |
|---|---|---|---|---|
| | 50/4 | | | |
| | 10/6 9/6 8/6 | | | 17 |
| 180 | 30/6 21/6 21/6 | Tan calcareous weather limestone with some shell | 27 | 32 |
| | 30/6 50/0 | | | 50+ |
| 185 | | | | |
| | 50/3 | Limestone | 28 | 50+ |
| 190 | 9/6 1/6 15/6 | Tan Silty weathered limestone | 29 | 16 |
| | 50/3 | Tan weathered limestone | 30 | 50+ |
| 195 | 8/6 3/6 13/6 | | | 16 |
| | 7/6 50/3 | drilling mud lost at 198 feet | | 50+ |
| 200 | 5/6 5/6 10/6 | | | 15 |
| | | Boring completed at depth 200.5 feet. | | |
| 205 | | | | |
| 210 | | | | |

NOTES: Weight of the Hammer 140 lbs Drop of the hammer 30" Grout hole, casing at 80"

FIELD TEST DATA ARE "BLOWS"/"INCHES DRIVEN". 140-LB HAMMER, 30-INCH FALL. (ASTM D-1586)

Figure 3.4 (continued).

Table 3.2 Energy BH-1.

| Drill | For Observed Drop | | SPT |
|---|---|---|---|
| String | Drop (in) | $ER_{FV}$ (%) | Blow Count |
| Length | (est.) | | N |
| 29.0 | 31.0 | **70.6** | 13 |
| 54.0 | 31.0 | **80.0** | 5 |
| 79.0 | 31.0 | **67.8** | 36 |

In order to test the five UF "cohesionless" soils, they were frozen inside the Shelby tube in order to solidified them. The tubes were then cut using a band-saw, and refrozen for ½ hour. The tube was then placed in a sample extruder, and the frozen tube slightly thawed using a blow-torch to break the bond between the frozen soil and tube. The frozen soil was then quickly extruded, trimmed, placed inside a rubber membrane, and onto the triaxial chamber pedestal. Suction (vacuum) was then applied to give the sample sufficient strength to stand while the dimensions were measured and the cell assembled. The samples were then back-pressured saturated, consolidated to the appropriate effective overburden stress, and sheared.

Table 3.7 (file: FDOT Test-2.xls) summarizes the triaxial test results, while Table 3.8 presents the testing details for the UF and FDOT-SMO tests, respectively. The data reduction approach by the University of Florida Lab assumes all the shear resistance developed in the sample is due to internal friction and does not consider cohesion; i.e., a c = 0 condition. Consequently, this assumption for the cohesionless soils tests results in higher values of friction angle, $\phi$. Conversely, the FDOT-SMO multiple confining pressures produced $\phi$-c results, or a lower $\phi$ value. Nevertheless, the results reflect friction angles near 40°, which are typical for sands, and cohesion values of $1000^{+}$ psf, which are reflective of a stiff clay.

## LABORATORY TESTS – 1-D CONSOLIDATION

FDOT-SMO performed seven 1-D consolidation tests, 3 from Borehole #1 and 4 from Borehole #2. The tests at 6 – 8 ft depths represent tests in the "hardpan." Table 3.9 summarizes the results of these consolidation tests, while Figures 3.5 to 3.11 present the e-log P' curves.

## FLEXIBLE WALL PERMEABILITY TESTS

FDOT-SMO performed 4 flexible wall permeability tests, 2 samples each from Boreholes #1 and #2. For comparison, Table 3.10 and Figure 3.12 compare these with the permeability results from consolidation tests. Except for those permeability tests in the hardpan (depth = 6-8 ft), the triaxial flex wall permeability values are in approximate agreement with those from the oedometer test. The permeability values are typically in the range of E-06 to E-07 cm/sec, which reflects the silty sands of the site.

# Table 3.3 Classification of GEC-1. (file:updated classification.xls)

AMDRILL SAMPLES
11/1/2002

| Boring No. | Sample No. | Depth (ft) | moisture content (%) | organic content (%) | AASHTO class. | Unified class. | passing 1/2" | passing 3/8" | passing #4 | passing #10 | passing #40 | passing #60 | passing #100 | passing #200 | % clay | % silt | % sand | LL/PI (%) |
|---|---|---|---|---|---|---|---|---|---|---|---|---|---|---|---|---|---|---|
| 1 | 1 | 0-2 | 16.1 | | A-3 | SP | | | | 100 | 98 | 87 | 33 | 2 | | | | |
| | 2 | 4-6 | 20.3 | 3.5 | A-2-4 | SM | | | | 100 | 97 | 86 | 43 | 16 | | | | |
| | 3 | 8-10 | 20.0 | | A-2-4 | SM | | | | 100 | 96 | 83 | 41 | 23 | | | | |
| | 4 | 11.5-13 | 26.8 | | A-3 | SP-SM | | | | | 100 | 93 | 62 | 7 | | | | |
| | 5 | 14-15.5 | 26.8 | | A-2-4 | SM | | | | 100 | 98 | 97 | 84 | 17 | | | | |
| | 6 | 16.5-18 | 26.6 | | A-3 | SP-SM | | | | | | 100 | 91 | 9 | | | | |
| | 7 | 19-20.5 | 25.7 | | A-2-4 | SM | | | | | | 100 | 96 | 19 | | | | |
| | 8 | 21.5-23 | 26.8 | | A-2-4 | SM | | | | 100 | 99 | 98 | 95 | 34 | 22 | 12 | 66 | 24 / 2 |
| | 9 | 24-25.5 | 24.4 | | A-3 | SP-SM | | | | 100 | 99 | 94 | 46 | 7 | | | | |
| | 10 | 27-28.5 | 26.9 | | A-2-4 | SP-SM | | | | | 100 | 99 | 80 | 11 | | | | |
| | 11 | 29-30.5 | 28.9 | | A-2-4 | SM | | | | | 100 | 99 | 83 | 25 | | | | |
| | 12 | 31.5-33 | 28.4 | | A-2-4 | SM | | | | | 100 | 99 | 97 | 25 | 13 | 13 | 74 | |
| | 13 | 34-35.5 | 31.2 | | A-4 | SC-SM | | | | | 100 | 98 | 90 | 43 | 20 | 23 | 57 | 28 / 6 |
| | 14 | 37.5-39 | 31.0 | | A-3 | SP-SM | | | | | 100 | 97 | 90 | 10 | | | | |
| | 15 | 39-40.5 | 24.9 | | A-4 | SC-SM | | | 100 | 99 | 86 | 79 | 63 | 39 | 12 | 27 | 61 | 20 / 5 |
| | 16 | 41.5-43 | 24.7 | | A-4 | SC-SM | | 100 | 99 | 95 | 83 | 78 | 60 | 45 | 23 | 22 | 55 | 21 / 6 |
| | 17 | 44-45.5 | 30.3 | | A-4 | SM | | | | 100 | 99 | 95 | 79 | 38 | 22 | 16 | 62 | NP |
| | 18 | 47.5-49 | 42.8 | | A-6 | SC | | | | 100 | 93 | 90 | 86 | 44 | | | | 34 / 15 |
| | 19 | 49-50.5 | 35.1 | | A-4 | (SC) w/ gravel | 96 | 93 | 85 | 84 | 78 | 76 | 73 | 45 | 17 | 28 | 55 | 28 / 10 |
| | 20 | 51.5-53 | 46.8 | | A-7-6 | sandy (CL) | 100 | 99 | 99 | 95 | 88 | 84 | 79 | 67 | 28 | 39 | 33 | 42 / 20 |
| | 21 | 54-55.5 | 19.6 | | A-1-b | SW-SM | 97 | 93 | 91 | 81 | 48 | 33 | 17 | 8 | | | | |
| | 22 | 56.5-58 | 25.6 | | A-1-a | (SW) w/ gravel | 95 | 92 | 77 | 50 | 23 | 15 | 9 | 3 | | | | |
| | 23 | 59-60.5 | 12.9 | | A-1-a | (SW-SM) w/ gravel | 78 | 75 | 59 | 37 | 20 | 15 | 10 | 5 | | | | |
| | 24 | 61.5-63 | 16.5 | | A-1-a | (SW) w/ gravel | 85 | 84 | 76 | 42 | 23 | 14 | 8 | 4 | | | | |
| | 25 | 64-65.5 | 17.5 | | A-1-b | (SW-SM) w/ gravel | 88 | 80 | 64 | 54 | 27 | 16 | 12 | 7 | | | | |
| | 26 | 66.5-68 | 28.9 | | A-1-a | (SW-SM) w/ gravel | 87 | 80 | 60 | 42 | 24 | 19 | 14 | 7 | | | | |
| | 27 | 69-70.5 | 46.2 | | A-1-b | SM | | 100 | 98 | 83 | 38 | 29 | 24 | 14 | | | | |
| | 28 | 71.5-73 | 28.9 | | A-1-b | (SW-SM) w/ gravel | 93 | 81 | 65 | 53 | 29 | 25 | 21 | 12 | | | | |
| | 29 | 74-75.5 | 48.1 | | A-1-b | SW-SM | | 100 | 88 | 73 | 33 | 26 | 20 | 11 | | | | 54 / 20 |
| | 30 | 76.5-78 | 27.2 | | A-4 | SM | | | 98 | 86 | 60 | 57 | 54 | 43 | | | | |
| | 31 | 79-80.5 | 33.8 | | A-4 | SM | | | 100 | 95 | 66 | 61 | 58 | 45 | | | | |
| | 32 | 81.5-83 | 34.4 | | A-1-b | SM | | | 99 | 95 | 48 | 35 | 31 | 22 | | | | |
| | 33 | 84-85.5 | 24.7 | | A-4 | SM | | | 100 | 98 | 72 | 56 | 52 | 38 | | | | |
| | 34 | 86.5-88 | 26.8 | | A-2-4 | SM | | | 100 | 98 | 67 | 49 | 44 | 30 | | | | |
| | 35 | 96.5-98 | 32.8 | | A-7-5 | SC | | | | 100 | 87 | 53 | 46 | 40 | 18 | 22 | 60 | 45 / 25 |
| | 36 | 99-100.5 | 22.8 | | A-1-b | (SM) w/ gravel | 91 | 85 | 66 | 55 | 39 | 34 | 29 | 24 | | | | |
| | 37 | 106.5-108 | 27.6 | | A-4 | sandy (ML) | 96 | 96 | 96 | 96 | 92 | 90 | 88 | 70 | | | | |
| | 38 | 109-110.5 | 23.3 | | A-4 | ML | | | | 100 | 98 | 98 | 97 | 76 | 10 | 66 | 24 | |
| | 39 | 111.5-113 | 26.4 | | A-1-b | SM | | 100 | 97 | 89 | 48 | 36 | 28 | 21 | | | | |
| | 40 | 114-115.5 | 27.7 | | A-1-b | SM | 93 | 89 | 89 | 77 | 44 | 33 | 26 | 19 | | | | |
| | 41 | 116.5-118 | 22.1 | | A-1-b | (SM) w/ gravel | 86 | 82 | 73 | 64 | 36 | 27 | 20 | 14 | | | | |
| | 42 | 119-120.5 | 22.1 | | A-1-b | (SM) w/ gravel | 73 | 68 | 66 | 62 | 38 | 28 | 20 | 14 | | | | |

Table 3.3 (continued).

| Boring No. | Sample No. | Depth (ft) | moisture content (%) | organic content (%) | AASHTO class. | Unified class. | passing 1/2" | passing 3/8" | passing #4 | passing #10 | passing #40 | passing #60 | passing #100 | passing #200 | % clay | % silt | % sand | LL/PI (%) |
|---|---|---|---|---|---|---|---|---|---|---|---|---|---|---|---|---|---|---|
| 1 | 43 | 121.5-123 | N/A | | A-1-b | SM | | 100 | 87 | 69 | 43 | 31 | 23 | 15 | | | | |
| | 44 | 124-125.5 | 19.7 | | A-1-b | (SM) w/ gravel | 88 | 86 | 84 | 78 | 45 | 31 | 22 | 14 | | | | |
| | 46 | 134-135.5 | 16.4 | | A-1-a | (SW-SM) w/ gravel | 80 | 70 | 54 | 43 | 23 | 16 | 10 | 5 | | | | |
| | 47 | 136.5-138 | 17.5 | | A-2-4 | SP-SM | 100 | 97 | 96 | 92 | 55 | 36 | 22 | 11 | | | | |
| | 48 | 139-140.5 | | | A-1-b | (SW-SM) w/ gravel | 81 | 77 | 73 | 69 | 43 | 28 | 17 | 8 | | | | |
| | 49 | 141.5-143 | 21.0 | | | | | | | | | | | | | | | |
| | 50 | 144-145.5 | 20.6 | | A-2-4 | SP-SM | | | 98 | 97 | 75 | 54 | 27 | 12 | | | | |
| | 51 | 146.5-148 | N/A | | A-1-b | (SW-SM) w/ gravel | 94 | 92 | 80 | 70 | 44 | 28 | 16 | 7 | | | | |
| | 52 | 152-153.5 | 27.6 | | A-2-4 | SM | | | 100 | 99 | 88 | 69 | 31 | 14 | | | | |
| | 53 | 154-155.5 | 29.3 | | A-2-4 | SP-SM | | | 100 | 99 | 86 | 66 | 38 | 11 | | | | |
| | 54 | 156.5-158 | 32.6 | | A-2-4 | SM | 99 | 98 | 98 | 97 | 76 | 56 | 36 | 23 | | | | |
| | 55 | 159-160.5 | | | A-2-4 | SM | | 100 | 99 | 99 | 78 | 57 | 28 | 13 | | | | |
| | 56 | 161.5-163 | 30.7 | | | | | | | | | | | | | | | |
| | 57 | 164-165.5 | 25.5 | | A-2-4 | SM | 98 | 98 | 97 | 95 | 76 | 55 | 28 | 15 | | | | |
| | 58 | 166.5-168 | 30.3 | | A-2-4 | SM | | | 100 | 98 | 78 | 59 | 30 | 13 | | | | |
| | 59 | 169-170.5 | 19.6 | | A-1-b | (SW-SM) w/ gravel | 85 | 79 | 68 | 62 | 40 | 25 | 15 | 8 | | | | |
| | 60 | 171.5-173 | | | A-2-4 | SP-SM | | 100 | 97 | 89 | 69 | 48 | 26 | 12 | | | | |
| | 61 | 174-175.5 | 23.7 | | | | | | | | | | | | | | | |
| | 62 | 176.5-178 | 16.8 | | A-2-4 | SM | | | 100 | 93 | 77 | 56 | 29 | 15 | | | | |
| | 63 | 179-180.5 | | | A-1-b | (SW-SM) w/ gravel | 100 | 95 | 81 | 70 | 45 | 29 | 17 | 9 | | | | |
| | 64 | 181.5-183 | 23.9 | | | | | | | | | | | | | | | |
| | 65 | 189-190.5 | | | A-1-b | SM | 100 | 99 | 91 | 83 | 48 | 34 | 24 | 16 | | | | |
| | 66 | 191.5-193 | 35.5 | | | | | | | | | | | | | | | |
| | 67 | 194-195.5 | 30.1 | | A-4 | ML | | | | 100 | 93 | 90 | 86 | 79 | 17 | 62 | 21 | NP |
| | 68 | 196.5-198 | N/A | | A-1-b | (SW) w/ gravel | 100 | 95 | 79 | 71 | 22 | 14 | 9 | 4 | | | | |
| | 69 | 199-200.5 | 27.9 | | A-5 | SC-SM | 98 | 98 | 96 | 94 | 74 | 67 | 59 | 49 | 24 | 25 | 51 | 24 / 7 |

Table 3.4 Classification of GEC-2. (file:updated classification.xls)

| Boring No. | Sample No. | Depth (ft) | moisture content (%) | organic content (%) | AASHTO class. | Unified class. | passing 1/2" | passing 3/8" | passing #4 | passing #10 | passing #40 | passing #60 | passing #100 | passing #200 | % clay | % silt | % sand | LL/PI (%) |
|---|---|---|---|---|---|---|---|---|---|---|---|---|---|---|---|---|---|---|
| 2 | 1 | 0-2 | 15.4 | 1.66 | A-3 | SP-SM | | | | 100 | 98 | 87 | 33 | 6 | | | | |
| | 2 | 2-4 | 20.0 | | A-2-4 | SM | | | | 100 | 67 | 57 | 43 | 32 | | | | |
| | 3 | 4-6 | 22.3 | 3.19 | | | no sample | | | | | | | | | | | |
| | 4 | 6-8 | 23.4 | | A-2-4 | SM | | | | | 100 | 99 | 85 | 18 | | | | |
| | 5 | 8-10 | 25.1 | | A-2-4 | SM | | | | | 100 | 99 | 84 | 17 | | | | NP |
| | 6 | 11.5-13 | 26.4 | | A-2-4 | SM | | | | 100 | 99 | 98 | 92 | 19 | | | | NP |
| | 7 | 14-15.5 | 23.6 | | | | no sample | | | | | | | | | | | |
| | 8 | 16.5-18 | 25.7 | | A-2-4 | SM | | | | | 98 | 95 | 81 | 28 | 12 | 16 | 72 | 24 / 5 |
| | 9 | 19-20.5 | 24.3 | | A-3 | SP-SM | | | | 100 | 98 | 92 | 49 | 7 | | | | |
| | 10 | 21.5-23 | 26.7 | | A-2-4 | SP-SM | | | | 100 | 99 | 98 | 78 | 12 | | | | |
| | 11 | 24-25.5 | 31.5 | | A-2-4 | SM | | | | | | 100 | 93 | 17 | | | | NP |
| | 12 | 27.5-29 | 36.5 | | A-4 | SM | | | | | 100 | 99 | 97 | 38 | | | | NP |
| | 13 | 29-30.5 | N/A | | A-2-4 | SC-SM | | | | 100 | 99 | 98 | 88 | 33 | | | | 26 / 5 |
| | 14 | 31.5-33 | 44.8 | | A-2-6 | SC | | | | 100 | 58 | 53 | 50 | 32 | 18 | 14 | 68 | 38 / 15 |
| | 15 | 34-35.5 | 31.5 | | A-6 | sandy (CL) | 96 | 94 | 91 | 79 | 78 | 78 | 77 | 70 | 8 | 62 | 30 | 32 / 11 |
| | 16 | 37.5-39 | 66.8 | | | | 100 | 99 | 97 | 94 | 87 | 57 | 45 | 38 | | | | |
| | 17 | 39-40.5 | 57.9 | | A-7-6 | (MH) w/sand | | | 100 | 97 | 97 | 97 | 94 | 78 | 20 | 58 | 22 | 51 / 19 |
| | 18 | 41.5-43 | 55.9 | | A-7-5 | sandy (CL) | | | | | | 100 | 96 | 65 | 18 | 47 | 35 | 43 / 18 |
| | 19 | 45-46.5 | 27.7 | | | | 100 | 96 | 79 | 71 | 47 | 38 | 24 | 10 | | | | |
| | 20 | 46.5-48 | 33.0 | | A-4 | SC-SM | | | | 100 | 99 | 98 | 96 | 42 | 12 | 20 | 68 | 24 / 5 |
| | 21 | 49-50.5 | 34.4 | | A-4 | SC | | | 100 | 99 | 93 | 90 | 86 | 49 | 10 | 39 | 51 | 28 / 8 |
| | 22 | 51.5-53 | 24.5 | | A-3 | SP-SM | | | 100 | 99 | 67 | 44 | 19 | 9 | | | | |
| | 23 | 54-55.5 | 17.5 | | A-3 | SP | 97 | 96 | 86 | 75 | 73 | 65 | 21 | 3 | | | | |
| | 24 | 57-58.5 | 22.0 | | A-1-b | (SW-SM) w/ gravel | 86 | 86 | 72 | 63 | 35 | 25 | 15 | 6 | | | | |
| | 25 | 59-60.5 | N/A | | | | | | | | | | | | | | | |
| | 26 | 61.5-63 | N/A | | A-1-b | (SW-SM) w/ gravel | 82 | 77 | 64 | 53 | 33 | 23 | 14 | 8 | | | | |
| | 27 | 64-65.5 | no sample | | | | | | | | | | | | | | | |
| | 28 | 66.5-68 | 36.8 | | A-1-b | SC | 100 | 97 | 86 | 71 | 40 | 31 | 24 | 14 | | | | 32 / 25 |
| | 29 | 69-70.5 | 43.1 | | A-7-5 | sandy (MH) | | | 100 | 97 | 84 | 81 | 78 | 64 | | | | 52 / 20 |
| | 30 | 71.5-73 | 31.1 | | A-1-b | (SM) w/ gravel | 88 | 85 | 75 | 68 | 40 | 34 | 30 | 19 | | | | |
| | 31 | 74-75.5 | 41.0 | | A-1-b | SM | 98 | 98 | 94 | 78 | 33 | 28 | 23 | 13 | | | | 46 / 14 |
| | 32 | 76.5-78 | 36.4 | | A-5 | sandy (ML) | 100 | 99 | 99 | 94 | 76 | 73 | 70 | 54 | | | | 44 / 10 |
| | 33 | 79-80.5 | 37.7 | | A-7-5 | SM | | | 100 | 97 | 71 | 67 | 64 | 48 | | | | 46 / 12 |
| | 34 | 81.5-83 | 38.9 | | A-2-7 | SC | | | 100 | 97 | 58 | 50 | 47 | 33 | 12 | 21 | 67 | 72 / 40 |
| | 35 | 84-85.5 | 33.5 | | A-1-b | SM | | 100 | 99 | 92 | 42 | 30 | 25 | 17 | 7 | 10 | 83 | 54 / 8 |
| | 36 | 86.5-88 | 23.5 | | A-4 | SM | | | 100 | 96 | 77 | 59 | 55 | 41 | | | | |
| | 37 | 89-90.5 | 29.7 | | A-2-6 | SC | | | 100 | 98 | 71 | 47 | 40 | 28 | 7 | 21 | 72 | 38 / 14 |
| | 38 | 91.5-93 | 31.6 | | A-2-7 | SC | | | 100 | 94 | 71 | 45 | 36 | 32 | 10 | 22 | 68 | 45 / 19 |
| | 39 | 94-95.5 | 25.7 | | A-2-4 | (SM) w/ gravel | 89 | 85 | 76 | 69 | 60 | 41 | 36 | 31 | 12 | 19 | 69 | 33 / 8 |

Table 3.4 (continued).

| Boring No. | Sample No. | Depth (ft) | moisture content (%) | organic content (%) | AASHTO class. | Unified class. | passing 1/2" | passing 3/8" | passing #4 | passing #10 | passing #40 | passing #60 | passing #100 | passing #200 | % clay | % silt | % sand | LL/PI (%) |
|---|---|---|---|---|---|---|---|---|---|---|---|---|---|---|---|---|---|---|
| 2 | 41 | 99-100.5 | 43.6 | | A-2-7 | SM | | | 100 | 99 | 70 | 45 | 36 | 33 | 4 | 29 | 67 | 58 / 26 |
| | 42 | 101.5-103 | N/A | | A-1-b | (SW-SM) w/ gravel | 92 | 82 | 70 | 62 | 32 | 21 | 15 | 9 | 14 | 38 | 48 | |
| | 43 | 104-105.5 | | | | | | | | | | | | | | | | |
| | 44 | 106.5-108 | 26.8 | | A-4 | sandy (ML) | 100 | 96 | 89 | 73 | 65 | 62 | 59 | 52 | 14 | 38 | 48 | |
| | 45 | 109-110.5 | 22.1 | | A-4 | sandy (ML) | | | | 100 | 90 | 86 | 81 | 64 | | | | |
| | 46 | 111.5-113 | 25.7 | | A-2-4 | SM | | | 100 | 99 | 67 | 53 | 43 | 35 | | | | |
| | 47 | 114-115.5 | 21.9 | | A-1-b | SM | | 100 | 97 | 80 | 42 | 31 | 23 | 16 | | | | |
| | 48 | 116.5-118 | 25.2 | | A-1-b | SM | | 100 | 92 | 76 | 45 | 32 | 24 | 17 | | | | |
| | 49 | 119-120.5 | 29.0 | | A-2-4 | SM | | 100 | 96 | 88 | 57 | 42 | 31 | 22 | | | | |
| | 50 | 121.5-123 | 16.8 | | A-1-b | SM | 93 | 93 | 89 | 81 | 47 | 34 | 24 | 16 | | | | |
| | 51 | 124-125.5 | | | | | | | | | | | | | | | | |
| | 52 | 131.5-133 | 20.2 | | A-1-b | (SW-SM) w/ gravel | 89 | 84 | 76 | 62 | 38 | 26 | 19 | 12 | | | | |
| | 53 | 134-135.5 | 19.9 | | A-2-4 | SM | 96 | 93 | 93 | 90 | 70 | 53 | 29 | 15 | | | | |
| | 54 | 136.5-138 | 20.2 | | A-2-4 | SW-SM | 97 | 96 | 89 | 84 | 55 | 39 | 23 | 12 | | | | |
| | 55 | 139-140.5 | 20.6 | | A-3 | SP-SM | 97 | 97 | 94 | 88 | 59 | 38 | 23 | 10 | | | | |
| | 56 | 144-145.5 | 23.5 | | A-1-a | SP-SM | 90 | 82 | 56 | 41 | 21 | 11 | 8 | 5 | | | | |
| | 57 | 149-150.5 | 25.2 | | A-2-4 | SP-SM | 95 | 94 | 93 | 91 | 71 | 47 | 26 | 12 | | | | |
| | 58 | 151.5-153 | 25.7 | | A-2-4 | SM | | | | 89 | 78 | 65 | 41 | 23 | | | | |
| | 59 | 154-155.5 | 34.4 | | A-2-4 | SM | | | | 100 | 91 | 74 | 50 | 28 | 8 | 20 | 72 | NP |
| | 60 | 156.5-158 | 33.4 | | A-2-4 | SM | | | 100 | 99 | 86 | 64 | 43 | 26 | | | | |
| | 61 | 159-160.5 | 28.3 | | A-2-4 | SM | | | | 100 | 89 | 72 | 49 | 29 | 8 | 19 | 71 | NP |
| | 62 | 161.5-163 | 19.4 | | A-2-4 | SM | 93 | 93 | 93 | 93 | 73 | 60 | 42 | 29 | | | | |
| | 63 | 164-165.5 | 26.4 | | A-2-4 | SM | | | 100 | 99 | 79 | 62 | 39 | 27 | | | | |
| | 64 | 169-170.5 | 30.9 | | A-2-4 | SM | | | | 100 | 83 | 65 | 44 | 28 | 6 | 22 | 72 | NP |
| | 65 | 171.5-173 | 23.8 | | A-2-4 | SM | | 100 | 99 | 98 | 78 | 60 | 38 | 26 | | | | |
| | 66 | 174-175.5 | 25.4 | | A-2-4 | SM | | | | 100 | 86 | 71 | 45 | 29 | 6 | 23 | 71 | NP |
| | 67 | 176.5-178 | 27.5 | | A-2-4 | SM | | | 100 | 99 | 83 | 68 | 42 | 26 | | | | |
| | 68 | 179-180.5 | 17.9 | | A-2-4 | SM | | | 100 | 98 | 62 | 42 | 24 | 14 | | | | |
| | 69 | 181.5-183 | N/A | | A-1-b | SW-SM | 95 | 92 | 91 | 89 | 49 | 31 | 18 | 9 | | | | |
| | 70 | 187-188.5 | no sample | | | | | | | | | | | | | | | |
| | 71 | 189-190.5 | 28.1 | | A-4 | sandy (ML) | | | | 100 | 91 | 85 | 78 | 69 | 13 | 56 | 31 | NP |
| | 72 | 191.5-193 | N/A | | A-1-b | SM | | 100 | 95 | 94 | 47 | 35 | 25 | 17 | | | | |
| | 73 | 194-195.5 | 29.5 | | A-4 | (ML) w/ sand | | | | 100 | 90 | 86 | 83 | 77 | 16 | 61 | 23 | NP |
| | 74 | 196.5-198 | 27.2 | | A-4 | (ML) w/ sand | | | | 100 | 87 | 83 | 78 | 72 | 22 | 50 | 28 | NP |
| | 75 | 199-200.5 | 27.5 | | A-2-4 | SM | | | | 100 | 56 | 41 | 28 | 13 | | | | |

# Table 3.5 U/C tests rock cores GEC –1.

PROJECT NO. 17946 (UCF DEEP FOUNDATION STUDY - AMDRILL SAMPLES)
ROCK CORE TESTING RESULTS

| BORING / CORE | SAMP. NO. | DEPTH TOP (ft) | DEPTH BOT. (ft) | MAX. LOAD (lbs) | LENGTH (in) | DIA. (in) | WET WT. (g) | WET UNIT WT (pcf) | L / D RATIO | CORR. FACTOR |
|---|---|---|---|---|---|---|---|---|---|---|
| **BORING ONE** | | | | | | | | | | |
| (50/0") | | | | | | | | | | |
| 1/1 | | 89.5' | 94.5' | | | | | | | |
| (50/2.5") | | | | | | | | | | |
| (50/1") | | | | | | | | | | |
| 1/2 | 1U | 101.5' | | 9220 | 3.539 | 2.394 | 613.8 | 146.8 | 1.48 | 1.0424 |
| | 2T | | | 2496 | 1.942 | 2.385 | 326.4 | 143.3 | 0.81 | |
| | 3U | | | 5709 | 3.201 | 2.394 | 547.9 | 144.9 | 1.34 | 1.0595 |
| | 4T | | | 2041 | 2.158 | 2.379 | 336.8 | 133.8 | 0.91 | |
| | 5U | | | 2423 | 3.602 | 2.398 | 626.3 | 146.7 | 1.50 | 1.0397 |
| | 6T | | | 3024 | 1.903 | 2.339 | 329.4 | 153.5 | 0.81 | |
| | 7U | | | 7506 | 3.515 | 2.384 | 626.7 | 152.2 | 1.47 | 1.0428 |
| | 8T | | 106.5' | 1224 | 2.392 | 2.377 | 331.4 | 119.0 | 1.01 | |
| (62/11.5") | | | | | | | | | | |
| (50/0.5") | | | | | | | | | | |
| 1/3 | 1T | 126.5' | | 6610 | 2.880 | 2.393 | 482.2 | 141.8 | 1.20 | |
| | 2T | | | 3706 | 2.229 | 2.360 | 340.5 | 133.1 | 0.94 | |
| | 3T | | | 3581 | 2.494 | 2.356 | 363.1 | 127.2 | 1.06 | |
| | 4T | | | 2577 | 2.566 | 2.382 | 340.6 | 113.5 | 1.08 | |
| | 5U | | | 9239 | 3.746 | 2.378 | 639.0 | 146.3 | 1.58 | 1.0324 |
| | 6U | | | 9827 | 3.535 | 2.402 | 604.5 | 143.8 | 1.47 | 1.0431 |
| | 7T | | | 3319 | 2.067 | 2.383 | 326.9 | 135.2 | 0.87 | |
| | 8U | | | 2112 | 3.730 | 2.351 | 534.4 | 125.7 | 1.59 | 1.0313 |
| | 9T | | | 1372 | 1.812 | 2.388 | 257.4 | 120.9 | 0.76 | |
| | 10T | | 131.5' | 1657 | 2.262 | 2.378 | 315.2 | 119.6 | 0.95 | |
| (50/2") | | | | | | | | | | |
| (50/0.5") | | | | | | | | | | |
| 1/4 | 1T | 147.0' | | 712 | 1.966 | 2.307 | 248.8 | 115.4 | 0.85 | |
| | 2T | | | 146 | 2.363 | 2.365 | 273.2 | 100.3 | 1.00 | |
| | 3T | | | sample broke during test set-up | | | | | | |
| | 4U | | | 912 | 3.582 | 2.342 | 467.8 | 115.6 | 1.53 | 1.0369 |
| | 5T | | | 1072 | 2.562 | 2.380 | 314.2 | 105.0 | 1.08 | |
| | 6T | | | 244 | 2.296 | 2.358 | 255.8 | 97.2 | 0.97 | |
| | 7T | | | 520 | 1.917 | 2.342 | 254.6 | 117.5 | 0.82 | |
| | 8T | | 152.0' | 3657 | 1.840 | 2.345 | 278.5 | 133.6 | 0.78 | |
| (50/1") | | | | | | | | | | |

| BORING / CORE | SAMP. NO. | w (%) | DRY UNIT WT (pcf) | S. T. STRENGTH (psi) | q (u) (psi) | STRAIN @ FAIL. (%) | % RECOV. / %RQD |
|---|---|---|---|---|---|---|---|
| **BORING ONE** | | | | | | | |
| NO TESTABLE MATERIAL | | | | | | | 16 / 0 |
| 1/2 | 1U | 9.4 | 134.2 | | 1965 | 1.48 | 92 / 48 |
| | 2T | 8.9 | 131.7 | 343 | | | |
| | 3U | 7.3 | 135.1 | | 1198 | 1.28 | |
| | 4T | 6.3 | 125.8 | 253 | | | |
| | 5U | 7.8 | 136.1 | | 516 | 0.57 | |
| | 6T | 8.1 | 142.0 | 433 | | | |
| | 7U | 7.7 | 141.3 | | 1613 | 1.93 | |
| | 8T | 4.3 | 114.1 | 137 | | | |
| 1/3 | 1T | 6.1 | 133.6 | 611 | | | 100 / 47 |
| | 2T | 6.9 | 124.5 | 449 | | | |
| | 3T | 9.9 | 115.8 | 388 | | | |
| | 4T | 7.9 | 105.2 | 268 | | | |
| | 5U | 5.8 | 138.3 | | 2015 | 2.14 | |
| | 6U | 6.7 | 134.8 | | 2080 | 1.94 | |
| | 7T | 8.1 | 125.1 | 429 | | | |
| | 8U | 14.1 | 110.2 | | 472 | 0.61 | |
| | 9T | 14.8 | 105.3 | 202 | | | |
| | 10T | 12.6 | 106.3 | 196 | | | |
| 1/4 | 1T | 24.8 | 92.4 | 100 | | | 95 / 32 |
| | 2T | 26.0 | 79.6 | 17 | | | |
| | 3T | | | | | | |
| | 4U | 22.8 | 94.1 | | 204 | 1.85 | |
| | 5T | 16.6 | 90.0 | 112 | | | |
| | 6T | 20.9 | 80.4 | 29 | | | |
| | 7T | 16.7 | 100.7 | 74 | | | |
| | 8T | 7.2 | 124.6 | 540 | | | |

Table 3.6 U/C rock cores GEC-2.

| BORING / CORE | SAMP. NO. | DEPTH TOP (ft) | DEPTH BOT. (ft) | MAX. LOAD (lbs) | LENGTH (in) | DIA. (in) | WET WT. (g) | WET UNIT WT (pcf) | L / D RATIO | CORR. FACTOR |
|---|---|---|---|---|---|---|---|---|---|---|
| **BORING TWO** | | | | | | | | | | |
| (50/1") | | | | | | | | | | |
| 2/1 | 1U | 126.5' | | 3763 | 4.506 | 2.376 | 724.3 | 138.1 | 1.90 | 1.0066 |
| | 2T | | | 2104 | 2.197 | 2.350 | 350.2 | 140.0 | 0.93 | |
| | 3T | | | 2038 | 2.666 | 2.377 | 385.6 | 124.2 | 1.12 | |
| | 4U | | | 1287 | 4.075 | 2.340 | 639.2 | 139.0 | 1.74 | 1.0178 |
| | 5T | | | 1191 | 1.970 | 2.365 | 297.1 | 130.9 | 0.83 | |
| | 6U | | | 4656 | 4.881 | 2.399 | 788.4 | 136.1 | 2.03 | 1.0000 |
| | 7T | | | 3825 | 2.032 | 2.375 | 338.0 | 143.0 | 0.86 | |
| | 8U | | | 5686 | 4.664 | 2.382 | 776.9 | 142.4 | 1.96 | 1.0026 |
| | 9T | | | 3254 | 2.820 | 2.325 | 449.6 | 143.1 | 1.21 | |
| | 10T | | | 2014 | 2.587 | 2.378 | 416.3 | 138.1 | 1.09 | |
| | 11T | | | 1180 | 2.669 | 2.374 | 391.7 | 126.3 | 1.12 | |
| | 12T | | 131.5' | 950 | 2.574 | 2.387 | 360.7 | 119.3 | 1.08 | |
| (50/6") | | | | | | | | | | |
| (50/0") | | | | | | | | | | |
| 2/2 | 1T | 182.0' | | 3051 | 1.823 | 2.390 | 281.9 | 131.4 | 0.76 | |
| | 2T | | 187.0' | 6551 | 2.230 | 2.389 | 347.8 | 132.6 | 0.93 | |
| (50/3") | | | | | | | | | | |

| BORING / CORE | SAMP. NO. | w (%) | DRY UNIT WT (pcf) | S. T. STRENGTH (psi) | q (u) (psi) | STRAIN @ FAIL. (%) | % RECOV / %RQD |
|---|---|---|---|---|---|---|---|
| **BORING TWO** | | | | | | | |
| 2/1 | 1U | 9.2 | 126.5 | | 843 | 1.33 | 95 / 68 |
| | 2T | 12.0 | 125.1 | 259 | | | |
| | 3T | 9.0 | 114.0 | 205 | | | |
| | 4U | 11.4 | 124.7 | | 294 | 0.82 | |
| | 5T | 14.4 | 114.4 | 163 | | | |
| | 6U | 12.0 | 121.6 | | 1030 | 0.97 | |
| | 7T | 9.7 | 130.4 | 505 | | | |
| | 8U | 9.3 | 130.4 | | 1273 | 1.78 | |
| | 9T | 11.3 | 128.7 | 316 | | | |
| | 10T | 10.9 | 124.5 | 208 | | | |
| | 11T | 14.6 | 110.2 | 119 | | | |
| | 12T | 18.7 | 100.5 | 98 | | | |
| | 1T | 3.2 | 127.3 | 446 | | | 53 / 13 |
| | 2T | 4.1 | 127.3 | 783 | | | |

Table 3.7 Triaxial test results. SPT 1 hard area on site, SPT 2 soft area on site.

| Boring | SPT-1 | | | | SPT-2 | | | |
|---|---|---|---|---|---|---|---|---|
| Triaxial | Test-1 | FDOT-1 | FDOT-3 | Test-2 | Test-3 | Test-4 | FDOT-2 | Test-5 |
| Depth (ft) | 3 | 36 | 7 | 55 | 7 | 17 | 36 | 56 |
| N-Value | 13 | 5 | 10 | 16 | 10 | 9 | 10 | 14 |
| N-Correct | 16 | 6 | 12 | 20 | 12 | 11 | 12 | 17 |
| Φ (degrees) | 46 | Clay | 35.4 | 40 | 39 | 45 | Clay | 43 |
| C (psf) | 0 | 1435 | 0 | 0 | 0 | 0 | 1688 | 0 |

Table 3.8 UF triaxial testing details. (file: FDOTtest-2.xls)

| Test # | Borehole & Tube | Depth (ft) | Test Type | Eff. Consolidation Stress, $\sigma'_{3c}$ (psi) | Eff. Consol. Stress @ Failure, $\sigma'_{3f}$ (psi) | Dev. Stress @ Failure, $\sigma'_{df}$ (psi) | Strain @ Failure, (%) | Eff. Friction Angle, ϕ' (deg) |
|---|---|---|---|---|---|---|---|---|
| 1 | BH #1 Tube #1 | 3-5 | CD | 5.31 | 5.31 | 26.35 | 7.8 | 45.4 |
| 2 | BH #1 Tube #4 | 57.5 – 58 | CU | 28.25 | 7.54 | 27.1 | 4.7 | 40.0 |
| 3 | BH #2 Tube #1 | 7.5 – 8.0 | CD | 5.0 | 5.0 | 16.95 | 4.2 | 39 |
| 4 | BH #2 Tube #2 | 18 – 19 | CD | 11.0 | 11.1 | 54.36 | 6.0 | 45.3 |
| 5 | BH #2 Tube #4 | 56.5 – 57 | CU | 30.0 | 6.02 | 26.1 | 11.7 | 43 |
| FDOT – SMO Triaxial Tests – Set #1 file: Boring 1UCF CU triaxial test data reduction | | | | | | | | |
| 1 | BH #1 Tube 3 | 35.5 – 37.5 | CU | 15 | 22.03 | 19.39 | 1.42 | ϕ'= 12.7 c'= 5.87 psi |
| 1a | BH #1 Tube 3 | | | 20 | 23.60 | 20.48 | 2.57 | ϕ' = 0 c'= 9.97 psi |
| FDOT – SMO Triaxial Tests – Set #2 file: Boring 1 tube 2 UCF CU triaxial test data reduction | | | | | | | | |
| 3 | BH #1 Tube 2 | 6 – 8 | CU | 6 | 75.98 | 90.7 | 10.14 | ϕ' = 28.1 c' = 7.25 psi |
| 3a | BH #1 Tube 2 | | | 3 | 27.12 | 45.96 | 13.6 | ϕ' = 35.4 c' = 0 psi |
| FDOT-SMO Triaxial Tests – Set #3 file: Boring 2 tube 3 UCF CU triaxial test data reduction | | | | | | | | |
| 2 | BH #2 Tube 3 | 35.5 – 37.5 | CU | 20 | 7.0 | 26.03 | 2.73 | ϕ' = 35.0 c' = 1.48 psi |
| 2a | BH #2 Tube 3 | | | 10 | 5.35 | 22.3 | 3.30 | ϕ' = 0 c' = 11.73 psi |
| 2b | BH #2 Tube 3 | | | 15 | 5.98 | 22.0 | 9.00 | |

Table 3.9  Summary of 1-D Consolidation Tests.

| BH #1 Tube 2, Depth = 6 – 8 ft, file: CF1_2_4 1-D consol | | | | | | | |
|---|---|---|---|---|---|---|---|
| Parameter | Load, tsf | | | | | | |
| | 0 | 0.5 | 1 | 2 | 4 | 8 | Eng. Props. |
| $e_o$ | 0.526 | .497 | .481 | .460 | .438 | .415 | $\gamma$ = 94.2 pcf |
| $t_{50}$, min | | 0.2 | 0.7 | 0.5 | 0.6 | 0.4 | $C_c$ = 0.075 |
| $C_v$, $in^2$/min | | .236 | .065 | .088 | .070 | .101 | $C_r$ = 0.005 |
| k, cm/s | | 1.12E-6 | 1.57E-7 | 1.06E-7 | 4.26E-8 | 3.11E-8 | $P_c' =$ 0.5 tsf |
| BH #1 Tube 4, Depth = 55.5 – 56.5 ft file: CF1_4_1 1-D consol | | | | | | | |
| $e_o$ | .712 | .683 | .665 | .649 | .621 | .576 | $\gamma$ = 99.3 pcf |
| $t_{50}$, min | | | | | 0.2 | 0.2 | $C_c$ = 0.145 |
| $C_v$, $in^2$/min | | | | | .203 | .187 | $C_r$ = 0.0 |
| k, cm/s | | | | | 2.14E-7 | 9.86E-8 | $P_c' \approx$ 2.6 tsf |
| BH #2 Tube 1, Depth = 6 – 8 ft file:CF2_1_1 1-D consol | | | | | | | |
| $e_o$ | 1.026 | .798 | .738 | .686 | .631 | .581 | $\gamma$ = 81.3 pcf |
| $t_{50}$, min | | 0.5 | | 0.4 | 0.4 | 0.2 | $C_c$ = 0.185 |
| $C_v$, $in^2$/min | | 0.074 | | 0.066 | 0.057 | 0.101 | $C_r$ = 0.01 |
| k, cm/s | | 6.08E-7 | | 1.62E-7 | 7.32E-8 | 6.66E-8 | $P_c' \approx$ 0.15 tsf |
| BH #2 Tube 3, Depth = 33.5 – 37.5 ft file:CF2_3_4 1-D Consol | | | | | | | |
| $e_o$ | 1.357 | 1.282 | 1.252 | 1.189 | 1.052 | 0.885 | $\gamma$ = 72.5 pcf |
| $t_{50}$, min | | 0.5 | 1.0 | 0.9 | 0.118 | 0.175 | $C_c$ = 0.54 |
| $C_v$, $in^2$/min | | .104 | .045 | .048 | .096 | .061 | $C_r$ = 0.02 |
| k, cm/s | | 1.52E_7 | 3.88E-8 | 1.83E-8 | 1.96E-8 | 6.77E-9 | $P_c' \approx$ 1.5 tsf |
| BH #2 Tube 2, Depth = 18 – 19 ft file: CF2_2_1 1-D Consol | | | | | | | |
| $e_o$ | 0.831 | 0.718 | 0.686 | 0.680 | 0.664 | 0.645 | $\gamma$ = 89.7 pcf |
| $t_{50}$, min | Not obtainable from time plots | | | | | | $C_c$ = 0.063 |
| $C_v$, $in^2$/min | | | | | | | $C_r$ = 0.006 |
| k, cm/s | | | | | | | $P_c' \approx$ 0.8 tsf |
| BH #1 Tube 4, Depth = 55.5 – 57.5 ft file: CF1_4_2 1-D Consol | | | | | | | |
| $e_o$ | 1.159 | 0.928 | 0.876 | 0.827 | 0.773 | 0.703 | $\gamma$ = 76.0 pcf |
| $t_{50}$, min | | 0.2 | 0.3 | 0.4 | 0.2 | 0.3 | $C_c$ = 0.20 |
| $C_v$, $in^2$/min | | 0.182 | 0.109 | 0.075 | 0.137 | 0.094 | $C_r$ = N/A |
| k, cm/s | | 3.48E-6 | 1.05E-6 | 1.85E-7 | 1.74E-7 | 6.18E-8 | $P_c' \approx$ 2.0 tsf |
| BH #2 Tube 4, Depth = 55.5 – 57.5 ft file: CF2_4_1 1-D Consol.xls | | | | | | | |
| $e_o$ | 1.108 | 0874 | .859 | .794 | .724 | .659 | $\gamma$ = 79.6 pcf |
| $t_{50}$, min | | | | 0.4 | 0.8 | 0.4 | $C_c$ = 0.23 |
| $C_v$, $in^2$/min | | | | 0.088 | 0.040 | 0.074 | $C_r$ = 0.033 |
| k, cm/s | | | | 2.71E-7 | 6.43E-8 | 6.15E-8 | $P_c' \approx$ 0.75 tsf |

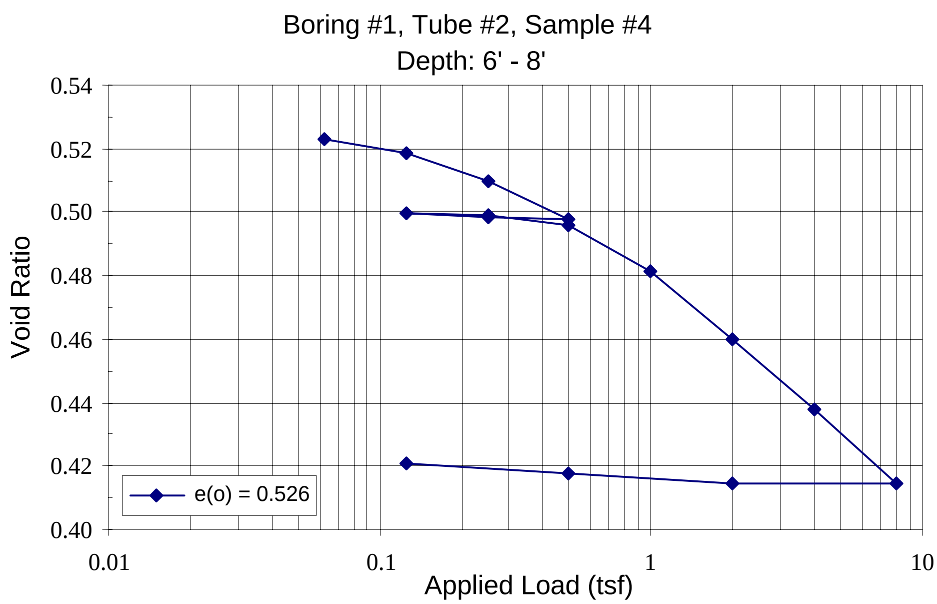


Figure 3.5 e-Log P' curve for BH #1 Tube 2.

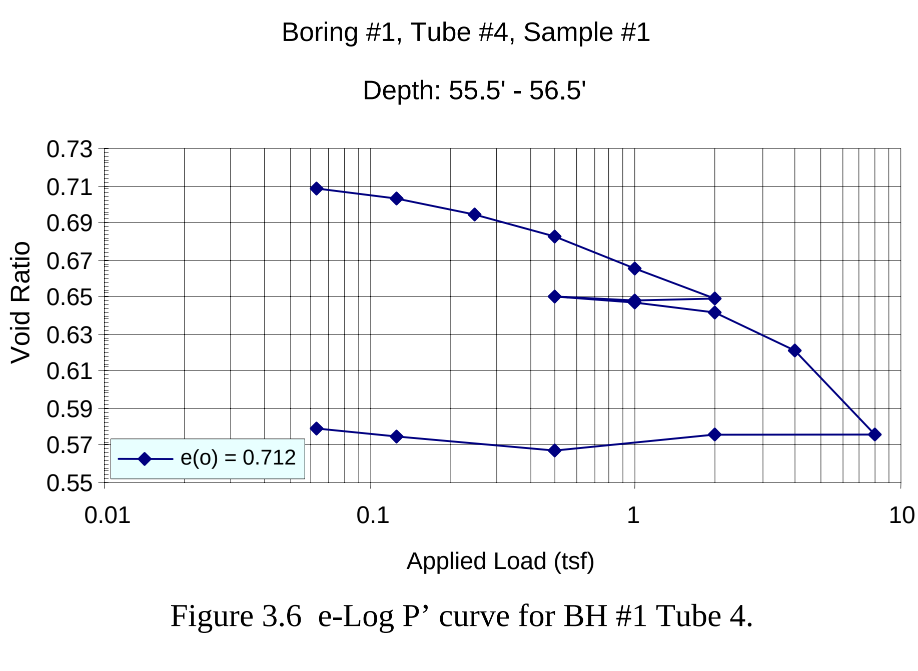


Figure 3.6 e-Log P' curve for BH #1 Tube 4.

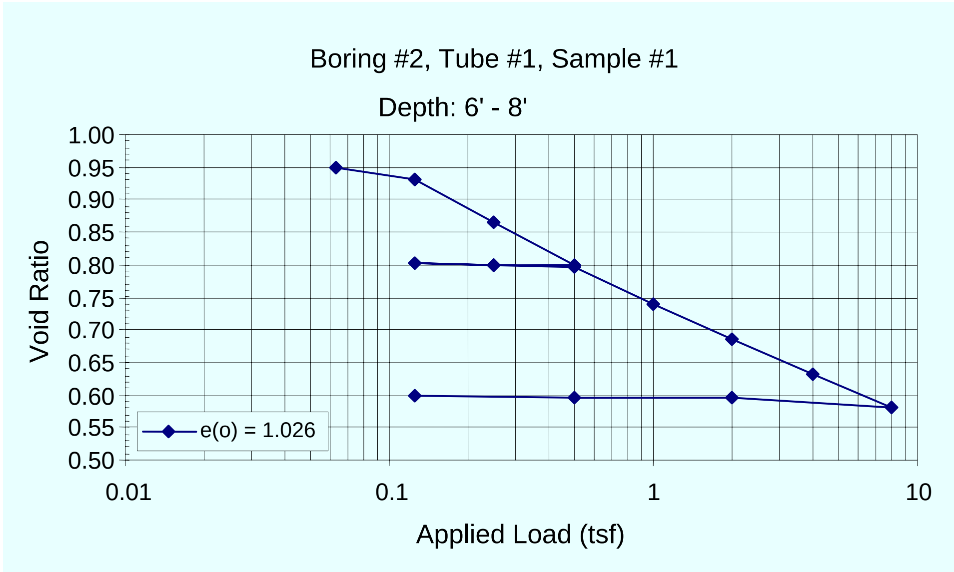


Figure 3.7 e-Log P’ curve for BH #2 Tube 1.

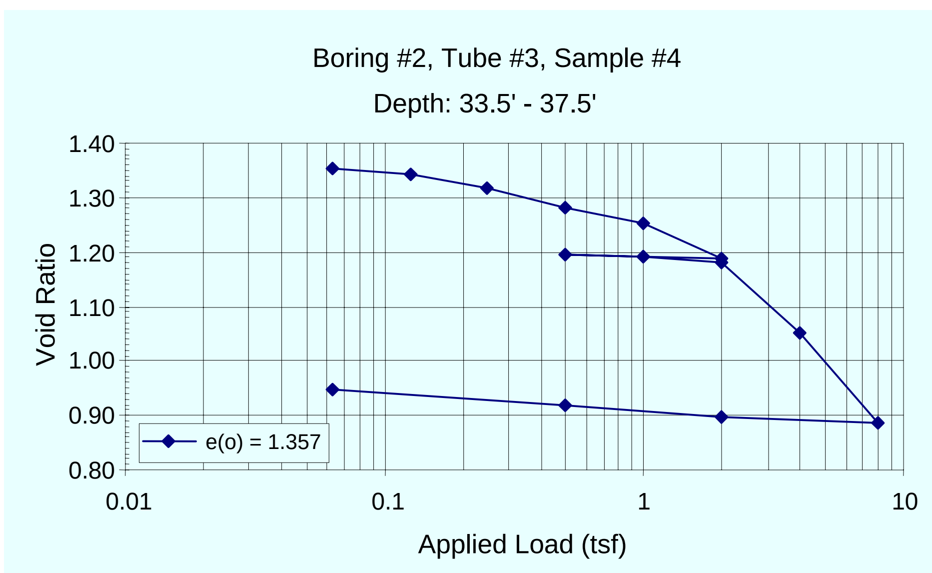


Figure 3.8 e-Log P’ curve for BH #2 Tube 3.

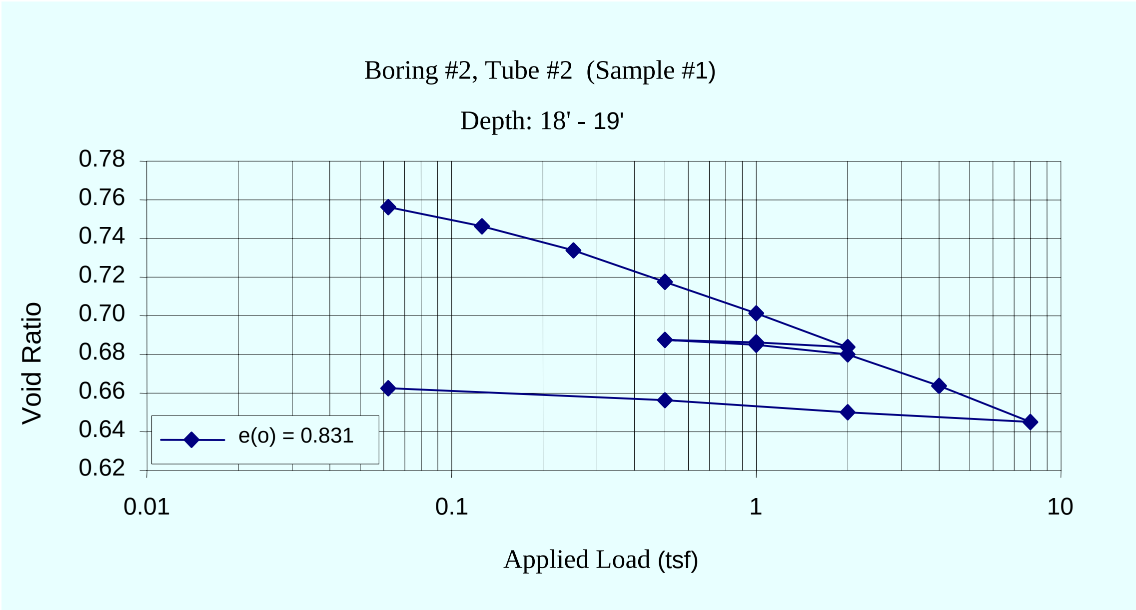


Figure 3.9 e-Log P' curve for BH #2 Tube 2.

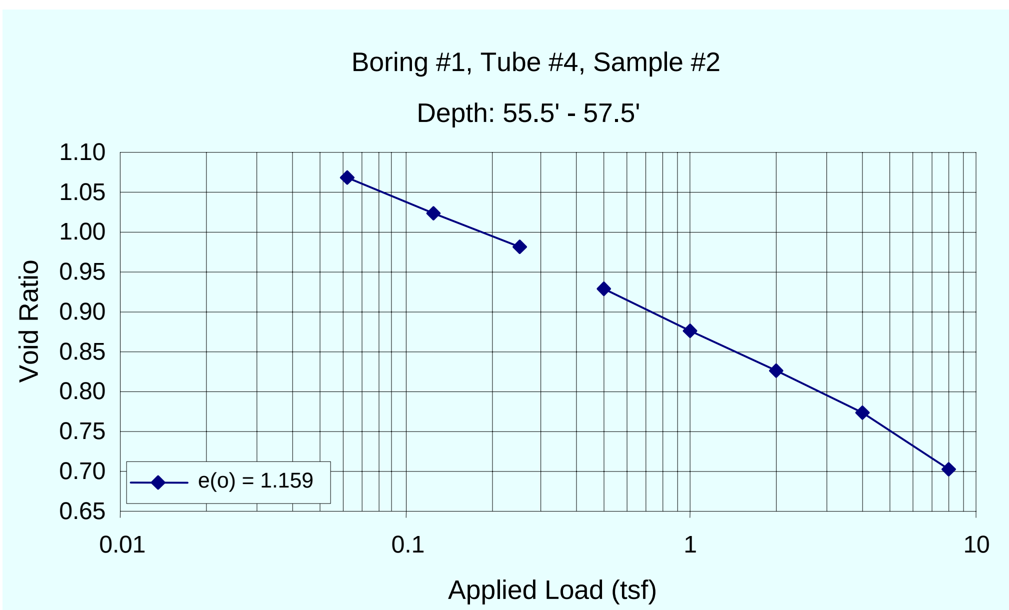


Figure 3.10 e-Log P' curve for BH #1 Tube 4.

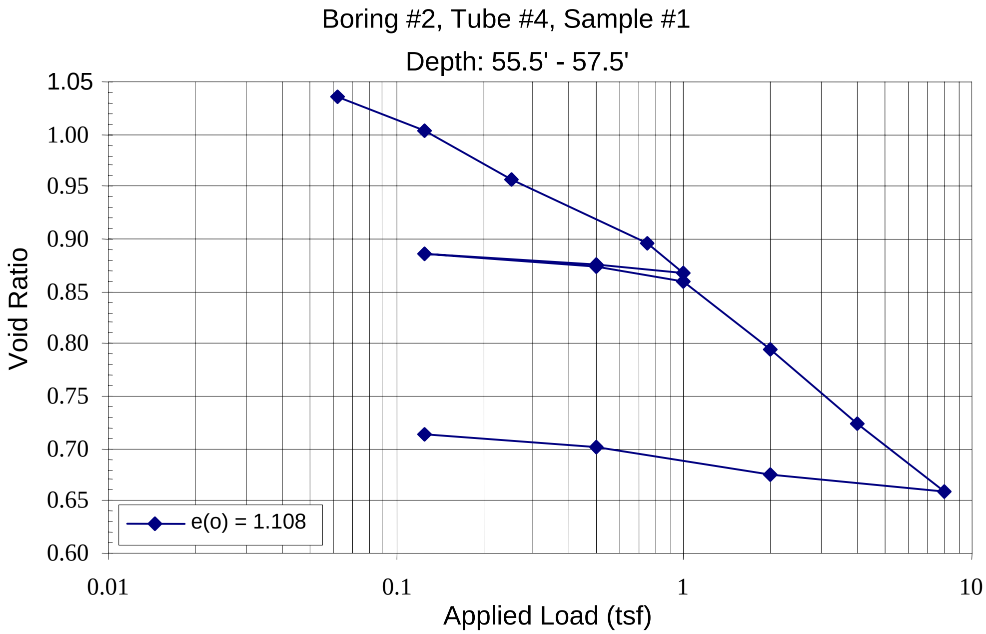


Figure 3.11 e-Log P' curve for BH #2 Tube 4.

Table 3.10 Summary of permeability values from triaxial flex wall vs. oedometer.

| BH # 1 Tube 2 Depth = 7ft; file: B1_T2_S3 flexperm.xls | | | | | |
|---|---|---|---|---|---|
| Permeability | Confining Stress or Load, tsf | | | | |
| | 0.29 | 0.5 | 1.01 | 2.02 | 4.03 |
| Flex Wall | 3.19E-04 | - | 1.24E-04 | 1.50E-04 | 8.76E-04 |
| Oedometer | | | 1.57E-07 | 1.06E-07 | 4.26E-07 |
| BH # 1 Tube 4, Depth = 58ft; file: B1_T4_S3 flexperm.xls | | | | | |
| Flex Wall | 6.47E-06 | 2.04E-06 | 9.92E-07 | 5.05E-07 | 3.84E-07 |
| Oedometer | - | - | - | - | 2.14E-07 |
| BH #2 Tube 2, Depth = 19ft; file: B2_T2_S2 flexperm.xls | | | | | |
| Flex Wall | - | 1.03 E-06 | 7.46 E-07 | 7.75 E-07 | - |
| Oedometer | - | - | - | - | - |
| BH # 2, Tube 3, Depth = 36ft; file: B2_T3_S3 flexperm.xls | | | | | |
| Flex Wall | 1.09 E-06 | | 9.83 E-07 | 6.73 E-07 | 4.15 E-07 |
| Oedometer | | | 3.88 E-08 | 1.83 E-08 | 1.96 E-08 |

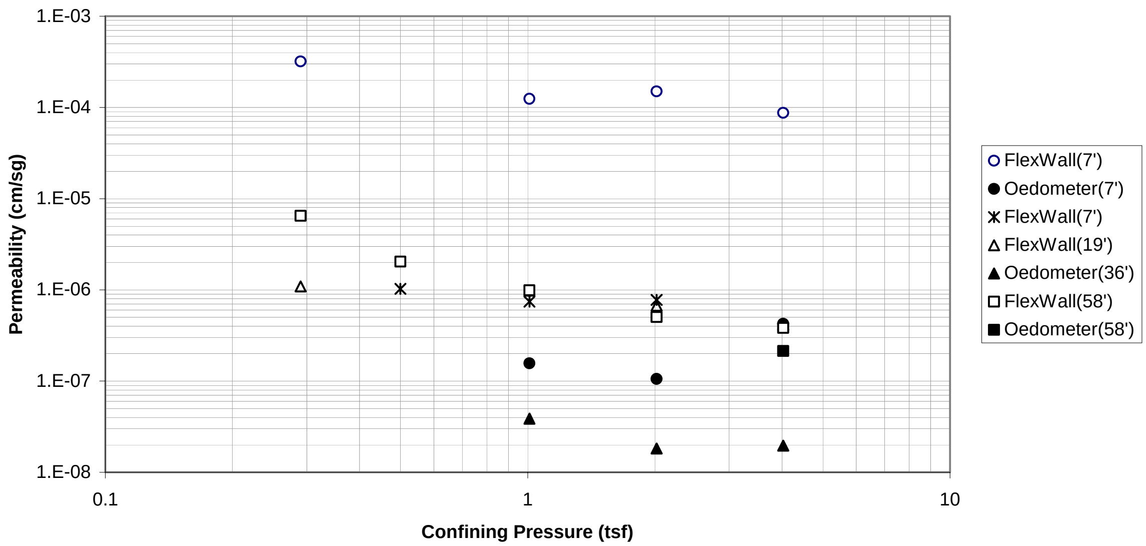


Figure 3.12 Comparison of permeability results for triaxial flex wall vs. oedometer.

# CHAPTER 4

# EVALUATION OF TRIAXIAL TESTING AND INSITU TEST CORRELATIONS

## INTRODUCTION

Engineering science is mainly based on human interpretation and modeling of Mother Nature physics phenomena. We try to reproduce through mathematical equations our understanding of the process in study. Geotechnical engineering deals with the most complicated civil engineering material: soil. Every soil mechanism we model, either by limiting equilibrium Mohr-Coulomb theory or deformation based theory, requires the basic input of soil engineering properties, i.e., unit weight, friction angle, cohesion, Young's modulus, Poisson's ratio, etc. In order to obtain these soil parameters, laboratory tests are necessary.

Unfortunately, laboratory testing requires the collection of high quality undisturbed sample material, transporting it back to the laboratory, and in many cases in Florida, requires freezing of cohesionless samples in order to have the appropriate consistency to set-up the lab test. Considering the fact that most construction sites in Florida consist of sands with very high water table elevation, undisturbed sampling of soil material becomes an almost impossible task. Therefore the use of insitu test as a way to estimate soil properties has become very popular; among these are SPT, CPT, DMT and PMT.

### Problem Statement

Historically, engineers have developed many types of correlations and curve fitting equations for use with the insitu tests, which provide the necessary soil parameters for engineering design.

These correlations are highly dependent on site geographic location, specific material tested, and technical expertise of the operator running the test. The generalized use of one or another equation disregarding the fact of different conditions for its application, can lead to erroneous results.

### Objectives

Based upon the aforementioned problems, the objectives of this chapter are:

1. To evaluate historically-used insitu test correlations with laboratory results data to obtain the desired soil properties parameters.
2. To select the most reliable insitu test and characteristic correlation of better use for this case-specific site.

## Testing Layout

In order to compare the results of soil characterization from insitu test with triaxial testing, two SPT tests were performed at the site by GEC agency. This was done in order to obtain undisturbed samples; Shelby tubes were taken at depths ranging from 2 to 55 feet. The location of the SPT under study are shown in Figure 4.1, the tests are denoted as SPT GEC –1 and 2. SPT GEC –1 is located on the "hard" side of the site; while SPT GEC –2 is located in the "soft" side.

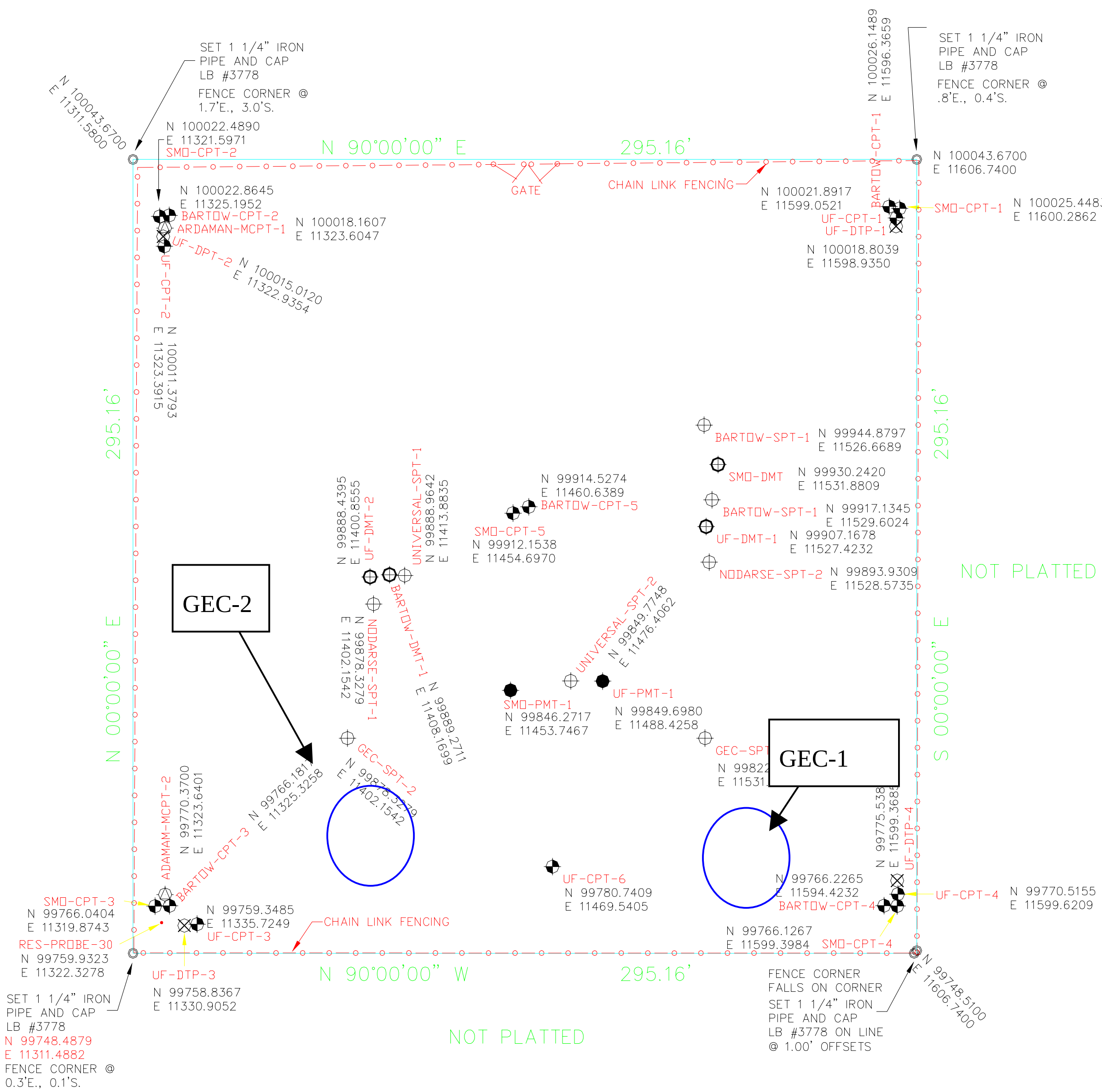


Figure 4.1 Location of SPT testing for extraction of Shelby tubes.

**SPT Correlations**

A series of different correlations relating internal friction angle vs. SPT blow counts, N-value, were plotted. Some of these correlations consider possible confinement of the sample by using “overburden-corrected” N-values, and therefore are directly related with sample position in the ground profile. The samples taken for triaxial laboratory testing were from 7, 17, 35, and 55 ft depths. Those correlations with confinement dependence are marked accordingly by (depth); e.g., (7’). A soil unit weight was assumed to be 120 pcf, and the water table elevation was assumed as 2-ft below the ground surface.

The equation used for overburden correction is:

$$C_N = 0.77 \log \frac{20}{\sigma_o^{'}} ,\ \sigma_o^{'} \text{ tsf}$$

The SPT based correlations used were:

Bowles, 1996 (7’ or 45’) : $\Phi = 25 + 28 \left( \frac{N_{55}}{\sigma_o^{'}} \right)^{1/2}$

Bowles, 1996 1 : $\phi = (18N_{70})^{0.5} + 15$

Bowles, 1996 2 : $\phi = 0.36N_{70} + 27$

Bowles, 1996 3 : $\phi = 4.5N_{70} + 20$

Kulhawy and Mayne (1990) : $\phi = \tan^{-1} \left[ \frac{N}{12.2 + 20.3 \log \sigma_o / P_a} \right]^{0.34}$

Insitu 2001 (p6.1) : $\phi = 20 + \sqrt{15.4 + (N_{1(60)})}$, with $N_{1(60)} = \frac{N_{60}}{\left[ \frac{\sigma_{vo}^{'}}{p_a} \right]^{0.5}}$

Peck et al. (1974) using uncorrected N-values as used in FL-PIER

$$\phi = 53.881 - 27.6034 * e^{-0.0147*N}$$

Ng (2000) Geotechnique: $\phi = 10 \log N + 27$

As shown in Figure 4.2, not all correlations plotted provided reliable information. For example, those given by the 2001 In-situ Conference, or the Bowles correlations were quite insensitive to N-values; i.e., a narrow range of ϕ values over a wide range of N-values. In other cases, results went extremely above expected values, as Kulhawy and Mayne 1990 (7’), or were similar to other correlation, as with the Bowles 1 and Bowles 2 expressions.

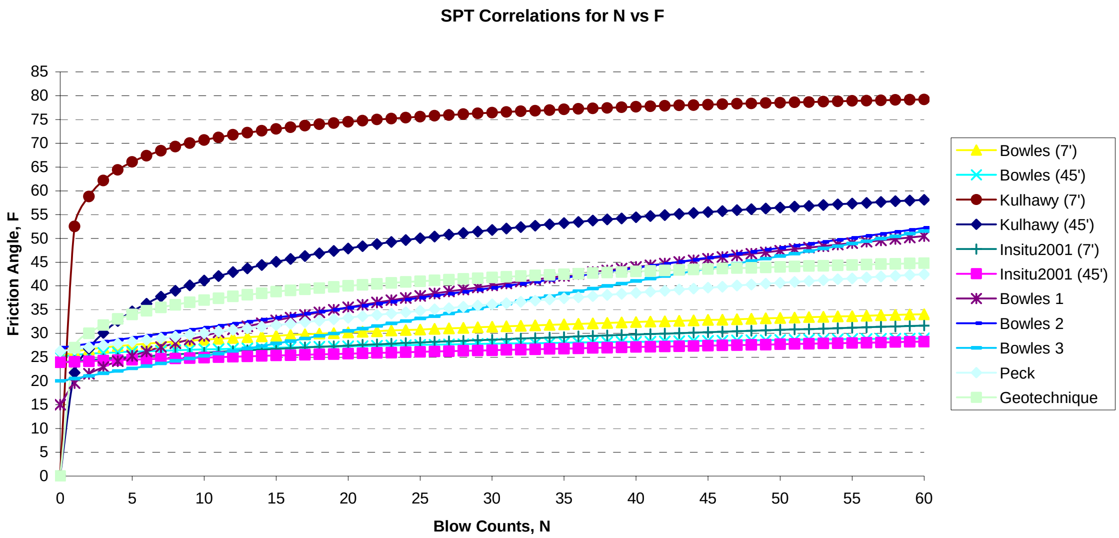


Figure 4.2 Different trends plotted by the use of correlations interpreting N-values as friction angle (ϕ ) of the soil.

We limited the analysis to those correlations shown in Figure 4.3. All seven laboratory results were plotted in this chart, two of them provided by the FDOT Lab. For laboratory test results see Table 4.1. Peck's (1974) correlation, used in FPIER software, and therefore widely used by consulting firms for this type of approach, falls below the plotted points, showing a considerable conservative analysis. For this data, the Geotechnique 2000 Conference expression fits very closely to our data, much better than the Kulhawy and Mayne (1990) (45') expression, which although plots close to our data distribution, it has very high values and is just applicable to samples at a depth of 45 ft.

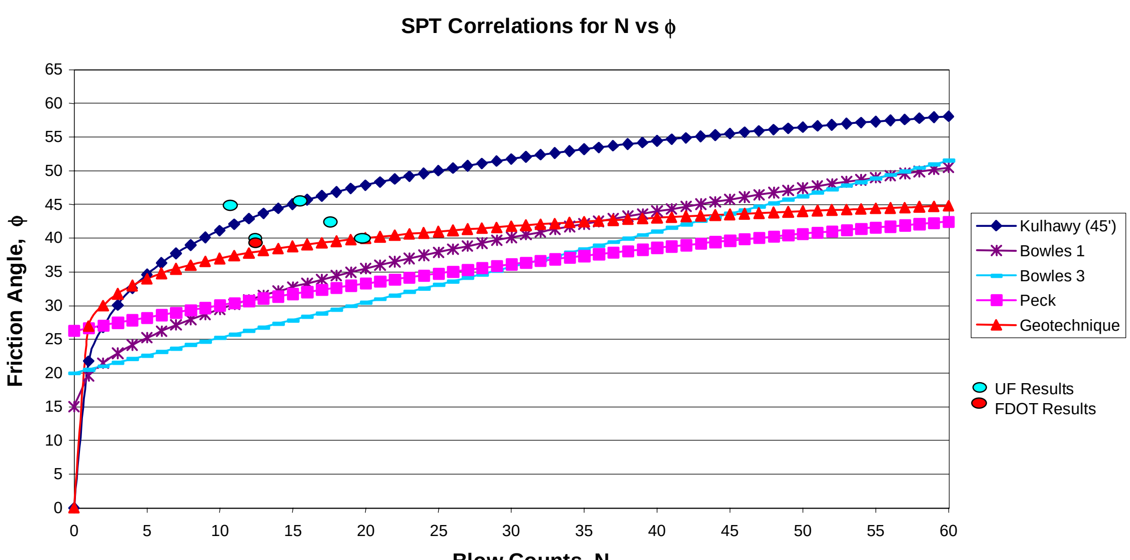


Figure 4.3 Best-fit $N_{SPT}$ correlations for triaxial laboratory results.

Table 4.1 Triaxial test results. SPT 1 hard area on site, SPT 2 soft area on site.

| Boring | SPT-1 | | | | SPT-2 | | | |
|---|---|---|---|---|---|---|---|---|
| Triaxial | Test-1 | FDOT-1 | FDOT-3 | Test-2 | Test-3 | Test-4 | FDOT-2 | Test-5 |
| Depth (ft) | 3 | 36 | 7 | 55 | 7 | 17 | 36 | 56 |
| N-Value | 13 | 5 | 10 | 16 | 10 | 9 | 10 | 14 |
| N-Correct | 16 | 6 | 12 | 20 | 12 | 11 | 12 | 17 |
| Φ(degrees) | 46 | Clay | 35.4 | 40 | 39 | 45 | Clay | 43 |
| C (psf) | 0 | 1435 | 0 | 0 | 0 | 0 | 1688 | 0 |

The data reduction approach by the University of Florida Lab assumes all the shear resistance developed in the sample is due to internal friction and does not consider cohesion; i.e., a c = 0 condition. Consequently, this assumption for the cohesionless soils tests results in higher values of friction angle, $\phi$.

### *SPT - $\phi$ Correlations – Navfac DM-7*

NavFac DM-7 presents two figures which can be used to estimate $\phi$-values from SPT tests. The method uses Figure 4.4 to obtain an estimate of relative density, $D_R$. Subsequently, Figure 4.5 is entered using the soil classification and the Figure 4.4 $D_R$ estimate to obtain $\phi$. Unfortunately, one must assume unit weight values, $\gamma$, to calculate effective vertical stress, $\sigma_v$', to use Figure 4.4, and then compare the assumed unit weight with values obtained from Figure 4.5. Hence an iteration procedure is required. Table 4.2 presents the results using this iterative DM-7 method for the UCF GEC –1 and –2 results. For these estimates a single uniform layer was assumed with a single unit weight, except for the Test #5 estimates.

The results presented in Table 4.2 reveal that the DM-7 method is quite insensitive to SPT – N blow count, estimating a range of $\phi$-values from 33.5° - 35° for blow counts ranging from 9 to 16. The DM-7 method is quite conservative and suffers implementation due to requiring an iterative procedure.

### *SPT vs. Cohesion*

The FDOT-SMO lab used 3 different confining pressures for samples from a single Shelby tube (boring 2). Consequently, a failure envelope tangent to the Mohr’s circles gave results closer to a clayey soil than a sandy soil, with a cohesion of 1435 psf, and a low effective friction angle of 12°. Data obtained from FDOT labs were plotted in Figure 4.6, with correlations relating cohesion with SPT blow counts, N-value.

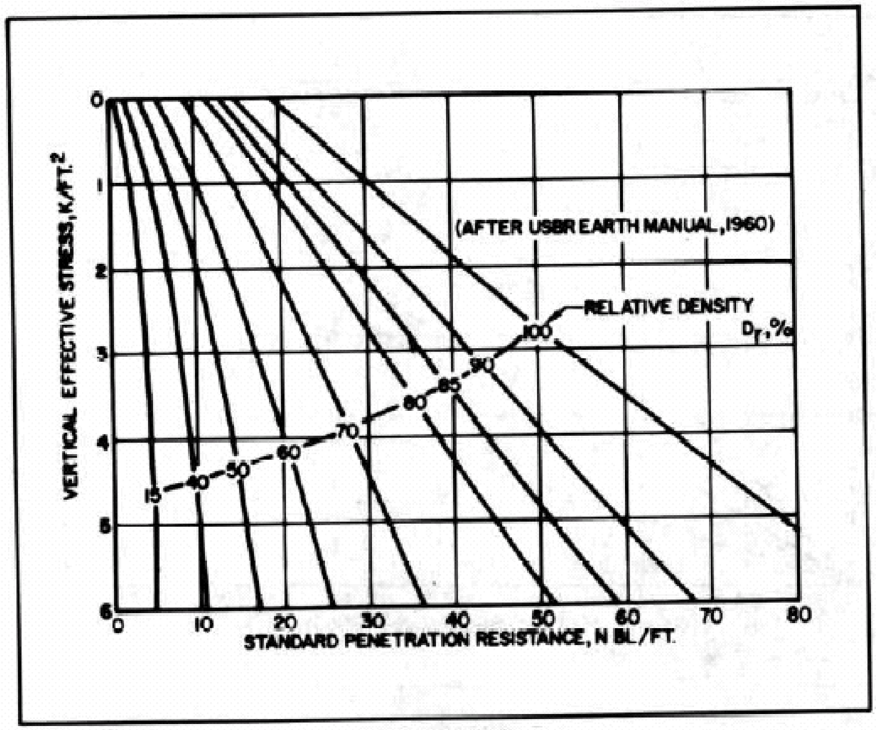


FIGURE 3
Correlations Between Relative Density and Standard Penetration Resistance in Accordance with Gibbs and Holtz

Figure 4.4 Figure 3 from DM-7.

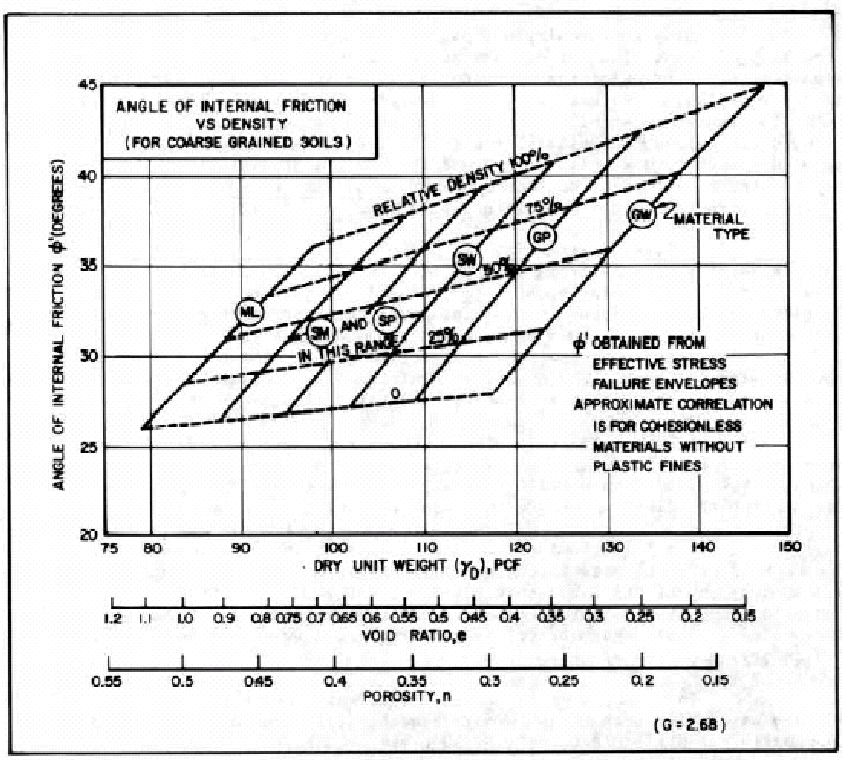


FIGURE 7
Correlations of Strength Characteristics for Granular Soils

Figure 4.5 Figure 7 from DM-7.

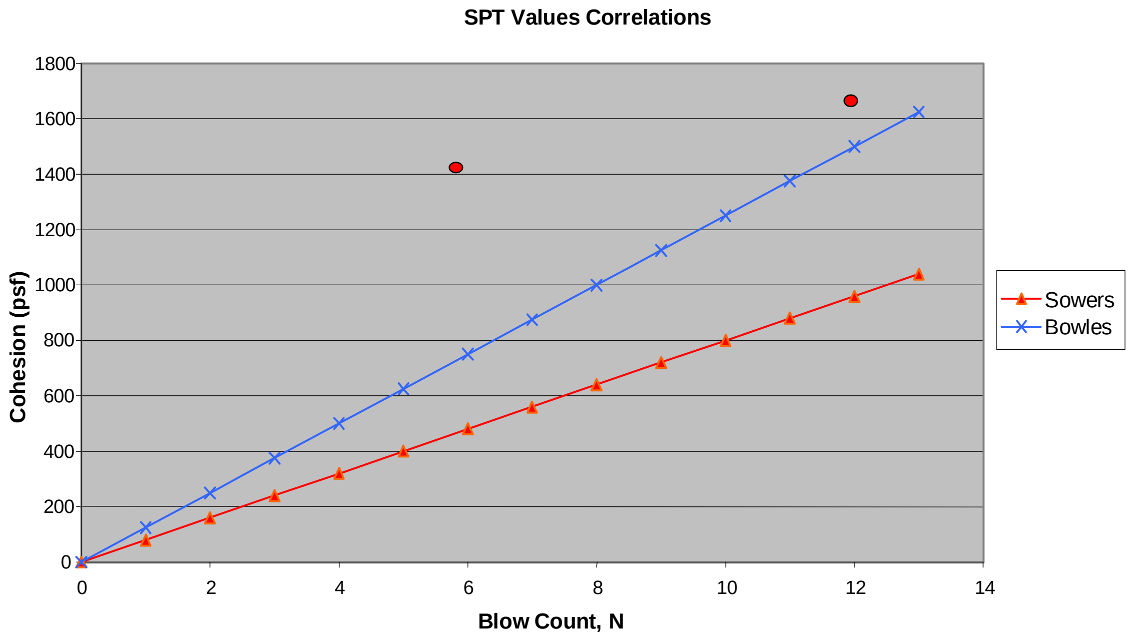


Figure 4.6 Comparison of measured and estimated cohesion values.

Table 4-2 Comparison of measured and DM-7 estimated ϕ - values.

| | Test #1 | Test #3 | Test #2 | FDOT #3 | Test #4 | Test #5 |
|---|---|---|---|---|---|---|
| Depth, ft | 3 | 7 | 55 | 7 | 17 | 56 |
| SPT – N | 13 | 10 | 16 | 10 | 9 | 14 |
| Soil Class | SM | SM | SW-SM | SM | SM | SP |
| Iteration #1 $\gamma_d$ assumed = 102.4 pcf, GWT @ 2ft | | | | | | |
| $\sigma_v$', ksf | 0.225 | 0.373 | 2.325 | 0.405 | 0.805 | 2.365 |
| $D_R$ Fig 3 | 78% | 69% | 60% | 65% | 60% | 50% (use SW as SP out of range) |
| $\gamma_d$ Fig 7 | 102 pcf | 101 pcf | 105 pcf | 101 pcf | 100 pcf | 112 pcf |
| Iteration #1a: $\gamma_d$ assumed = 102.4 pcf for 0 – 10 ft, GWT @ 2ft, but for Test # 5 $\gamma_d$ = 112.4 10 – 60 ft. | | | | | | |
| $\sigma_v$', ksf | | | | | | 2.825 |
| $D_R$ Fig 3 | | | | | | 58% |
| $\gamma_d$ Fig 7 | | | | | | 113 pcf |
| ϕ Fig 7 | 35 | 33.5 | 34 | 33.5 | 33 | 35 |
| $\phi_{measured}$ | 46 | 39 | 40 | 39 | 45 | 43 |

The correlations used were:

Sowers, 1979: $C_{tsf} = 0.04\,N$

Bowles, 1996: $C_{tsf} = 0.0625\,N$

As shown, these correlations are quite conservative and greatly underestimate cohesion values.

**CPT and DMT Discussion**

Laboratory friction angles ($\phi$) in this case, were also compared with some estimated values from other insitu tests; specifically, CPT and DMT.

Table 4.3 gives a general idea of the nature of the soil surrounding the two SPT borings from were the samples were extracted. The values of friction angle shown are based on the interpretation performed by CONEPLOT, software develop by University of British Columbia, Vancouver, Canada, using correlations developed by Robertson and Campanella (1983)

Table 4.3 General friction angle at UCF site based on CPT correlations. SPT-2 soft area, SPT-1 hard area.

| | Depth (ft) | qc (tsf) | CPT, $\phi$ (°) Campanella | $\phi$ (°) Triaxial | SPT |
|---|---|---|---|---|---|
| CPT 019 | 2 | 30 | 45 | - | SPT 2 |
| UF cpt 3 | 7 | 60 | 43 | 39 | |
| SW corner | 18 | 42 | 39 | 45 | |
| | 36 | 60 | 37 | $\phi = 0°$ | |
| | 56 | 100 | 39 | 43 | |
| CPT 213 | 2 | 33 | 47 | - | |
| Bartow cpt 3 | 7 | 50 | 43 | 39 | |
| SW corner | 18 | 50 | 39 | 45 | |
| | 36 | 70 | 35 | Clay | |
| | 56 | 100 | 39 | 43 | |
| UCF | 2 | 80 | 47 | 46 | SPT 1 |
| UF cpt 4 | 7 | 140 | 47 | - | |
| SE corner | 18 | 80 | 41 | - | |
| | 36 | 25 | Clay | Clay | |
| | 56 | 100 | 39 | 40 | |
| UCF 214 | 2 | 100 | 47 | 46 | |
| Bartow cpt 4 | 7 | 160 | 47 | - | |
| SE corner | 18 | 70 | 41 | - | |
| | 36 | 10 | Clay | Clay | |
| | 56 | 100 | 39 | 40 | |
| UCF 6 | 2 | 54 | 47 | 46 | In-between |
| South center | 7 | 54 | 43 | 39 | |
| | 18 | 36 | 39 | 45 | |
| | 36 | 20 | 31 | Clay | |
| | 56 | 100 | 39 | 40-43 | |

Due to the fact that the comparison of the friction angle on Table 4.3 was too general, a narrower approach was considered. For a better comparison only the reduced data from the test in the vicinity of the SPT's were considered.

Table 4.4 and Figures 4.7 and 4.8 present values obtained for the comparison between the results from triaxial testing and CPT, DMT in areas located in the immediate vicinity of the SPT tests.

Table 4.4 Summary of comparison between triaxial testing, CPT and DMT.

| CPT | Depth (ft) | CPT, ϕ (°) Campanella | DMT, ϕ (°) | ϕ (°) Triaxial | SPT | DMT |
|---|---|---|---|---|---|---|
| CPT 019 UF cpt 3 SW Corner | 2 | 45 | 42 | - | SPT 2 | UF DMT 2 |
| | 7 | 43 | 43 | 39 | | |
| | 18 | 39 | 42 | 45 | | |
| | 36 | 37 | 36 | Clay | | |
| | 56 | 39 | - | 43 | | |
| UCF 214 SMO cpt 4 SE Corner | 2 | 47 | 43 | 46 | SPT 1 | UF DMT 1 |
| | 7 | 47 | 40 | - | | |
| | 18 | 41 | 39 | - | | |
| | 36 | Clay | Clay | Clay | | |
| | 56 | 39 | - | 40 | | |

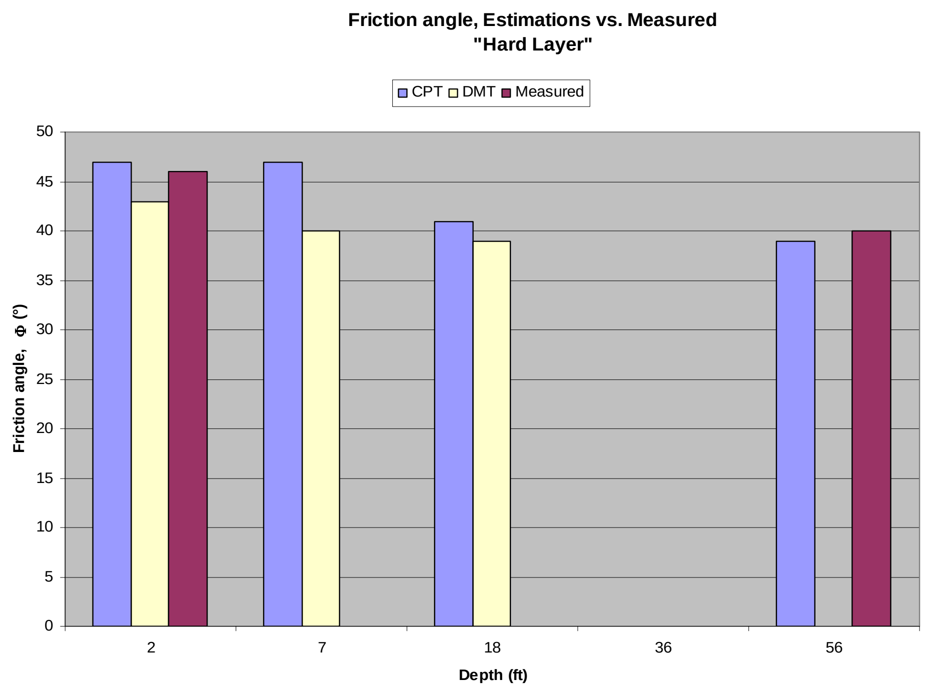


Figure 4.7 Friction angle comparison; insitu testing vs. measured (triaxial) at "hard" area of site (SPT-1).

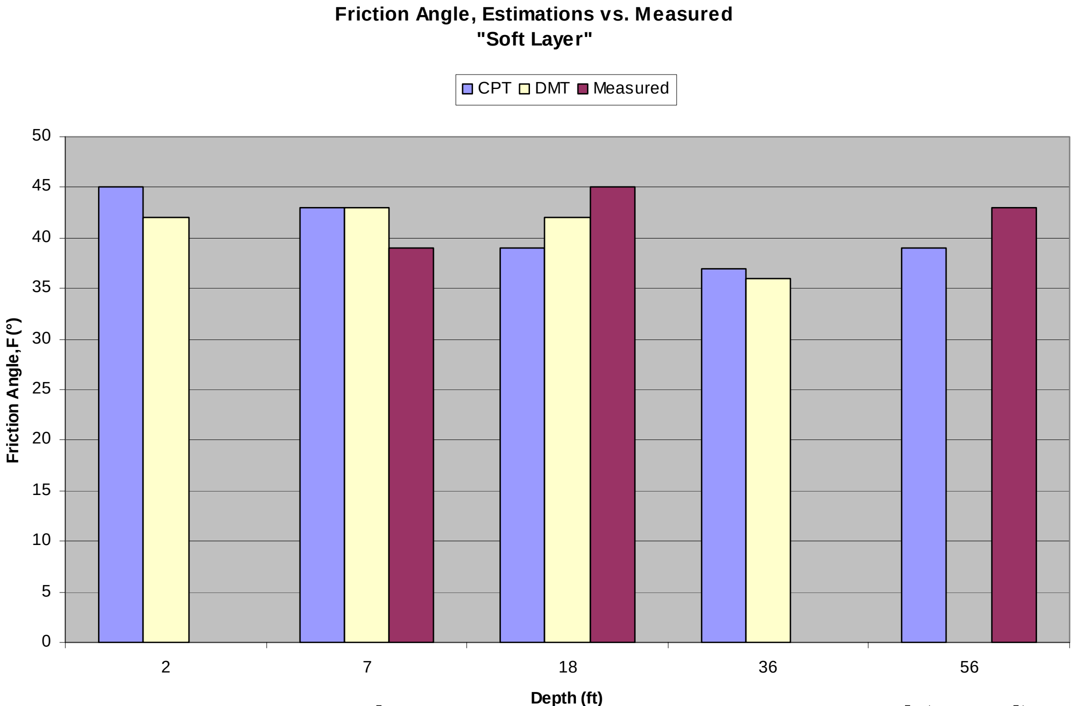


Figure 4.8 Friction angle comparison; insitu testing vs. measured (triaxial) at "soft" area of site (SPT-2).

The information collected shows a general agreement of the values measured vs. the ones collected by CPT and DMT, with the exception of the case of the SPT –2 at a depth of 36 feet. The CPT and DMT data indicate the existence of sand to this depth, but measured values from triaxial testing indicate the existence of clay. A further analysis of the reduced data collected by DMT and CPT indicate the existence of thin layers of sand within the large layer of silty clay, which is in concert with the laboratory results. Figure 4.9 depicts the profile of the soil in the vicinity of the SPT's based on the previous information.

### *Cohesion from Insitu Tests*

Table 4.5 presents a comparison between triaxial test cohesion values and those estimated from SPT, CPT, and DMT correlations. As shown, the insitu correlations compare poorly with the laboratory measured values.

Table 4.5 Comparison of laboratory and field cohesion values.

| Location | #1, psf | #2,psf |
|---|---|---|
| SPT[a] | 480 | 880 |
| CPT[b] | 1107 | 7774 |
| DMT | 376 | 2654 |
| Triaxial Measured[c] | 1435 | 1688 |

a. Sowers c (tsf) = 0.04N

b. $c = \dfrac{q_c - \sigma}{15}, \sigma = 36\,ft \times 94.2\,pcf = 3391\,psf$

c. FDOT-1, and FDOT-2 Table 4.1

### *Constitutive Behavior – SPT*

Table 4.6 and Figure 4.10 present a comparison between triaxial test modulii values and those estimated from SPT correlations. PLAXIS uses $E_{50}$, which is the modulus at 50% of the maximum deviator stress, for FEM modeling. The comparison is based upon the FL-Pier correlations:

E (psf) = 20,000 $N_{60}$ Sands

E (psf) = 30,000 $N_{60}$ OC Sands

E (psf) = 10,000 $N_{60}$ Sands with fines

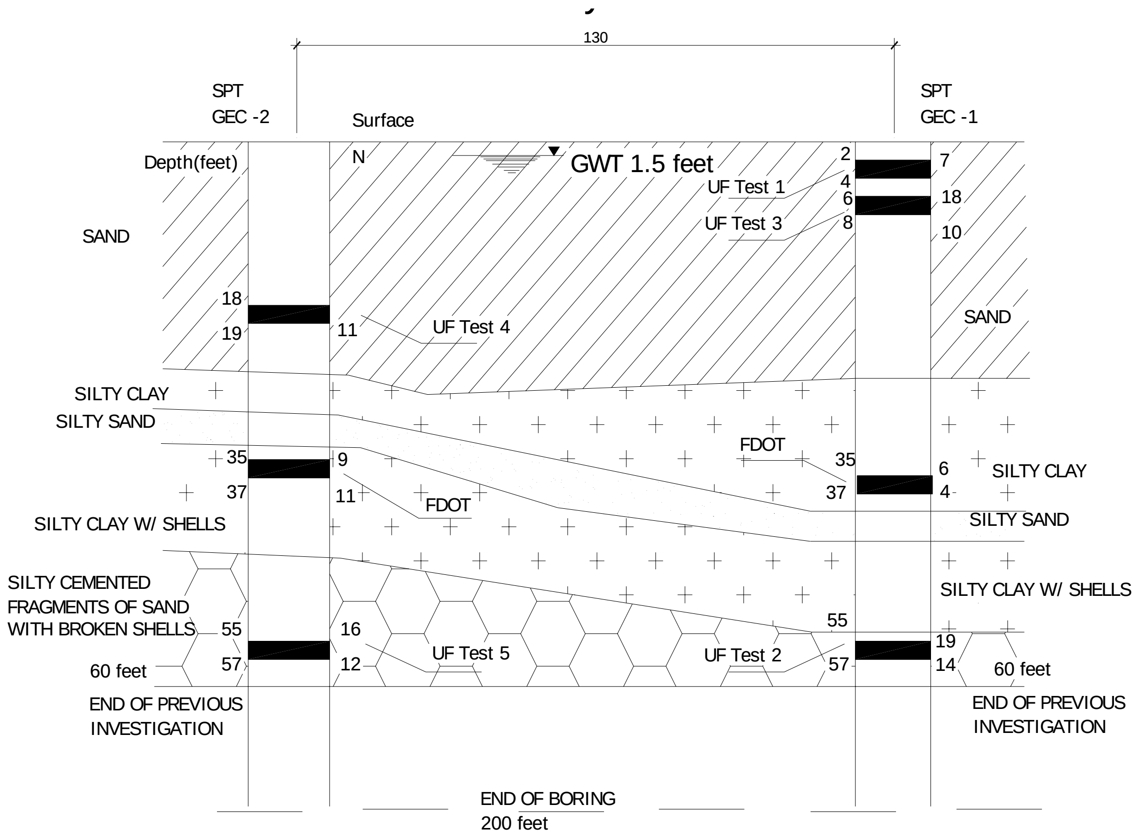


Figure 4.9 Soil profile based on information collected by CPT, DMT, SPT and triaxial testing.

Table 4.6 Comparison of triaxial $E_{50}$ and estimated SPT derived E-values.

| Test ID | $\sigma_{Dmax}$ | $\sigma^{50}_{Dmax}$ | $\varepsilon_{50}$(%) | $E_{50}$ (psi) | $\sigma'_{3f}$ (psi) | σ'o est (psi) | Janbu E (psi) | SPT $N_{corr}$ | SPTE (psi) |
|---|---|---|---|---|---|---|---|---|---|
| UF1 | 26.35 | 13.18 | 0.200 | 6588 | 5.31 | 1.56 | 4073 | 16 | 3333 |
| UF2 | 27.10 | 13.55 | 1.006 | 1347 | 7.54 | 14.88 | 992 | 20 | 2778 |
| UF3 | 16.95 | 8.48 | 0.946 | 896 | 5.00 | 2.59 | 538 | 12 | 833 |
| UF4 | 54.36 | 27.18 | 0.698 | 3894 | 11.00 | 5.59 | 3465 | 11 | 1528 |
| UF5 | 26.10 | 13.05 | 0.262 | 4975 | 6.00 | 16.40 | 3270 | 17 | 2361 |
| FDOT 3 | 90.70 | 45.35 | 1.189 | 3814 | 6.00 | 2.59 | 2507 | 12 | 1667 |
| FDOT 3 | 46.00 | 23.00 | 1.002 | 2295 | 3.00 | 2.59 | 1067 | 12 | 1667 |

σ'o est (psi) = (2ft) (94.2 pcf) + (55-2 ft) (36.9 pcf) ÷ 144 = 14.88 psi

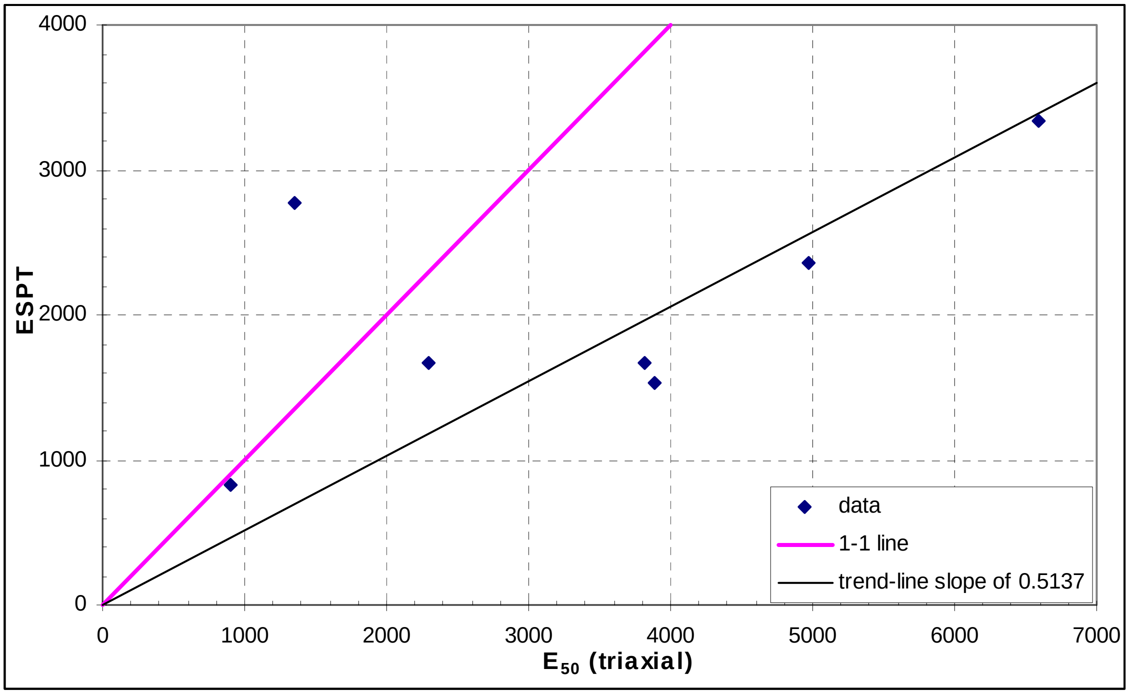


Figure 4.10 Comparison of triaxial $E_{50}$ and SPT estimated moduli values.

The SPT N-values were corrected for overburden pressure using unit weights (γ) from oedometer tests (Table 3.1) or γ = 94.2 pcf for 0 - 2 ft, and γ' = 36.9 pcf for depths below 2 ft. That is to say, the ground water table is placed at 2-ft. The triaxial test $E_{50}$ values also were corrected to 1 tsf using Janbu's approach and modulus number for sands m = 0.5; that is:

$$E_{50}^{corrected} = E_{50}^{txl}\left(\frac{\overline{\sigma}_{3f}}{1\,\text{tsf}}\right)^{0.5}$$

Admittedly, there is a mixture of C/U and C/D triaxial tests, but by using $\overline{\sigma}_{3f}$, the effective triaxial stress is considered; however, the field effective stress during SPT testing is unknown. As shown, the SPT estimated values are about half those measured via triaxial tests.

***Constitutive Behavior – CPT***

Table 4.7 and Figure 4.11 present the comparisons between triaxial $E_{50}$ values and those estimated from CPT tests. Schmertmann (1978) suggested $E = \alpha\, q_c$, where $\alpha \approx 2.5 - 4.0$. Figure 4.10 suggests $\alpha = 3.2$ as an average for the tests, with a range of 1.0 to 5.4.

Table 4.7  Comparison of laboratory triaxial E and CPT $q_c$ values.

| Test ID | $\sigma_{Dmax}$ | $\sigma^{50}_{Dmax}$ | $\varepsilon_{50}$(%) | $E_{50}$ (psi) | $\sigma'_{3f}$ (psi) | σ'o est (psi) | Triax. Mod E (psi) | CPT Qc (psi) |
|---|---|---|---|---|---|---|---|---|
| UF1 | 26.35 | 13.18 | 0.200 | 6588 | 5.31 | 1.56 | 3570 | 782.3 |
| UF2 | 27.10 | 13.55 | 1.006 | 1347 | 7.54 | 14.88 | 1892 | 1449.7 |
| UF3 | 16.95 | 8.48 | 0.946 | 896 | 5.00 | 2.59 | 645 | 829.9 |
| UF4 | 54.36 | 27.18 | 0.698 | 3894 | 11.00 | 5.59 | 2776 | 634.4 |
| UF5 | 26.10 | 13.05 | 0.262 | 4975 | 6.00 | 16.40 | 8225 | 1392.9 |
| FDOT 3 | 90.70 | 45.35 | 1.189 | 3814 | 6.00 | 2.59 | 2506 | 2348.5 |
| FDOT 3 | 46.00 | 23.00 | 1.002 | 2295 | 3.00 | 2.59 | 2133 | 2348.5 |

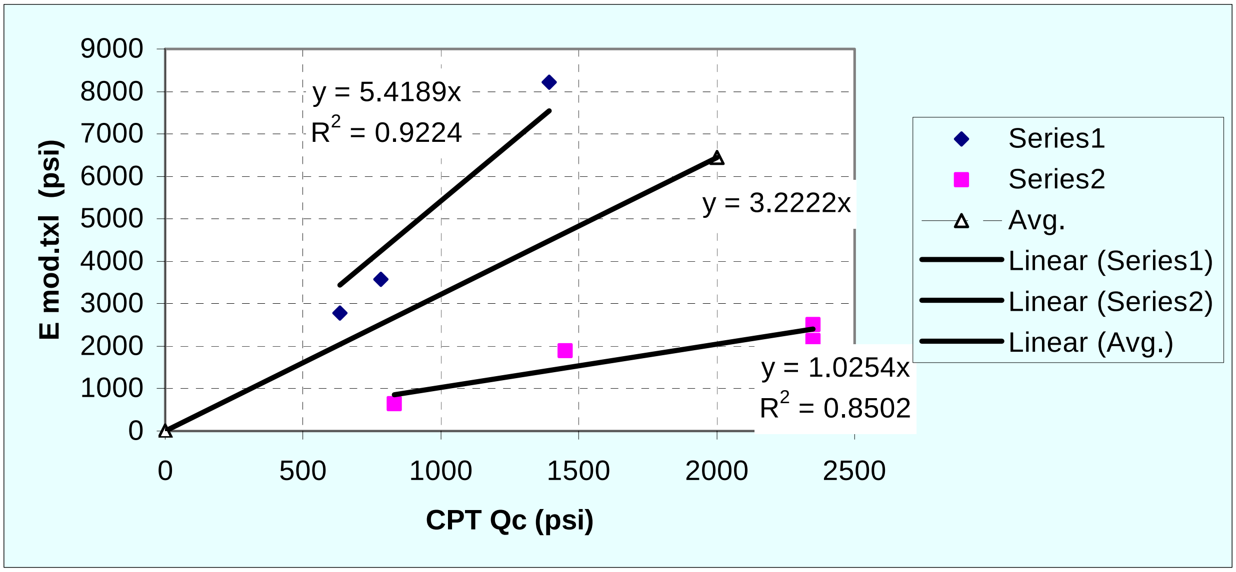


Figure 4.11  Comparison of laboratory triaxial E and CPT $q_c$ .

***Constitutive Behavior – DMT***

Table 4.8 and Figure 4.12 present a comparison of laboratory triaxial $E_{50}$ values vs. DMT-based estimates of E using UF DMT-1 and-2 data . The DMT does not directly measure E, but returns an estimate of the constrained modulus, M. Consequently, one must assume a value of Poisson's ratio (typically $\nu \approx 0.3$) to calculate E. $E = \frac{(1+\nu)(1-2\nu)}{(1-\nu)} M, \approx 0.8 M_{DMT}$, if $\nu = 0.25 - 0.3$. Although Marchetti et al. (2001) shows this relationship between E and $M_{DMT}$, the results presented in Figure 4.12 reveal no correlation between E and $M_{DMT}$.

Table 4.8 Comparison of triaxial E vs. DMT E.

| Triaxial Test ID | $\sigma_{Dmax}$ | $\sigma^{50}_{Dmax}$ | $\varepsilon_{50}$(%) | $E_{50}$ (psi) | $\sigma'_{3f}$ (psi) | σ'o est (psi) | Triax. Mod E (psi) | DMT E $\mu = 0.3$ (psi) |
|---|---|---|---|---|---|---|---|---|
| UF1 | 26.35 | 13.18 | 0.200 | 6588 | 5.31 | 1.56 | 3570 | 10576 |
| UF2 | 27.10 | 13.55 | 1.006 | 1347 | 7.54 | 14.88 | 1892 | 4198 |
| UF3 | 16.95 | 8.48 | 0.946 | 896 | 5.00 | 2.59 | 645 | 8010 |
| UF4 | 54.36 | 27.18 | 0.698 | 3894 | 11.00 | 5.59 | 2776 | 3919 |
| UF5 | 26.10 | 13.05 | 0.262 | 4975 | 6.00 | 16.40 | 8225 | 7581 |
| FDOT 3 | 90.70 | 45.35 | 1.189 | 3814 | 6.00 | 2.59 | 2506 | 29753 |
| FDOT 3 | 46.00 | 23.00 | 1.002 | 2295 | 3.00 | 2.59 | 2133 | 29753 |

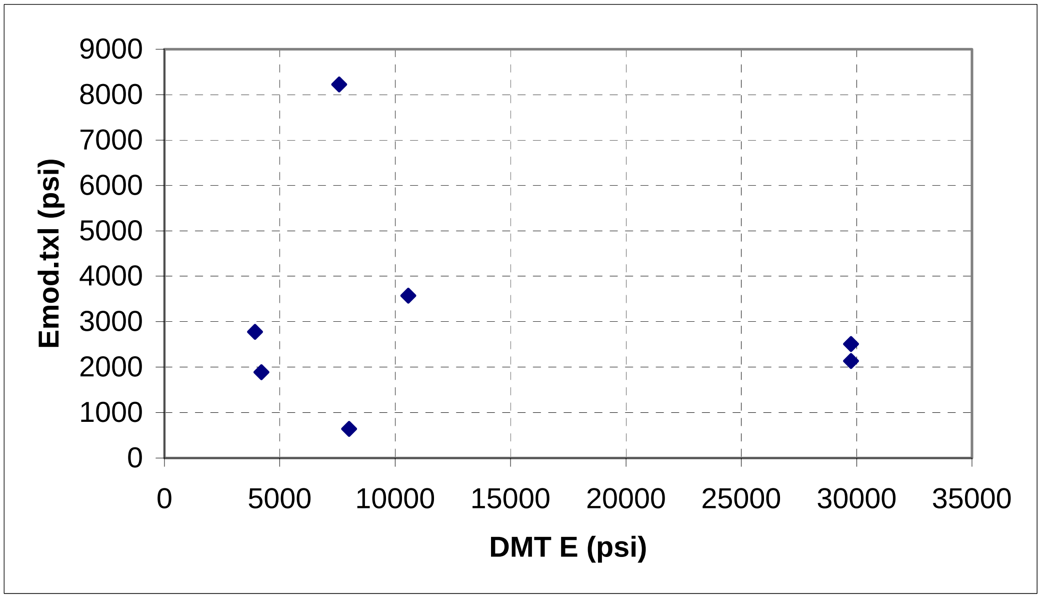


Figure 4.12 Comparison of triaxial based E vs. DMT E values.

*Constitutive Behavior – Consolidation Oedometer Tests*

Seven (6 had useable data) consolidation oedometer tests were performed, from which the constrained modulus, $M = \frac{1}{m_v}$, where $m_v$ = volumetric compressibility or; $\frac{\Delta e}{\Delta \sigma}$ can be obtained. As shown in Table 4.9, the effective overburden stresses, $\sigma_o'$, are quite low. Consequently, the unload-reload portion of the e- log P' curve was used to calculate M.

Table 4.9 Consolidation oedometer - M values vs. E values.

| SPT GEC Boring # | Depth ft | $\sigma'_o$ psi | Consolidation test | Mu-r tsf | E, $\mu$=0.3 psi |
|---|---|---|---|---|---|
| 1 | 7 | 1.56 | 1_2_4 | 125 | 1284.7 |
| | 55.5 | 14.88 | 1_4_1 | 187.5 | 1927.1 |
| 2 | 7 | 2.59 | 2_1_1 | 75 | 770.8 |
| | 18.5 | 5.59 | 2_2_1 | 250 | 2569.4 |
| | 35 | 9.76 | 2_3_4 | 100 | 1027.8 |
| | 56 | 16.4 | 2_4_1 | 33 | 39.2 |

**Summary of Constitutive Parameters**

Figure 4.13 presents a summary of the insitu test estimated and laboratory triaxial and oedometer measured moduli values, E. PMT values are not shown as PMT does not directly provide a modulus, E. Also, Townsend and Anderson (2001) showed E from PMT is a function of $P_L$, for which laboratory and PMT test depths were not compatible. Figure 4.13 results show that the oedometer consolidation test provided the lowest estimates, while DMT tended to be the highest.

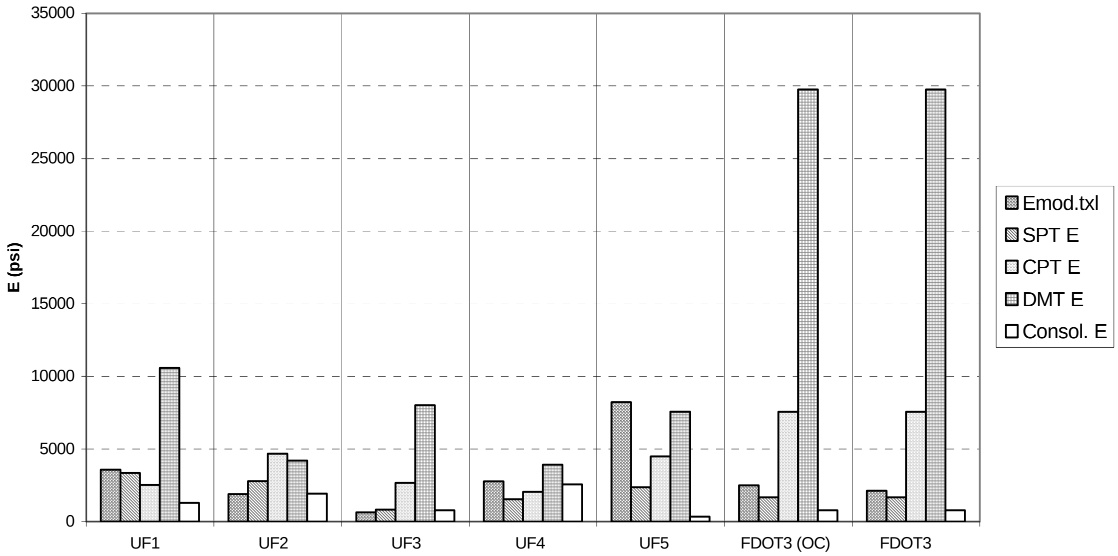


Figure 4.13 Comparison of laboratory vs. insitu moduli estimates.

# CHAPTER 5

# FDOT-UCF SITE - GEOPHYSICAL TEST RESULTS

## TEST SCOPE

There were several non-tested spots at the FDOT-UCF site. Ground Penetration Radar (GPR) profiling was proposed as a solution to increase the amount of data available, and to cover the non-tested areas at the site. The objectives of the testing were:

- Obtain a series of profiles in order to generate a general characterization of the site.
- Compare results with data collected with the CPT, DMT and SPT in order to determine reliability of GPR test.

## TEST LAYOUT

The test was performed by All Coast Engineering, Inc., using a 100 mhz antenna (Ramac GPR) shown in Figures 5.1 and 5.2. A total of 22 scans were made at the FDOT–UCF site. The scans were made from East to West, covering the entire site from North to South. A distance of 15 to 18 feet was left between each pass. Additionally 2 scans were made in diagonal direction. Scan 21, runs from NE corner to SW corner and scan 22 from NW to SE corner. The location of scanning runs is shown in Figure 5.3.

Figure 5.1 Test was performed using the Ramac GPR, a 100 mHz Antenna, shielded with fiber optics in order to avoid external interference.

Figure 5.2  All Coast Engineering Inc., crew performing the test.

Figures 5.4 and 5.5 show that the GPR test had good accuracy in the representation of the upper layers of the soil profile at the FDOT-UCF site. Comparison with data collected with CPT, DMT, and SPT shows total agreement.

The existence of a well-defined layer of silty clay to clayey silt from depth 33 to 50 feet at the entire site, and the location of the water table as high as 1.5 feet below grade introduced attenuation of the signal. Poor information was gathered below a depth of 35 feet.

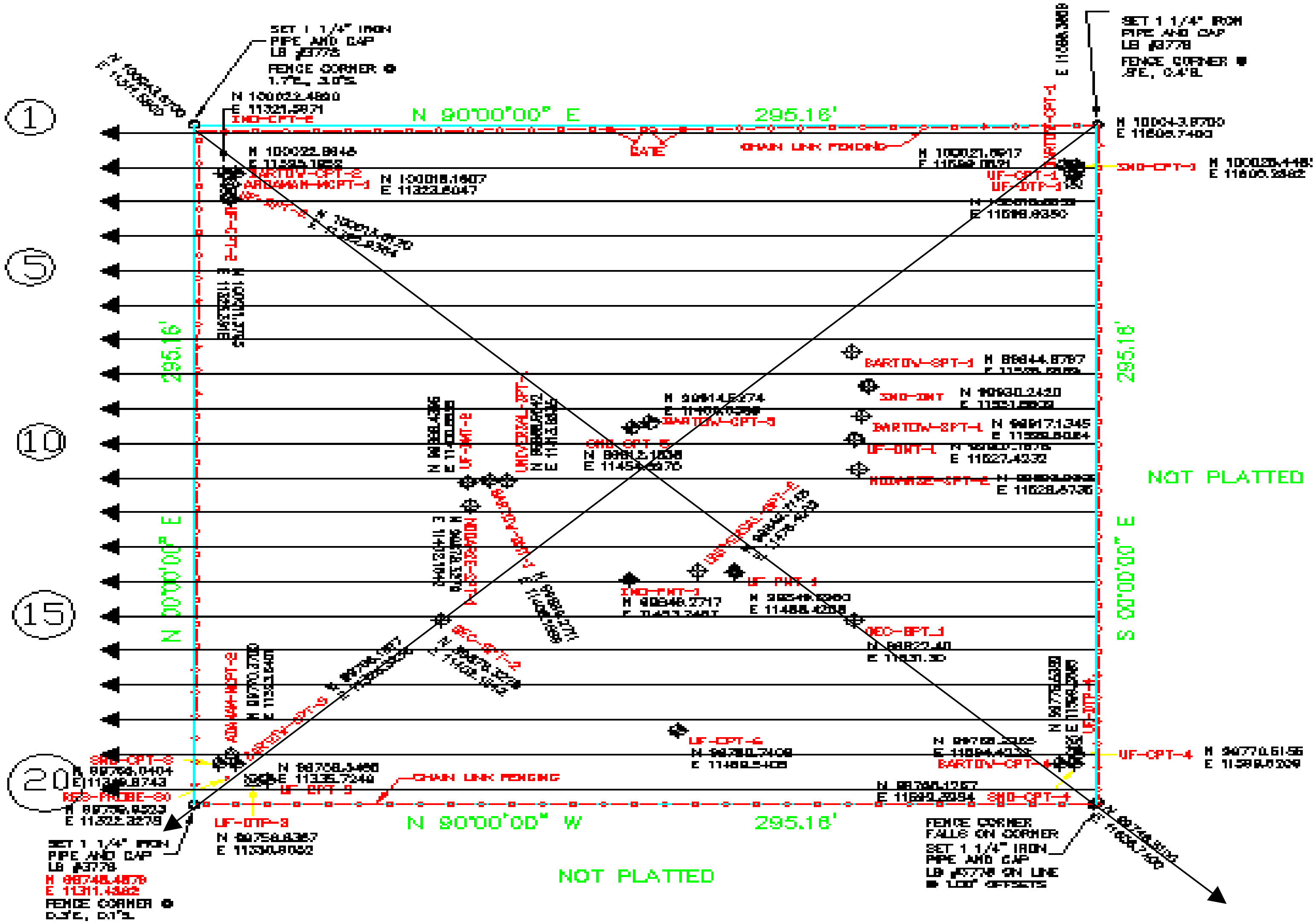


Figure 5.3 Location of GPR Test at FDOT-UCF research.

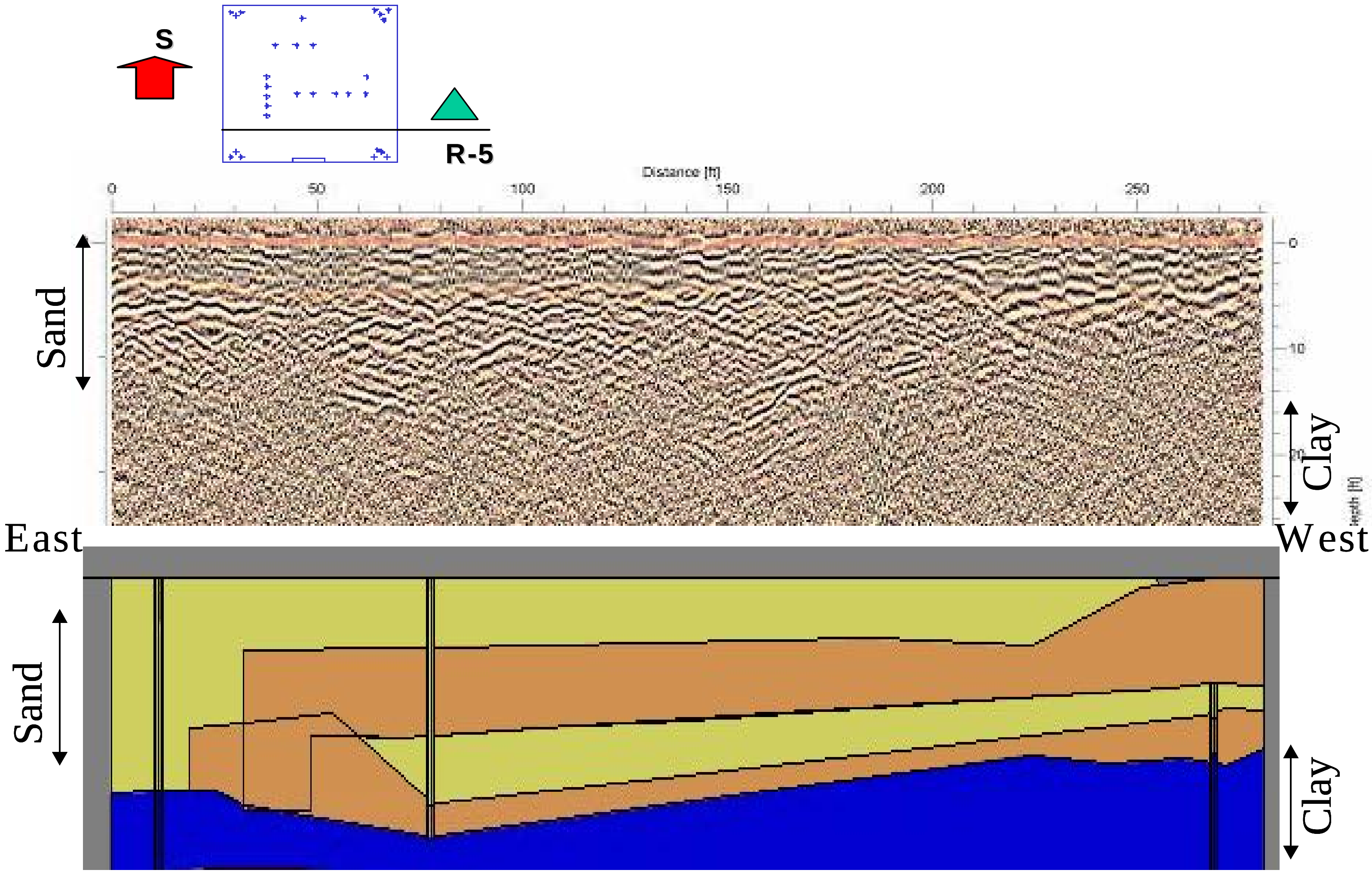


Figure 5.4  Comparison of the GPR output from pass #5 with GMS soil profile at same location – Depth = 0 to 27 ft..

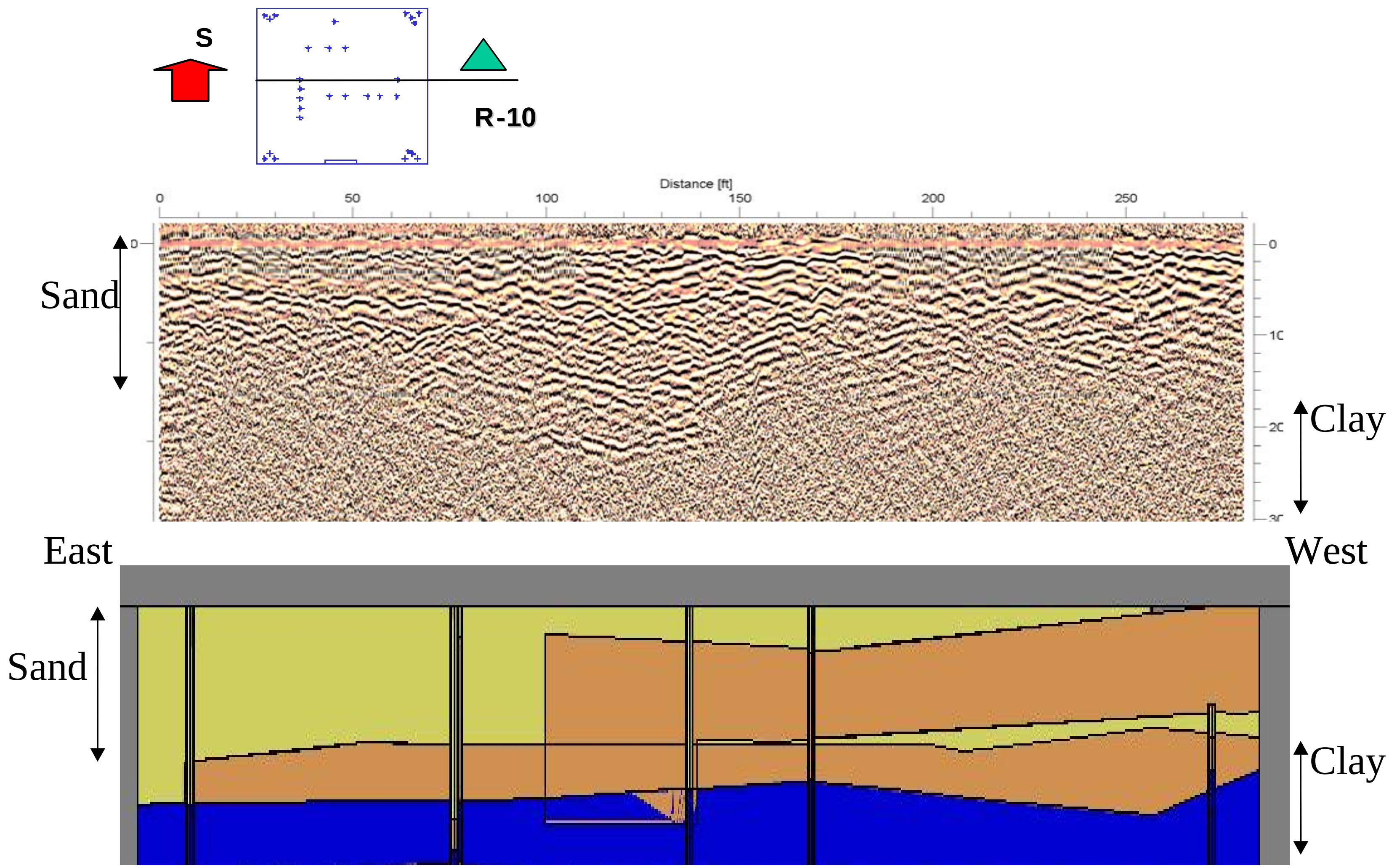


Figure 5.5 Comparison of the GPR output from pass #10 with GMS soil profile at same location – Depth = 0 to 30 ft..

## ELECTRO RESISTIVITY TEST

### Test Scope

Three electro-resistivity surveys were performed at the FDOT-UCF site, as part of the geophysical study. The tests were performed in order to compare results with the reduced data obtained from the insitu testing i.e., SPT, CPT, DMT. The objective was to correlate ER results with other insitu tests.

As was explained in the literature review section, the process of reducing the data obtained with the electro-resistivity test is a trial and error process. The software reduces the data using a fast iterative process (seconds), without introducing error of human interpretation to the results. However, as with any software the computer program requires proper input data from the field. The existence of backup data from other insitu testing techniques is very important in order to obtain good quality comparison results. The main results are stratigraphic profiles, without soil properties.

### Test Layout

#### *Survey (Run) #1*

The test was performed at the center of the site in a South-North direction, perpendicular to the gate. The length of the run was 87 feet (27) m, using a spacing of 3 feet (0.91 m). The North side of the test is located in the immediate vicinity of the SMO and Bartow CPT- 5 test locations. The South side is located in the vicinity of Universal SPT- 2; see Figure 5.6 for location of the test.

Figure 5.7 shows the reduced data obtained from the output of the RES2DINV software, designed for this propose. The plot is a two-dimensional graph of length of the test vs. depth of penetration of the test. On the X-axis bar is shown the number of electrodes used in the test (30) and the spacing between them, 0.91 m (3 feet). The rainbow-colored scale displayed below the graph is the range of true resistivity of the soil, for this specific test.

The two-dimensional profile shows the existence of at least four visible layers.

- From 0 to 2 feet = Sand
- From 2 to 7 feet = Wet sands
- From 7 to 12 feet = Sand to silty sand
- From 12 to 13.8 feet = Sandy clay.

In a comparison of this profile with the data interpretation of the SPT and CPT data in the vicinity of the test, it was determined that the results from the electro-resistivity test were very close to those inferred from the SPT and CPT results. Comparison of the data is shown in Figure 5.7. Further study of the CPT borings results indicates the location of the sandy clay layer to a depth of 5 feet below the depth found in the electro-resistivity profile.

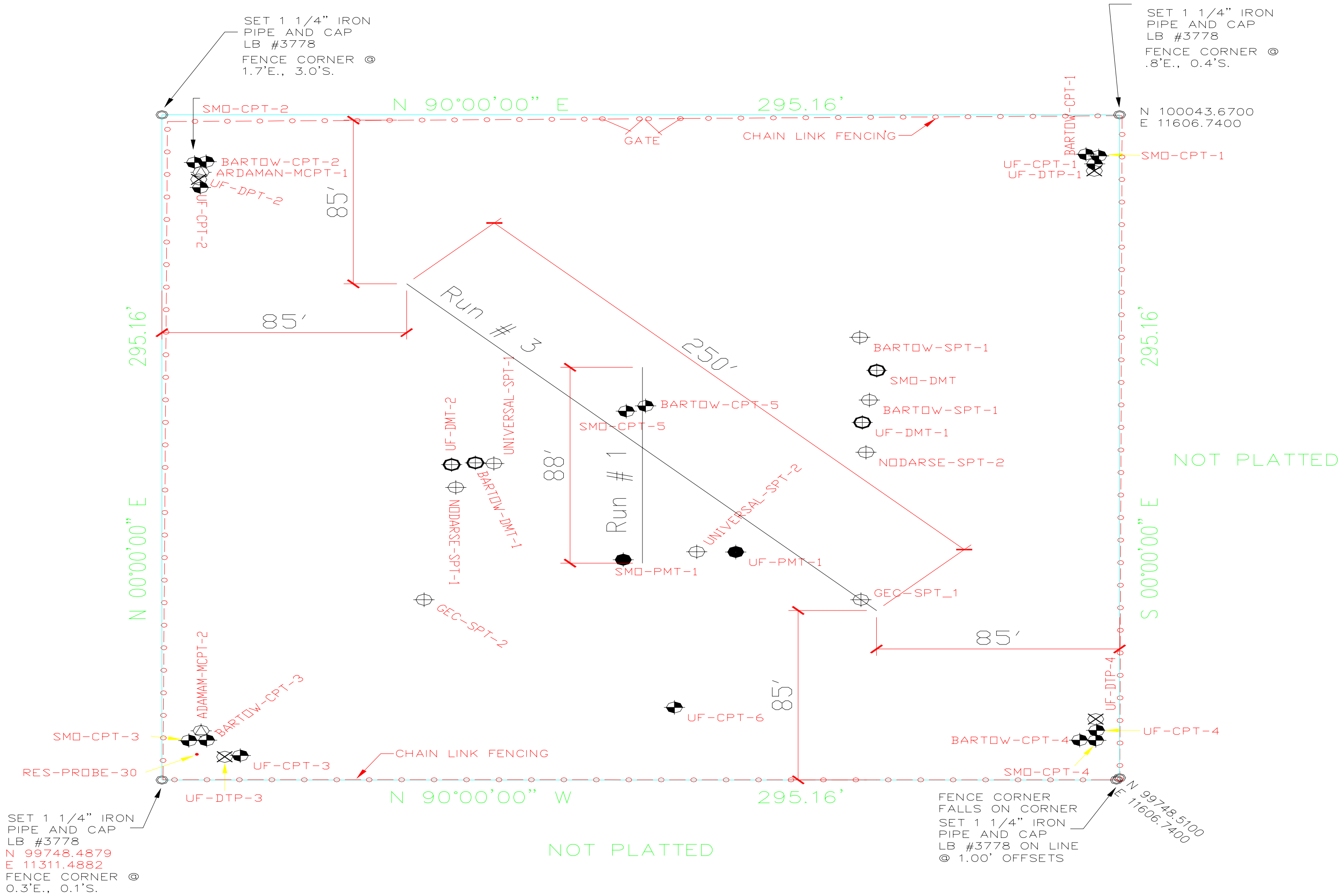


Figure 5.6 Location of electro-resistivity surveys Runs #1 and 3 at the UCF site.

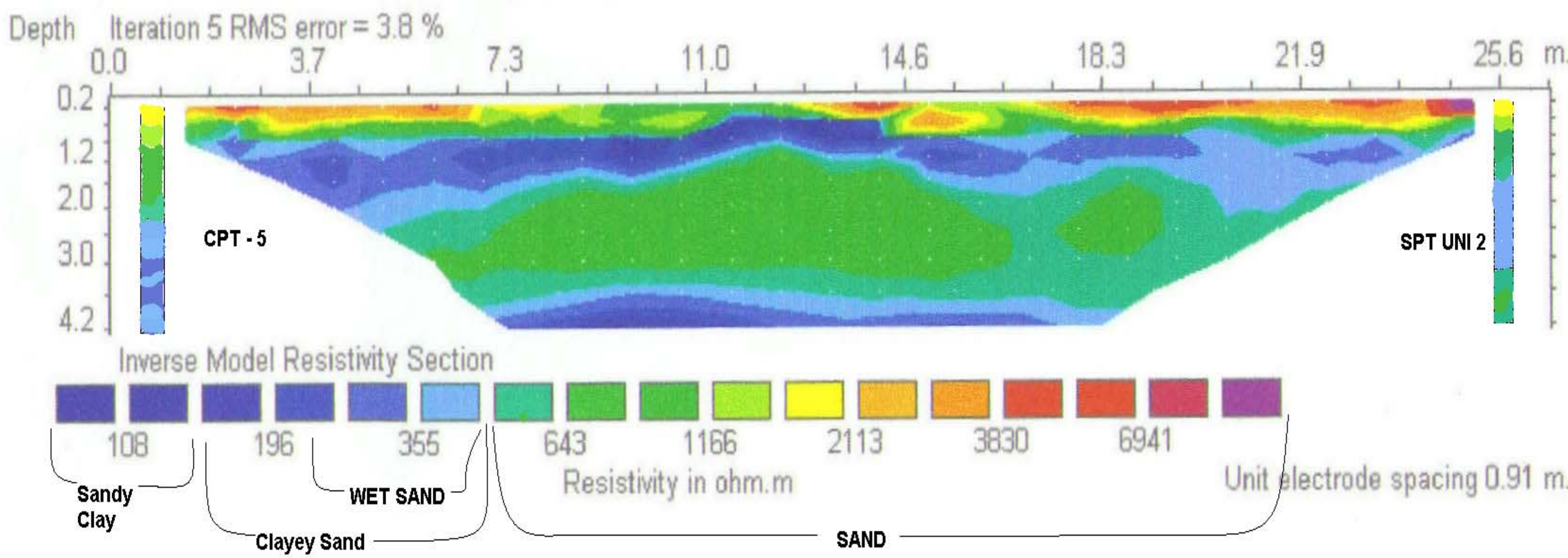


Figure 5.7 Interpretation of soil profile from test Run #1. CPT 5 and SPT Universal 2 was added to figure for visual comparison.

***Survey (Run) #2***

The results obtained from this run were discarded due to corruption of the input data obtained at the site. The performance of the test was affected by the magnetic field created by the perimeter fence. The data reduced by the software did not match the previous information given by the rest of the insitu testing performed at the site. As a result of this experience the personnel of SMO decided to keep a significant distance from the perimeter fence and perform another survey.

***Test Run #3***

The survey was performed at the center of the site in a Southeast-Northwest direction. The length of the run was 250 feet (76) m, using a spacing of 8.9 feet (2.7 m). The center of the test is located in the immediate vicinity of SMO and Bartow CPT- 5 and Universal SPT- 2. The South end is located in the vicinity of GCE SPT- 2. The north end of the test is located in a "blind" area of the site but is close enough to the NW corner to be fairly well represented by the CPT data in that corner. See Figure 5.6 for location of the test.

The results obtained with the use of the RES2DINV software indicate a complex configuration in the soil profile. Visual comparison of this profile with the profile developed for the same area of the site, using of the GMS software indicate a strong similarity of results. A thorough comparison of the data presented using CPT and SPT data in the vicinity of this electro-resistivity survey, confirms that the electro-resistivity test results provide a fairly accurate soil profile for the experimental site area. The profile shown in Figure 5.8 indicates a sand layer that tends to be flat in the Northwest direction merging into a silty sand layer. In the Southeast direction the layer increases in thickness.

The Electro-Resistivity Test has shown good accuracy in the representation of the soil profile at the FDOT-UCF site. The existence of SPT and CPT data was of key importance to properly calibrate the results. Inasmuch as the ER data reduction software is a "signal-matching" operation, knowledge of the site data allowed us to reduce the assumptions in the trial and error inconvenience in the process of selection and calibration of parameters.

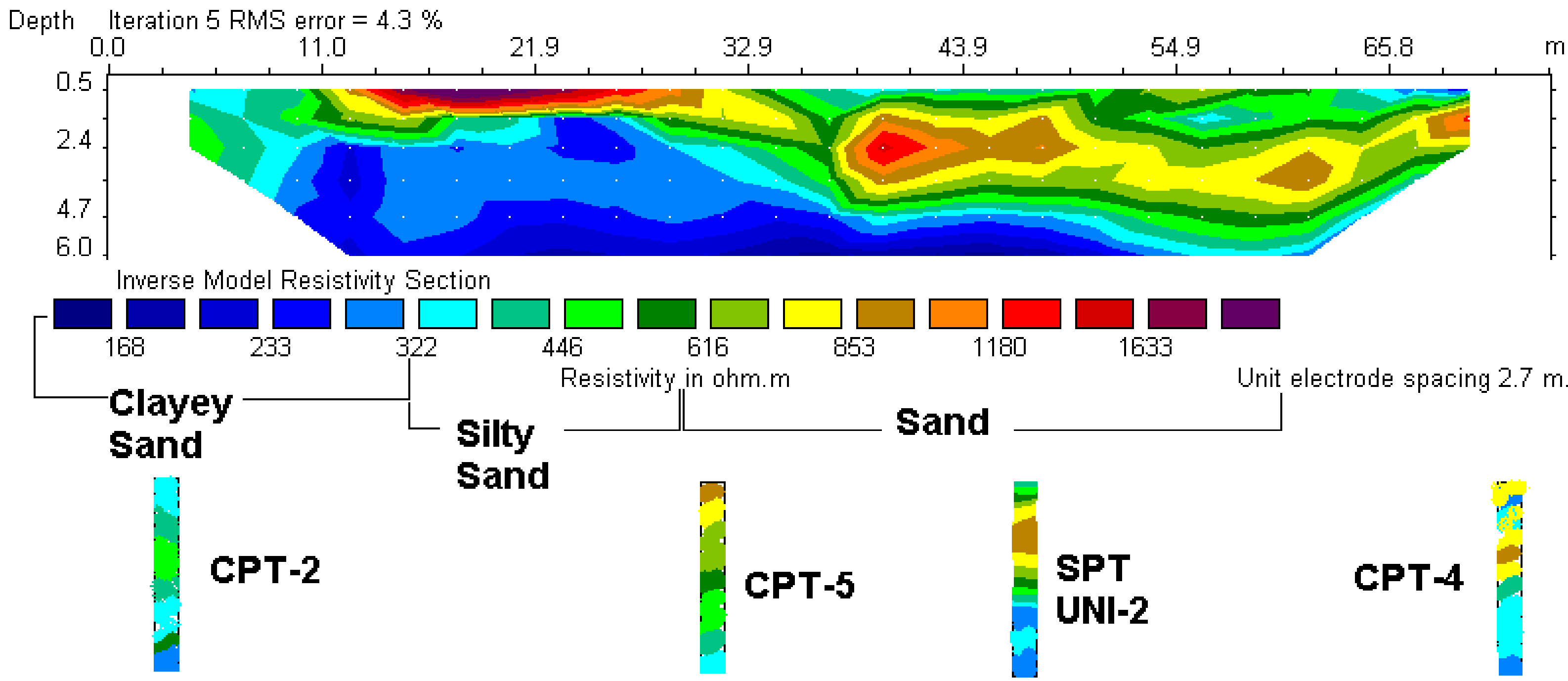


Figure 5.8 Comparison of soil profile from test Run #3 and Insitu Tests

# CHAPTER 6

# PMT TESTING AND CALIBRATION

## FRICTION REDUCER EVALUATION

### Evaluation Plan

To evaluate the friction reducer ring effects, two tips, (one with and one without a friction reducer ring) were tested at two Gainesville sites (cohesive and a cohesionless).

- Lake Alice. A site where UF has performed considerable insitu testing in the last two years as part of the instruction course "CEG-5250 Insitu Measurement of Soil Properties" offered by the University to graduate students every Spring. This site is considered cohesive, mixed with sand and silts. See Figure 6.1 for soil profile.
- The Archer Road Landfill. This cohesionless site has previously been tested by PhD graduates, Brian Anderson and Landy Rahelison.

The evaluation of the friction ring effect required three critical points.

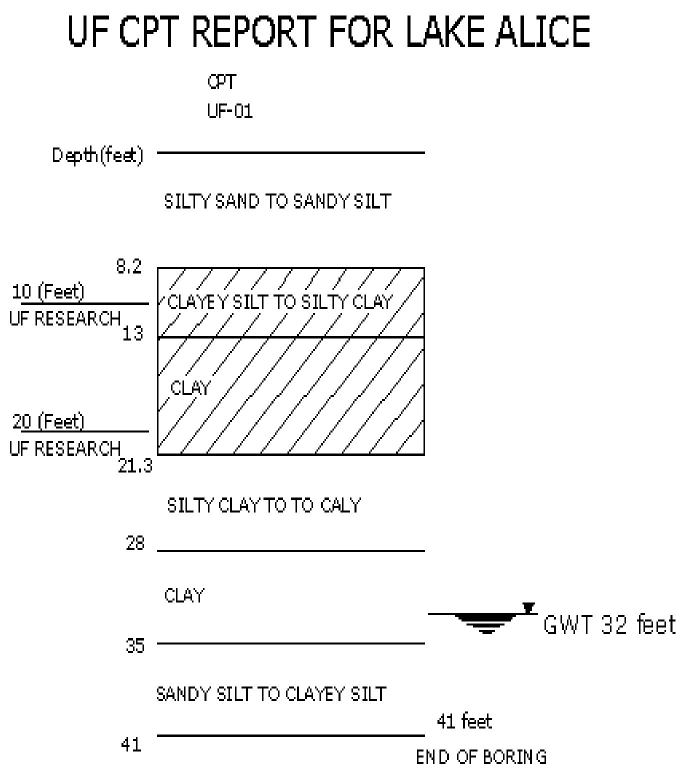


Figure 6.1 Sketch of general soil profile at Lake Alice. Highlighted are the main clay layers tested in this research.

- Uniform site conditions or soil properties. Test performed in a cohesive or in a cohesionless soil.
- Same test and calibration routine.
- Same data reduction procedure.

## TEST COMPARISON (friction reducer ring vs. no friction reducer ring)

### Comparison at Lake Alice (Cohesive Site)

#### *Characteristics of the Site.*

This site is considered cohesive, mixed with sand and silts. The objective was to perform comparison tests at the same depth using the two different cone tips, with and without a friction reducer ring. The tests were performed at depths 5, 10, 20 and 40 feet on two separate boreholes close enough for comparison yet located a safe distance from each other to avoid disturbance. See Figure 6.2 for location of the boring in the area of study. The tests were compared with results of several tests previously performed in the area by UF students. The soil profile at the site is shown in Figure 6.1.

The soil profile shown in Figure 6.1, is based on the interpretation of the data obtained from the reduction of the ECPT test. The relative location of the PMT and ECPT tests used for this research are shown in Figure 6.2. The reduced data are shown on the attached CD. (file: Lake Alice ECPT)

### PMT Test Results - Lake Alice Location

Membrane rupture at the Lake Alice field test site resulted in the use of a different membrane for each test with and without the friction reducer. This situation implied the use of a new calibration and different membranes each time the test was performed.

The following Figures 6.3 to 6.6 show the corrected curves Pressure vs. Volume from pressuremeter test at depths of 5, 10, 20 and 40 feet.

A comparative examination of these PMT results show:

1. The limit pressure, $P_{L,}$ is higher for the ring on tip at the 5, and 40 ft depths. At 10 ft no difference between tips is observed. However, at 20 ft the ring on tip results are lower. Please note that the 5-ft and 40-ft depths are sand, while the 10-ft and 20-ft are in clay.

2. The initial P-V curve is "S"-shaped for the ring on tip at 5, 10, and 20 ft depths. Apparently the ring oversizes the hole and more volume is required for contact between probe and borehole wall. At 40 ft sufficient overburden stress "closes" the hole lessening the volume required for contact.

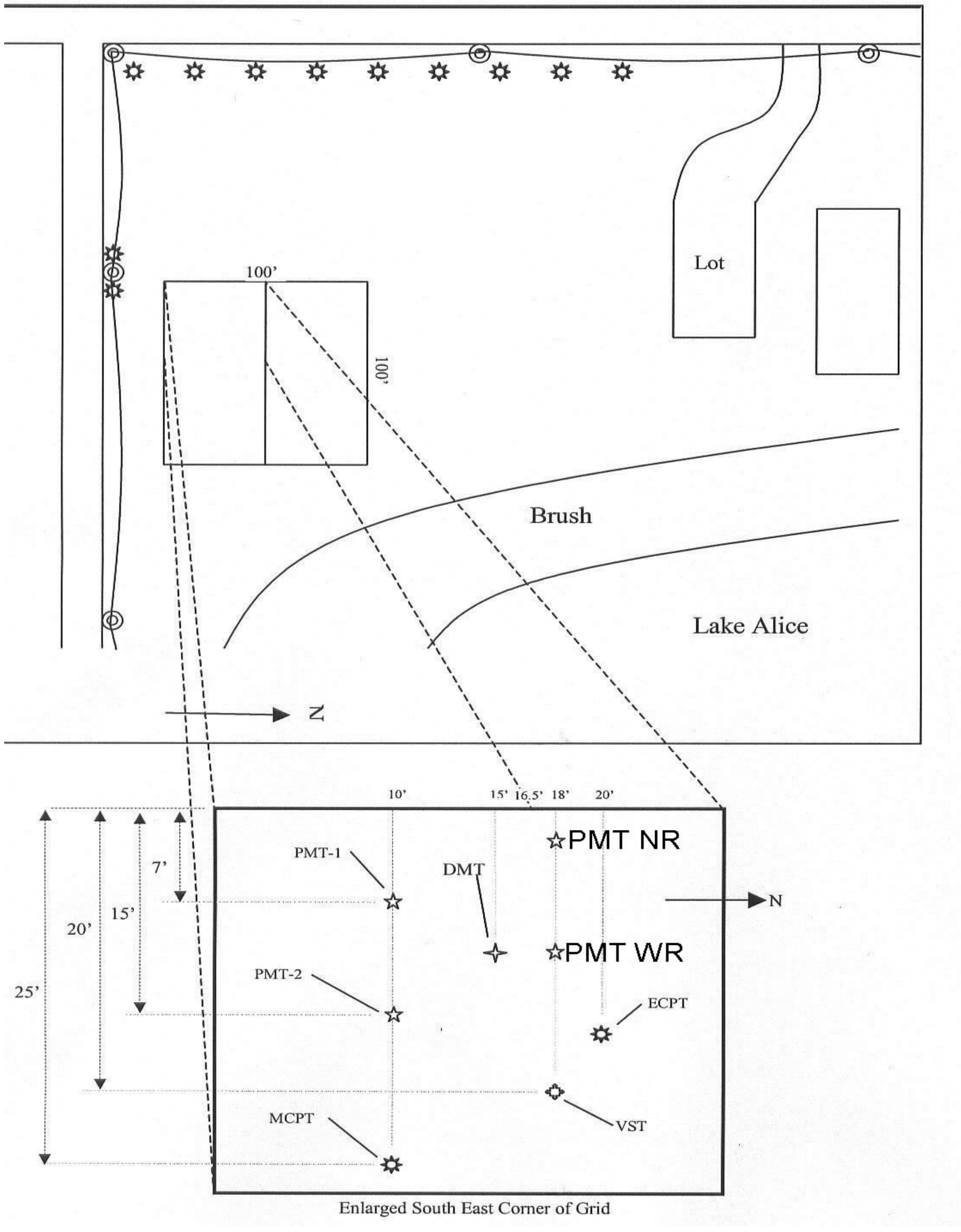


Figure 6.2 Sketch of research site at Lake Alice showing relative location of new PMT testing (denoted NR and WR).

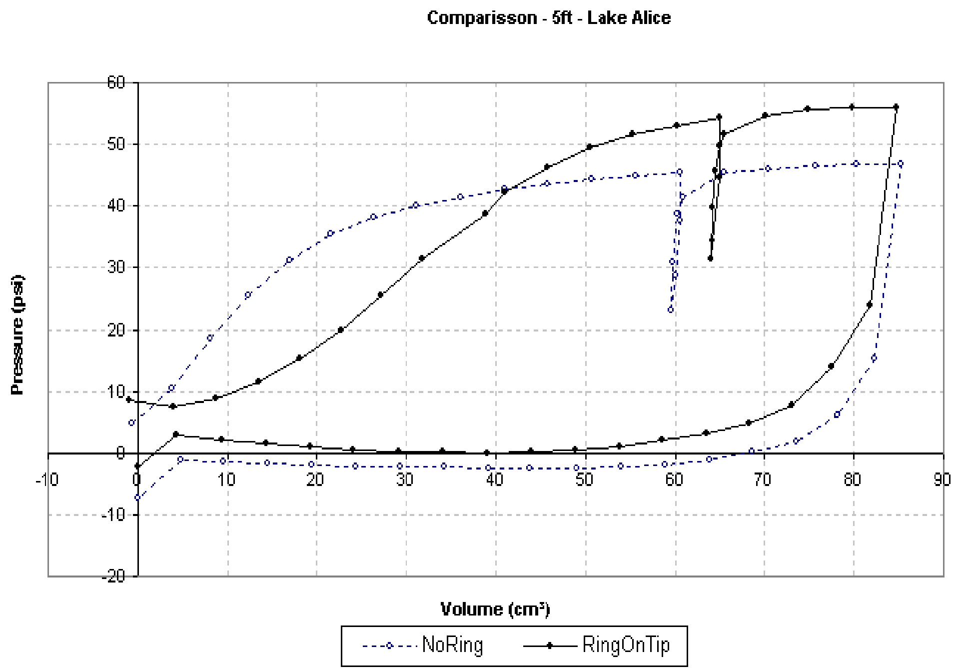


Figure 6.3 Lake Alice comparison of different friction reducer at depth of 5 feet.

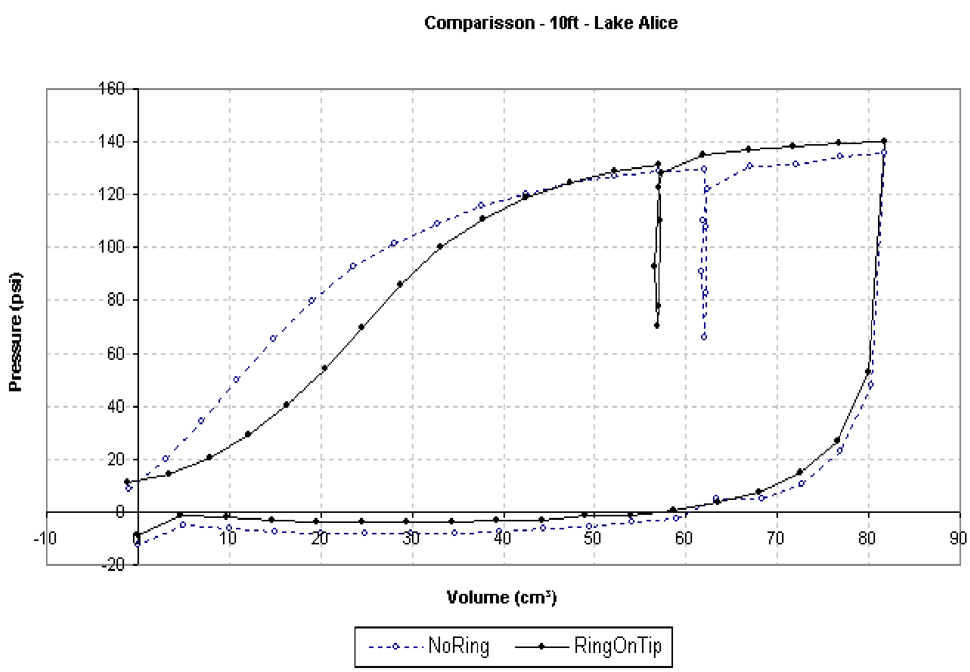


Figure 6.4 Lake Alice comparison of different friction reducer at depth of 10 feet.

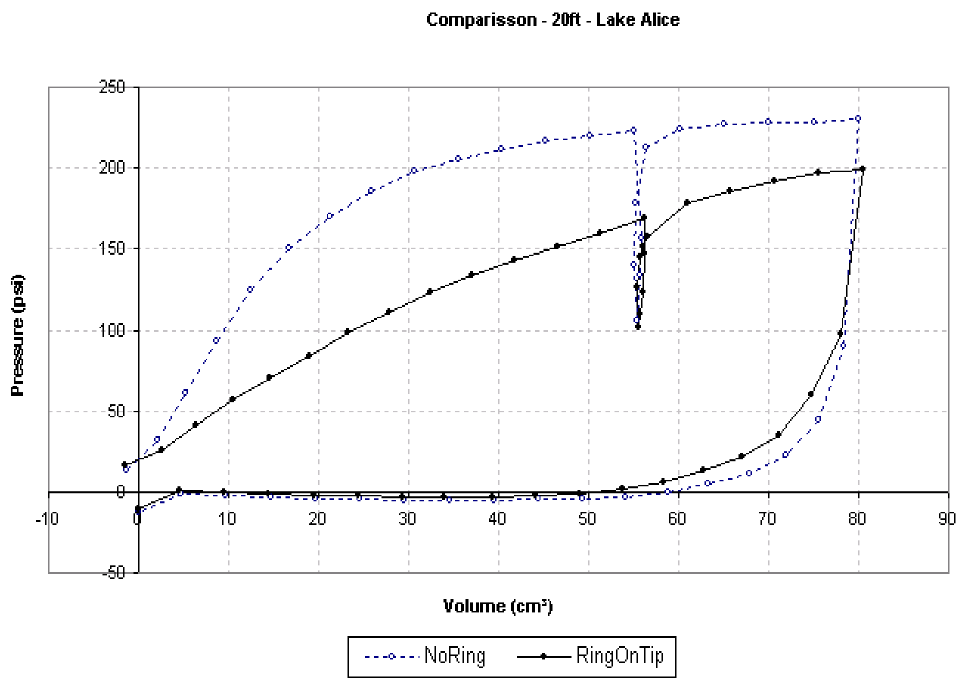


Figure 6.5 Lake Alice comparison of different friction reducer at depth of 20 feet.

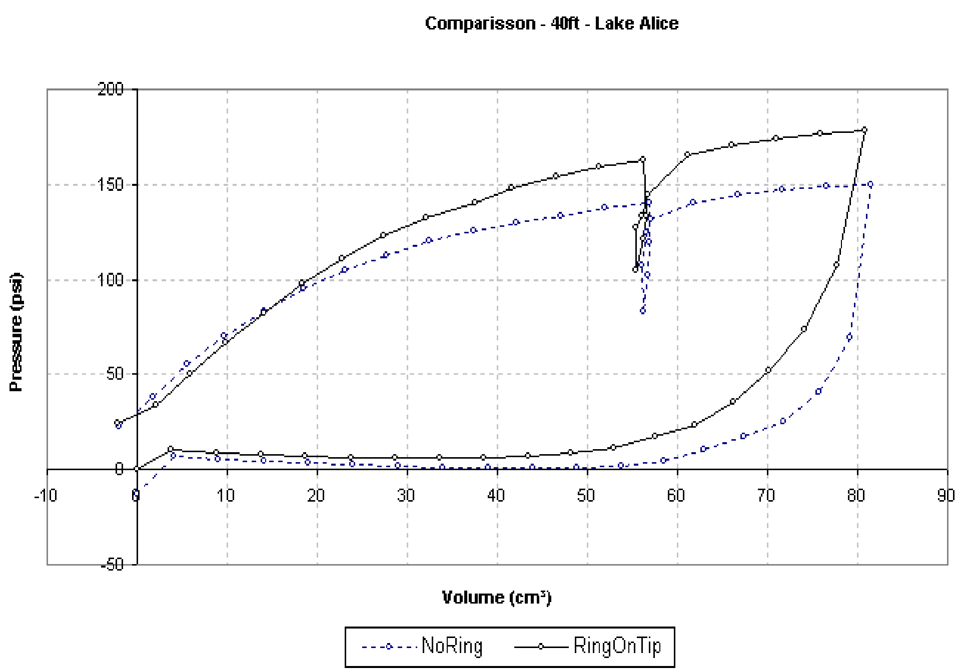


Figure 6.6 Lake Alice comparison of different friction reducer at depth of 40 feet.

The data reduction from the tests show that only at the depth of 20 feet below grade, is an obvious discrepancy observable between the test results using the two different tips. Thus, the results of the comparison data between the two different tips do not indicate significant differences between the two tests. This result indicates that the friction reducer ring has no significant effect in cohesive soils. Consequently, the finding of "no difference" eliminates the friction reducer ring as being the reason for the difference observed between the UF and SMO PMT tests at the FDOT-UCF site.

**Comparison at Archer Landfill (Cohesionless Site)**

For several years the Archer Landfill has been used by UF to conduct insitu testing research. The landfill site is essentially forty feet of sand overlying limerock. A sketch of the site general profile is shown in Figure 6.7

The objective again was to perform comparison tests at depths previously studied, using the two different cone tips; i.e., with and without a friction reducer ring. The tests were performed at depths of 5, 10, and 20 feet in two separate boreholes close enough for comparison yet located sufficiently far apart to avoid influence from the results of the adjacent borehole location.

A sketch of the approximate location of the research site is shown in Figure 6.8. Additional insitu test data from the CPT can be found on the attached CD.

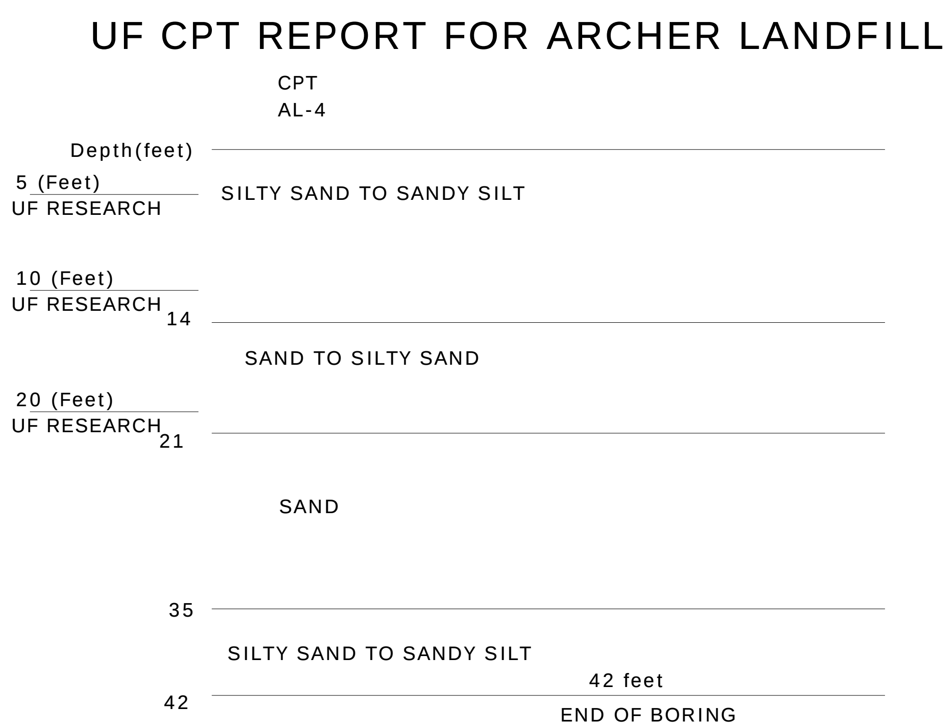


Figure 6.7 Archer Landfill Soil profile based CPT data from previous research.

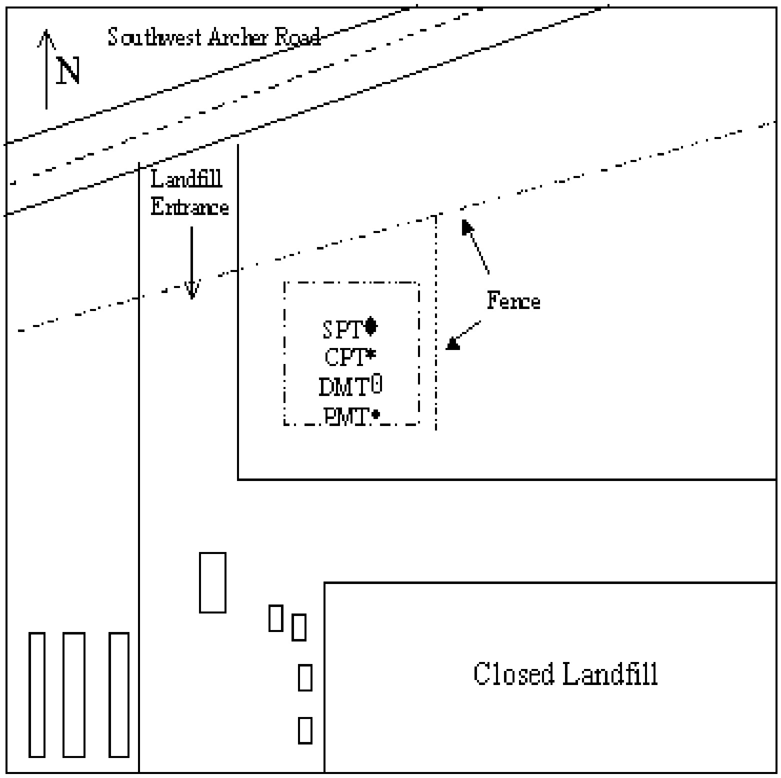


Figure 6.8 Location of research site at Archer Landfill.

**Test Conditions and Results from Work at Lake Alice Location**

In the case of the Archer testing site the circumstances were propitious for utilizing the equipment belonging to UF and FDOT, which simulates the actual conditions at the FDOT-UCF site; i.e., use of a different probe and operator for each test with and without the friction reducer. This situation implied the use of a new calibration and different membrane each time the test was performed.

Due to the poor quality and variability in the results of the data collected using the ring tip, it was necessary to substitute these data with ones collected by Anderson (2001) in previous research. The 20 feet mark was fixed as the limit depth of testing, due to the lack of data at greater depths, from the previous report.

Figures 6.9 to 6.11 show the comparisons of the corrected PENCEL Pressuremeter curves. (file Archer –FDOT (no ring) vs. UF (ring))

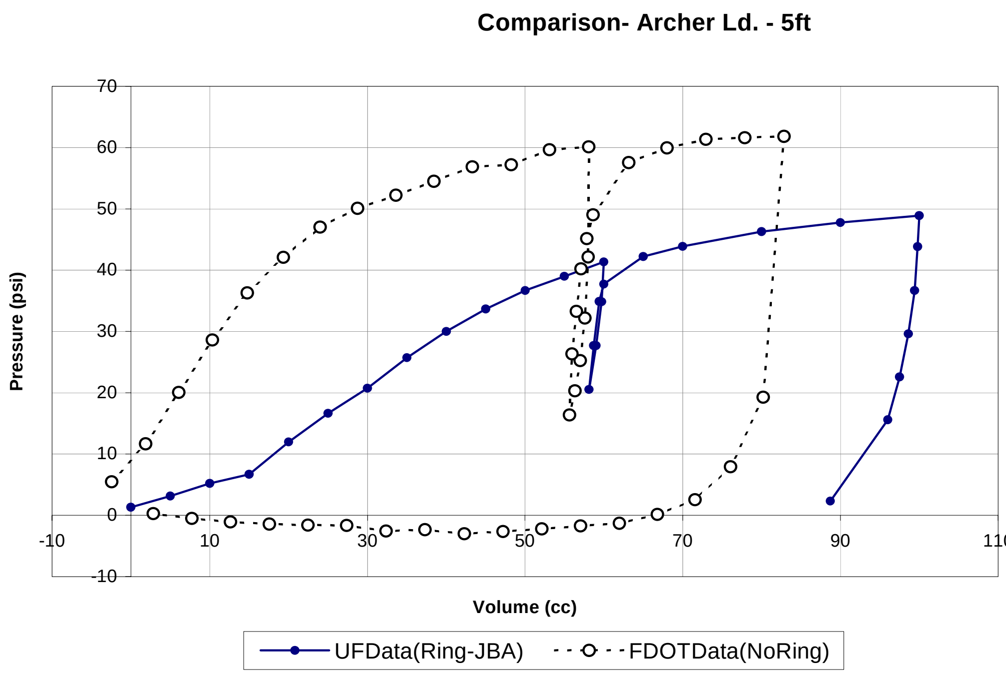


Figure 6.9 Archer Landfill comparison of different friction reducer at depth 5 feet.

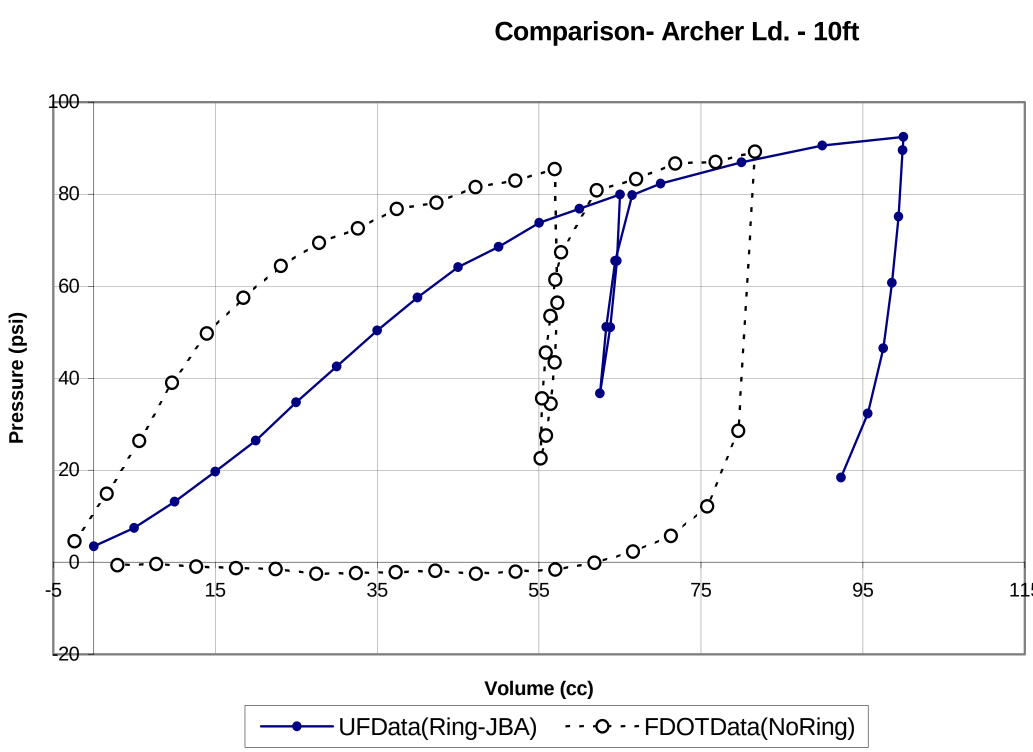


Figure 6.10 Archer Landfill comparison of different friction reducer at depth 10 feet.

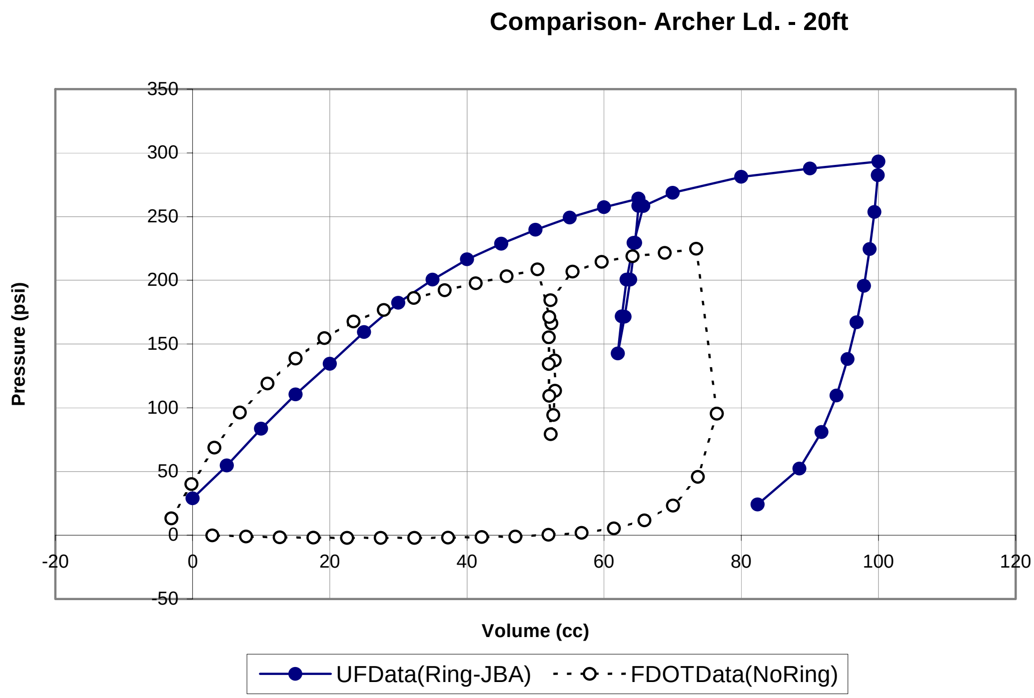


Figure 6.11 Archer Landfill comparison of different friction reducer at depth 20 feet.

Based on the information collected and data shown in Figures 6.9 to 6.11, it is concluded that:

1. At the shallow 5-ft depth the ring on tip produces lower $P_L$ values. At 10-ft there is no effect, and at 20-ft. the ring on tip produces higher $P_L$ values. An explanation for this behavior is; (a) at the shallow depths the surface sands are lightly cemented and the larger ring over-stresses and fractures the cementation resulting in a lower $P_L$, (b) at the greater depths the additional confinement due to the overburden allows the ring to over-stress (over-consolidate) the soil causing a greater $P_L$. However, the 5-ft. results in sand at Lake Alice did not follow this behavior, as the ring on tip gave a higher $P_L$.

2. For the two shallower depths, the ring on tip produces an initial "S"-shaped curve representing a larger borehole and the additional volume required to make contact. However, for the greater depths the larger lateral stresses tend to close the borehole after the ring passes.

3. Table 6.1 presents the moduli comparisons, and reveals little difference due to the tip type. Originally, when the ring on tip was developed for membrane protection, it was assumed that moduli values would be unaffected. Similarly, the Lake Alice site also shows little differences in moduli values based upon tip type.

Table 6.1 Comparison (Ei) at Archer Landfill site.

| Depth (ft) | Ei PMT Pencel (psi) | |
|---|---|---|
| | Research | B. Anderson |
| | No Ring tip | Ring tip |
| 5 | 512 | 591 |
| 10 | 1188 | 1074 |
| 20 | 3349 | 3719 |

### Effect of Tip Type on p-y Curves

Initially the ring on the tip was to minimize membrane breakage caused by limestone fragments prevalent to Florida. Previous UF research for FDOT using the PMT to develop p-y curves used ringed tips. The p-y curve used 10 points from the unload-reload portion of the pressure vs. volume curve. The thought was that although the ring on the tip over bored the hole upon reloading, the effect would be minimal. These previous comparisons show that the ring significantly affects the $P_L$ and consequently the p-y curve. However, the initial portion of the curve along the unload – reload part is not affected. That is to say only the portion of the p-y curve responsible for large deformations is affected. Fortunately, the effects of the ring on tip are smallest for the shallow depths, and it is the p-y curves at the shallow depths that are most influential on the pile head deformations.

Consequently, if the PMT data are to be used for obtaining modulus values or p-y curves, use of the friction ring is up to the discretion of the operator as little effect by the ring was observed for these applications.

# CHAPTER 7

## PMT INTERAGENCY COMPARISONS AND WORKSHOP RESULTS

### BACKGROUND

The Task 2 objective of the project was to resolve the differences in testing results between SMO and UF that were observed at the FDOT-UCF site. All PMT tests reported in this chapter were performed **without** a friction reducing ring on the tip. Accordingly,

1. Companion PMT tests were performed by SMO and UF at the previously mentioned Archer Landfill (cohesionless) site.
2. In addition, a PMT workshop was held June 12 – 13, 2003 during which companion PMT tests were performed by FDOT- SMO, UF, Prof. Paul Cosentino (FIT), and Prof. J. Brian Anderson (UNCC).

### PMT RESULTS – ARCHER LANDFILL

The Archer Landfill site was previously described in Chapter 6. Companion PMT tests were performed by FDOT- SMO and UF at depths of 5, 10, 20, and 40 ft. Figures 7.1 to 7.4 present the pressure–volume test results (file Archer-FDOT vs. UF No ring.xls). Table 7.1 summarizes the comparisons (file: Archer-summary.xls). As shown, there is excellent agreement between the testing agencies at depths of 5, 10, and 20-ft. The tests at 40-ft are discredited as a valid comparison, in that, the stiff limestone bedrock was encountered and consequently different materials most likely were tested.

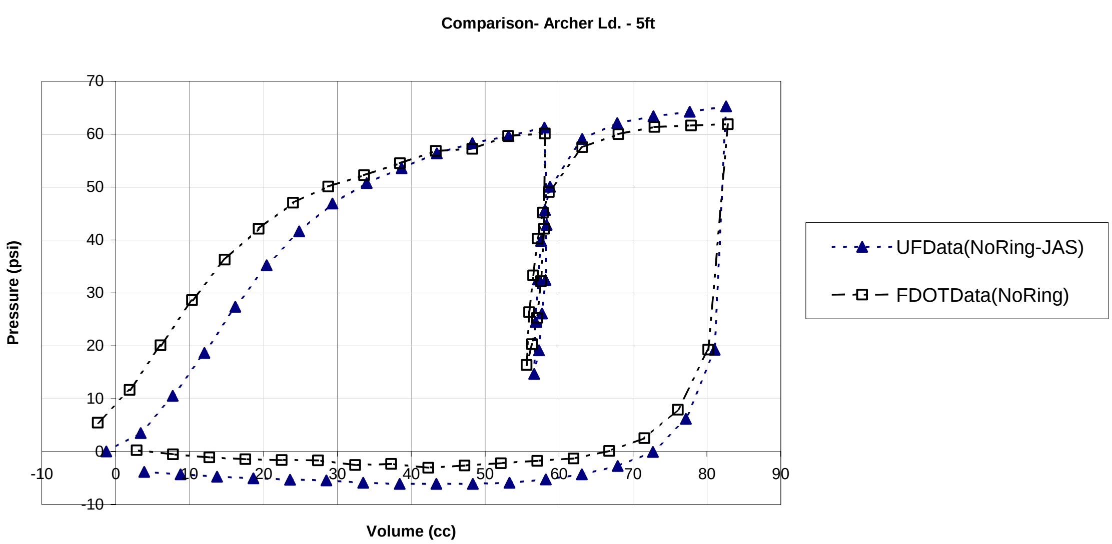


Figure 7.1 Comparison of FDOT-SMO vs. UF PMT at 5-ft depth.

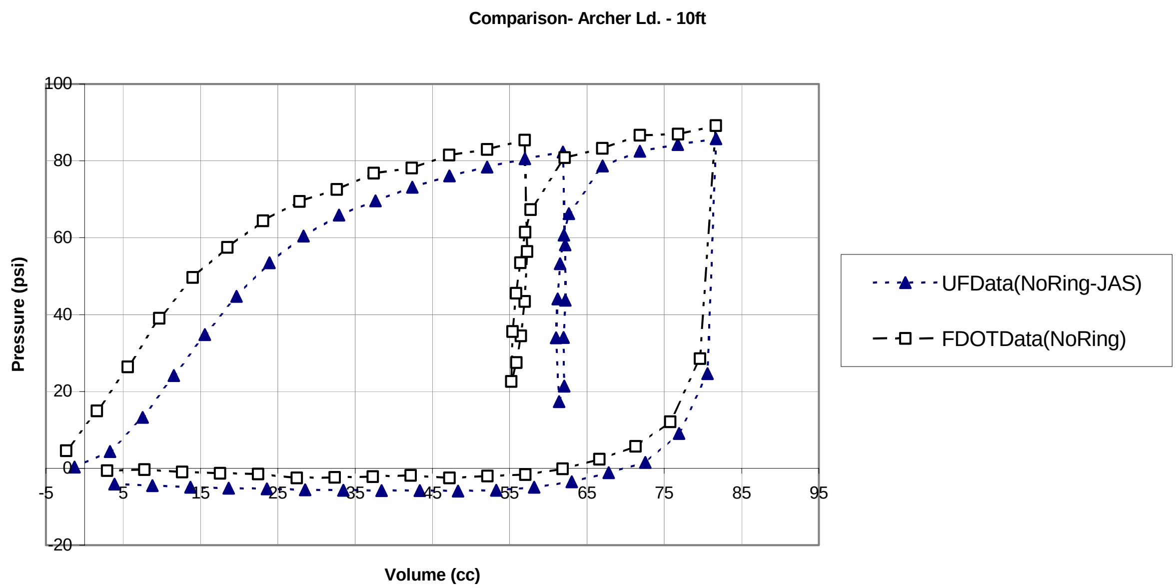


Figure 7.2 Comparison of FDOT-SMO vs. UF PMT at 10-ft depth.

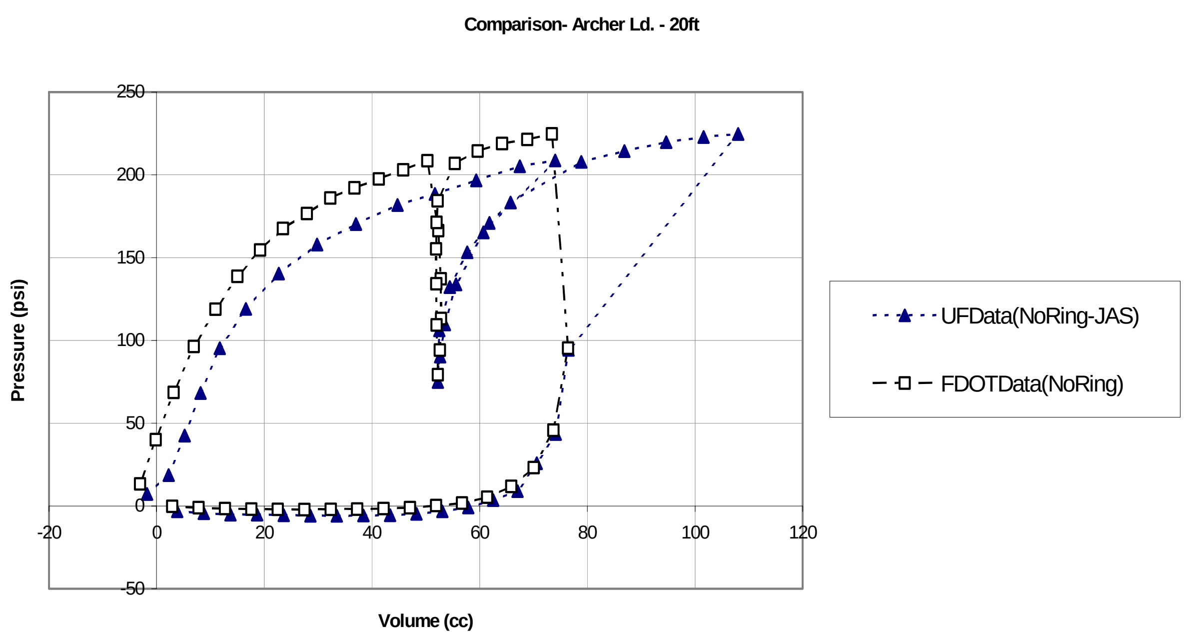


Figure 7.3 Comparison of FDOT-SMO vs. UF PMT at 20-ft depth.

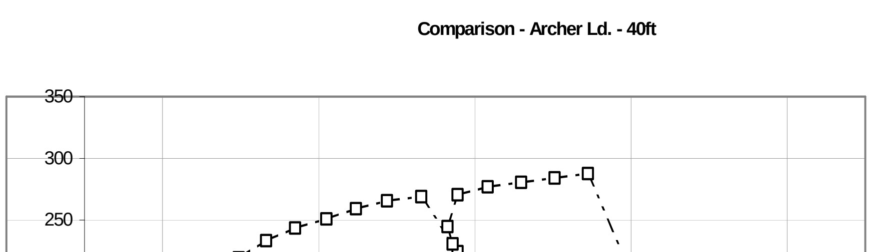

Figure 7.4  Comparison of FDOT-SMO vs. UF PMT at 40-ft depth.

**PMT RESULTS – LAKE ALICE**

The description of the Lake Alice testing site has been previously presented in Chapter 6. As part of the PMT workshop 4 agencies: FDOT-SMO, UF, FIT, and UNCC performed PMT tests at depths of 5, 10, 20, and 40-ft.  The 5 and 40-ft depths are sandy, while the 10 and 20-ft depths are clay.  The ground water table is at 27.5 ft.  All agencies were individually responsible for their calibrations and data reduction.  However, FDOT, UF, and UNCC used similar methods and spreadsheets, as developed by Dr. Anderson's PhD research.  Figures 7.5 – 7.8 present the testing comparisons (file: Lake Alice – FDOT vs UF vsUNCCvsFIT-No Ring-modif).

Unlike the Archer Landfill results, which produced excellent agreement between just 2 agencies, these figures reveal considerable discrepancy between the testing agencies.  Figure 7.9 summarizes the limit pressure values.  This figure shows:

1. At 5-ft, there is good agreement for 3 agencies, except FIT's value is lowest

2. At 10-ft, there is good agreement for 3 agencies, except UF's value is lowest

3. At 20-ft, FDOT and UNCC agree with the highest values, and FIT's value is lowest

4. At 40-ft, there is no agreement with UNCC being the highest and FDOT being the lowest.

Table 7.1 Comparison of limit pressure and moduli values FDOT-SMO vs. UF Archer Landfill.

DATE OF CALIBRATION (UF): 6/02/2003

COMPARISON OF PPMT DATA: FDOT vs. UF NO RING ON TIP ARCHER LANDFILL

| Soil Parameters | Depth: 5 ft | | | Depth: 10 ft | | | Depth: 20 ft | | | Depth: 40 ft | | |
|---|---|---|---|---|---|---|---|---|---|---|---|---|
| | FDOT Data | UF Data | % Differ-ence | FDOT Data | UF Data | % Differ-ence | FDOT Data | UF Data | % Differ-ence | FDOT Data | UF Data | % Differ-ence |
| E (psi) | 751 | 786.6 | 4.5 | 1136.9 | 1041.2 | 8.4 | 3088.7 | 3148.9 | 1.9 | 3939.1 | 1816.9 | 53.9 |
| Po = $\sigma_{oh}$(psi) | 11.6 | 10.5 | 9.5 | 14.9 | 13.3 | 10.7 | 13.3 | 19.7 | 28.9 | 19.1 | 20.9 | 8.6 |
| $P_L$ (psi) | 62.5 | 67.1 | 6.9 | 91.9 | 91.3 | 0.7 | 237.5 | 219.6 | 7.5 | 300 | 175.7 | 41.4 |
| $P^*_L$ (psi) | 50.9 | 56.6 | 10.1 | 77 | 78 | 1.3 | 224.2 | 200.9 | 10.4 | 280.9 | 154.8 | 44.9 |
| $E/P^*_L$ | 14.8 | 13.9 | 6.1 | 14.8 | 13.3 | 10.1 | 13.8 | 15.7 | 12.1 | 14 | 11.7 | 16.4 |
| $\alpha$ | (1/2) | (1/2) | | (1/2) | (1/2) | | (1/2) | (1/2) | | (1/2) | (1/3) | |
| Eo (psi) = E/$\alpha$ | 1502 | 1573.2 | 4.5 | 2273.8 | 2082.4 | 8.4 | 6177.4 | 6297.8 | 1.9 | 7878.2 | 5450.7 | 30.8 |
| | | | | | | | | | | | | |
| Vo (cc) | 1.9 | 7.7 | | 1.6 | 7.5 | | -3.1 | 2.2 | | -3.6 | 2.1 | |
| Vf (cc) | 14.7 | 20.4 | | 9.7 | 19.7 | | 6.9 | 8.2 | | 5.9 | 12.9 | |
| Po (psi) | 11.6 | 10.5 | | 14.9 | 13.3 | | 13.3 | 18.7 | | 19.1 | 20.9 | |
| Pf (psi) | 36.3 | 35.2 | | 39 | 44.8 | | 96.3 | 68.3 | | 120.2 | 71.6 | |

Comparisons - Lake Alice - 5ft - No ring on tip

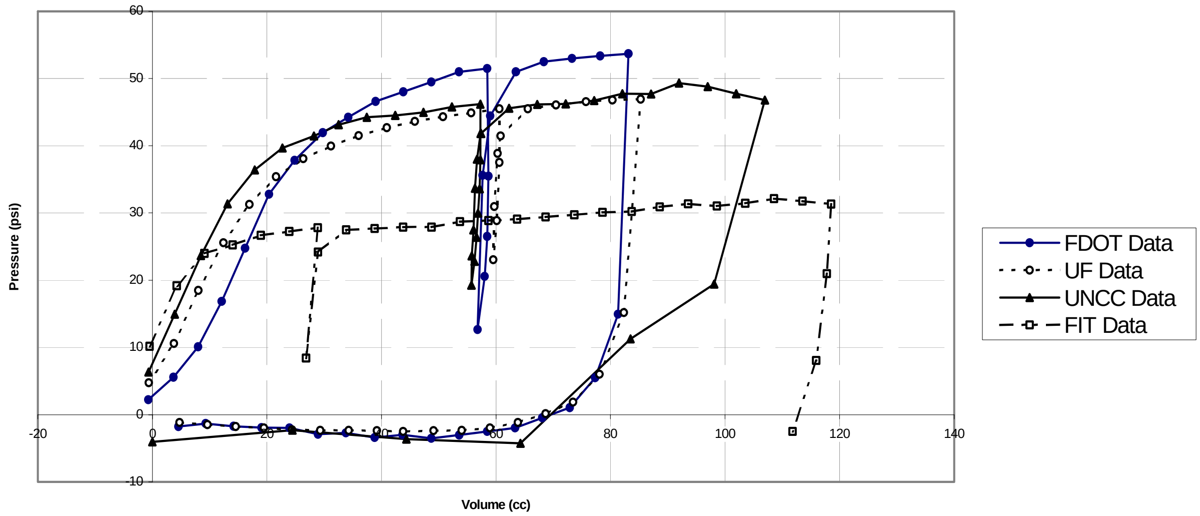


Figure 7.5 Comparison of FDOT-SMO vs. UF vs. UNCC vs. FIT at 5-ft depth.

Comparisons - Lake Alice - 10ft - No ring on tip

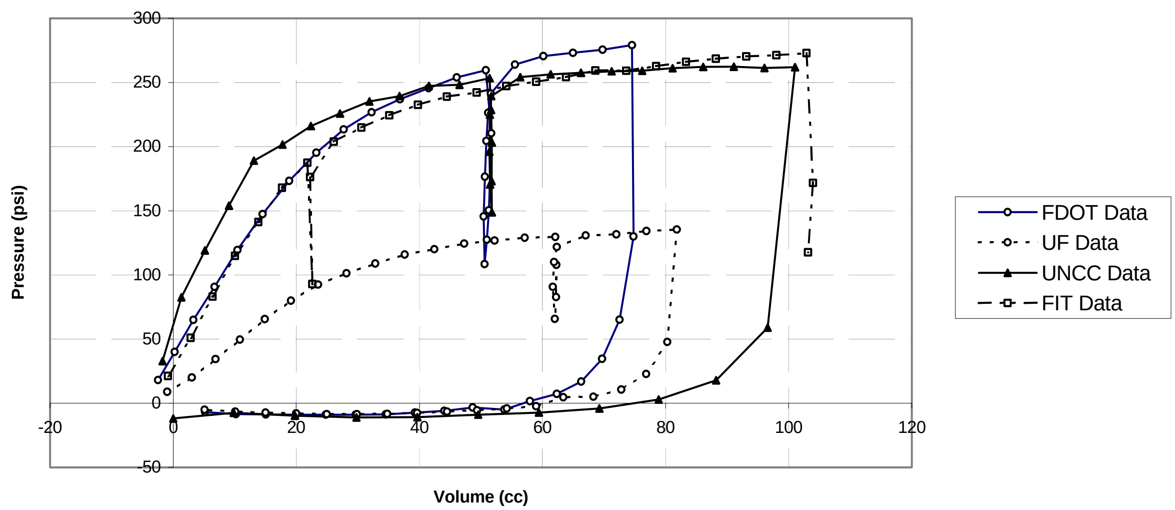


Figure 7.6 Comparison of FDOT-SMO vs. UF vs. UNCC vs. FIT at 10-ft depth.

Comparisons - Lake Alice - 20ft - No ring on tip

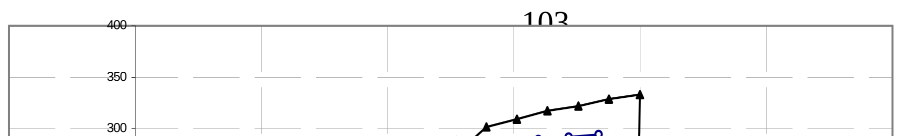

Figure 7.7  Comparison of FDOT-SMO vs. UF vs. UNCC vs. FIT at 20-ft depth.

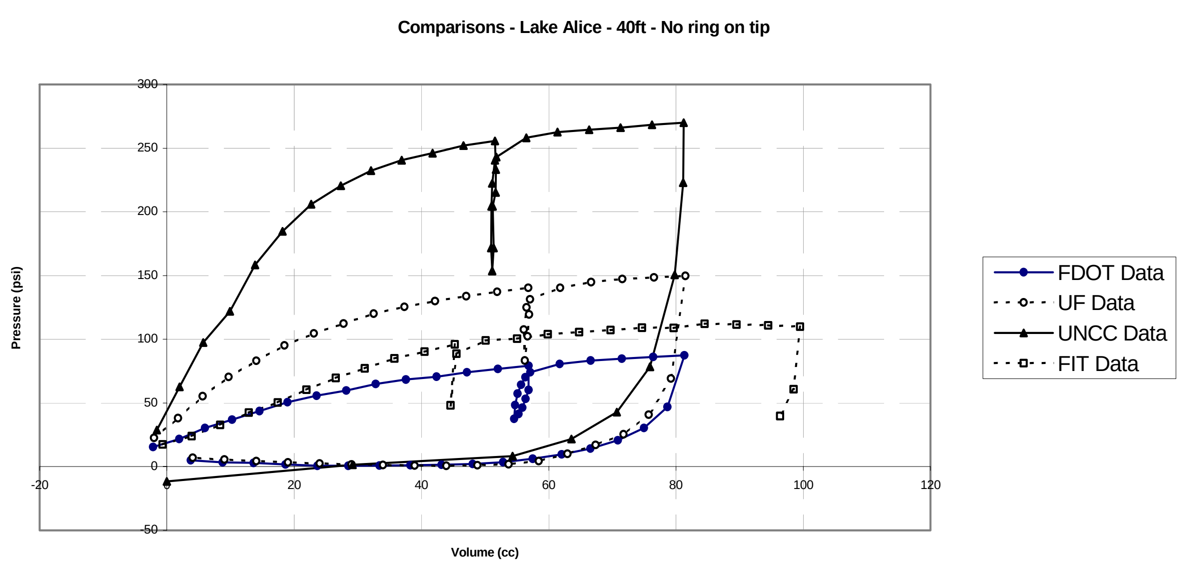


Figure 7.8  Comparison of FDOT-SMO vs. UF vs. UNCC vs. FIT at 40-ft depth.

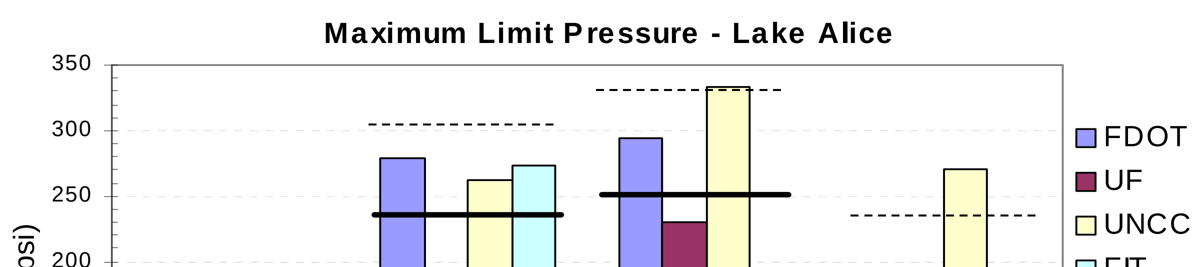

Figure 7.9  Comparison of Lake Alice limit pressure values.

## DISCUSSION

There is confusion between the Archer Landfill and Lake Alice test events; that is to say, from agreement among 2 agencies to total disagreement for 4 agencies.  For background, at both sites the FDOT and UF tests were done simultaneously and UNCC and FIT were performed a week after the FDOT and UF tests.  Several hypotheses could be presented to explain this anomaly.

1. Site variability and soil type

2. Membrane calibration changes during testing

3. Calibration differences

4. Operator differences

5. Pencel pressuremeter differences.

**Site Variability –**

The Archer Landfill site is quite uniform sand with no water table effects.  Excellent agreement was obtained until the 40-ft depth where the limestone interface caused divergence in results.  To investigate site variability at Lake Alice, the week after PMT testing, 2 ECPT soundings were performed solely for this purpose.  These results are presented in Figure 7.10 and Table 7.2 and show:

1. At 5- and 10-ft, the interpreted soil type and SPT – N-values are comparable.  However, UNCC and FIT agreement is only at the 10-ft depth and FIT is weaker at 5-ft.

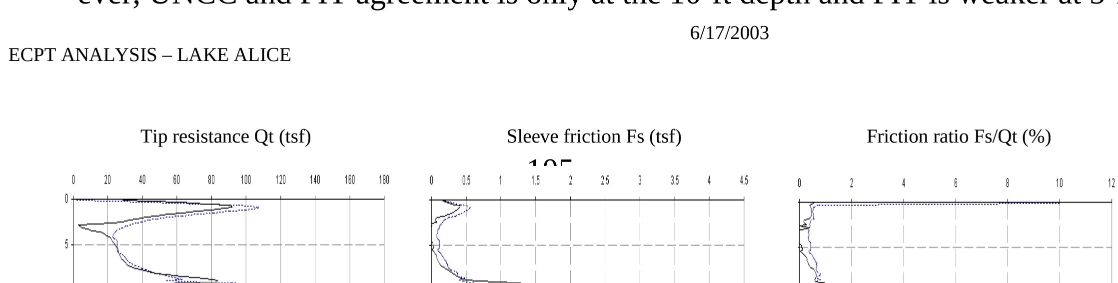

Figure 7.10  ECPT boring for UNCC and FIT PMT Lake Alice.

Table 7.2  Interpreted soil type and N-value.

| | UNCC | | FIT | |
|---|---|---|---|---|
| Depth (ft) | Soil Type | N-Value | Soil Type | N-Value |
| 5 | Silty Sand | 8 | Silty Sand | 8 |
| 10 | Silty Sand | 29 | Clay | 24 |
| 20 | Silty Clay | 16 | Clay | 9 |
| 40 | Silty Clay | 6 | | |
| 37.1 | | | Silty Clay | 26 |

2. At 20-ft, the FIT location is a clay and weaker (N = 9), whereas the UNCC location is silty clay and stronger (N = 16). Consequently, the FIT lower $P_L$ is justified.

3. At 40-ft, both locations are classified silty clay, yet the FIT site is stronger (N = 26 vs. 6). (However, my personal observation for the UNCC PMT test was that the soil was quite stiff and not representative of a SPT N = 6 blows.) Nevertheless, FIT's $P_L$ value is considerably lower than UNCC – 112 psi vs. 270 psi.

In summary, site variability can explain most of the observed discrepancies. The Lake Alice site suffers from site variability for depths greater than 10-ft. Only the 5-ft FIT lower result is unexplainable for site variability.

**Membrane Calibration Differences During Testing –**

The protective metal strips of the "Chinese lantern" cause a testing problem due to soil becoming trapped between the strips. That is to say, after the PMT is inflated, upon unloading, soil particles become trapped and the membrane does not fully decompress. Unfortunately, the change in membrane stiffness due to particle entrapment is unknown and random. An examination of Figures 7.5 to 7.8 show a random behavior in $P_L$ values. Although speculative, for research, this could be verified by recalibrating the PMT probe after each depth.

**Calibration Differences –**

This is not considered as a culprit for the observed differences. FDOT, UNCC, and UF all use the same procedure and spreadsheet developed by Prof. Anderson. The calibration spreadsheet utilizes a "macro" to develop a 3rd order trendline for calibration. The authenticity of this trend-line has been checked with a hand-solution as show in Figure 7.11 (file: A mano-5ft.-No ring-UF.xls)

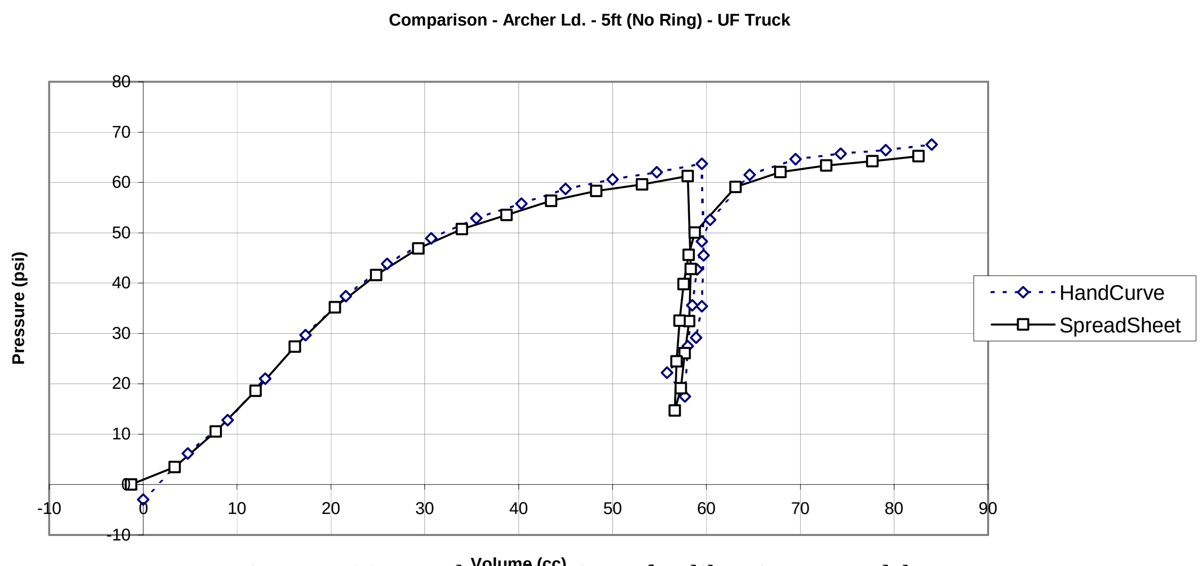


Figure 7.11 Hand verification of calibration spreadsheet.

**Operator Differences –**

During the testing at specific depths, all operators attempted to wait 30 sec. after reaching the desired volume prior to recording the pressure. However, the delay time after reaching the testing depth, which affects the pore pressure dissipation, was not controlled. This effect would be more pronounced in the clayey 10- , 20- , and 40-ft depths, and as shown, the standard deviation is greatest for these 3 layers. It is interesting, that for the Archer Landfill (cohesionless) site with rapid pore pressure dissipation, there was good agreement between UF and FDOT-SMO

PMT tests. For future research, it is recommended that the "rest" time after reaching depth be approximately 2 minutes for free-draining soils, and 5 minutes for impermeable soils.

**Pencel Pressuremeter Differences –**

All pressuremeters were manufactured by ROCTEST and had a length of approximately 24-inches. Any tubing compliance issues should have been mitigated by the calibration procedure. Consequently, the differences are not attributed to the equipment. However, it is noted that for 50-ft of tubing the compliance is quite soft. That is, the "lift-off" pressures occur at a volume of approximately 6-$cm^3$. Considering that the maximum testing volume is approximately 95-100 $cm^3$, this represents a "softness" of 6%. Perhaps future research could consider using more compliant tubing.

## PENCEL TESTING RECOMMENDATIONS

During the course of the workshop, the following testing recommendations evolved:

1. During pressure calibration inside a steel tube, expand the membrane until contact is made with the sides of the steel tube, and then begin calibration. Calibrate at equal increments of <u>pressure</u> not <u>volume</u>.

2. During volume calibration in air, after reaching the desired volume, wait 30 sec. prior to recording the pressure.

3. During testing when advancing the PMT to a deeper depth there usually is a pressure build-up. It is recommended to wait 2 min. for free-draining soils and 5-min. for impermeable soils prior to testing.

4. During testing, wait 30 sec. prior to recording the pressure reading.

5. For the volume calibration curve, the trend-line should be forced through zero. For the pressure calibration curve, the trend-line need not be forced through zero.

6. During unloading, it is best to unload in ½ cc increments and record the pressure.

# CHAPTER 8

# SUMMARY AND CONCLUSIONS

## SUMMARY

### FDOT-UCF Research Site

#### *Site Profile*

Based on comparisons of the data collected through the different insitu and geophysical tests and with the use of the GMS software, a general soil profile of the site was drawn. Figure 8.1 shows a cross section of the site.

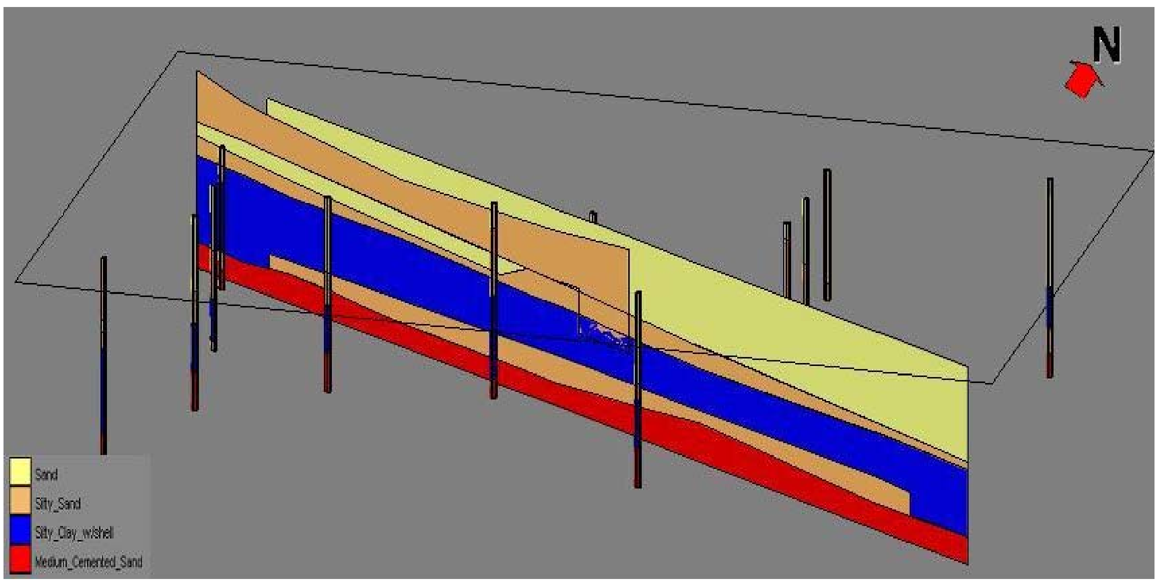


Figure 8.1 FDOT-UCF site soil profile along the SE to NW edge.

- From 0-5 feet a medium sand.
- From 5-33 feet as shown on the profile on the NW side there are successive layers of sand interspersed with silty sand layers; versus the SE side of the site where the layer is mostly formed by sand.
- From 33-48 feet clayey sands to clayey silt and some shell.
- From 48-52 feet silty sand.
- From 52-60 feet shelly silty cemented sand (gravely sand).

- From 60 – 75 feet, sand with gravel
- From 75-83 feet, sand
- From 83-153 feet, intermittent sand with gravel, and thin silt layers
- From 153-168 feet, dense sand
- From 168-200 feet, dense sand w/gravel and thin silt layers

The existence of a hardpan layer from the 8 to 15 feet of depth was located on the center eastward of the site. This information was corroborated by the information obtain with SPT, CPT and DMT.

Water level was found as high as 1.5 feet below surface.

## CONCLUSIONS

Based upon the data collected, the following conclusions are drawn:

1. A comparison of the geophysical data with the traditional insitu test data shows excellent agreement. However, the SPT and CPT compliment and assist geophysical interpretation.
2. A comparison of SPT estimated $\phi$ values with laboratory triaxial tests suggests, the Geotechnique 2000 expression best fits the triaxial testing $\phi$ angle. The Peck SPT estimate used in FB-PIER is comfortably conservative.
3. A comparison of SPT vs. triaxial cohesion values shows the Sowers (1979) and Bowles (1996) correlations are quite conservative and greatly underestimate cohesion values.
4. A comparison of CPT and DMT vs. triaxial test measured $\phi$ values shows good agreement.
5. Comparisons of triaxial test Young's moduli with estimates from FB-PIER SPT correlations were poor (about ½).
6. Comparisons between triaxial $E_{50}$ values and those estimated from CPT tests suggested $E = \alpha\, q_c$ , with $\alpha = 3.2$ as an average for the tests, with a range of 1.0 to 5.4, instead of the customary $\alpha \approx 2.5 – 4.0$.
7. DMT moduli estimates were poor with triaxial based values.
8. A testing program implemented to investigate PMT differences at the FDOT-UCF revealed:
    a. A comparison of two different probes (ring and no-ring on tip) at cohesive soils shows no apparent differences between them.

b. The comparison of two different probes (ring and no ring on tip) in cohesionless soils shows total discrepancy between them when depth is increased beyond 10 feet.

c. A comparison of data reduced with the computer generated correction curves with results reduced by hand shows agreement.

9. Interagency (FDOT-SMO, UF, UNCC, and FIT) PMT tests revealed:

   a. Excellent agreement between FDOT-SMO and UF at the cohesionless Archer Landfill site.

   b. Total disagreement occurred between the 4 agencies at the cohesive Lake Alice site. Although site variability may explain some of the disagreement, other unknown factors are occurring.

   c. A standard PMT test and calibration procedure is presented in Chapter 7.

## LIST OF REFERENCES


Advanced Geosciences, Inc. (1998). Sting R1 Instruction Manual Release 2.5.5., Austin, Texas.

American Society for Testing Materials, (D1586-84), (1989). "Standard Method for Penetration Test and Split-Barrel Sampling of Soils (D1586-84)," Annual Book of Standards, Vol. 4.08, ASTM, Philadelphia.

Anderson, J.B. (2001). "Finite Element Modeling of Florida Soil with The PENCEL Pressuremeter," Dissertation Presented to the Graduate School, University of Florida, Gainesville, Florida.

Annan, A.P. (1992). "Ground Penetration Radar, Work Shop Notes," Sensors and Software, Inc., Ontario, Canada.

Baguelin, F., Jézéquel, J.F., and Shields, D.H. (1978). The Pressuremeter and Foundation Engineering, Trans Tech Publications, Clausthal, Germany.

Baligh, M.M. "Theory of Deep Site Static Cone Penetration Resistance," Research Report R 75-76, No. 517, MIT, Cambridge, Massachusetts.

Bustamante, M. and Gianeselli, L. (1981) "Prevision de la Capacite Portante des Pieux Isoles sour Charge Vertical: Regles Prossiometriques et Penetrometriques," Bull. Liasion Labo. P. et Ch. 113, May-June

Bowles, J.E. (1996). Foundation Analysis and Design, Fifth edition, The MacGraw-Hill Companies, Inc.

Briaud, J.L. and Shields, D.H. (1979). "A Special Pressuremeter and Pressuremeter Test for Pavement Evaluation and Design," Geotechnical Testing Journal, ASTM, Vol. 2, No. 3.

Briaud, J.L. (1989). The Pressuremeter Test for Highway Applications, FHWA Publ. FHWA-IP-89-008

Cambridge Insitu, "Self-Boring Pressuremeters – An Introduction" http://www.cambridge-insitu.com/csbp_leaflet2.htm .

Cambridge Insitu, "Full Displacement Pressuremeter" http://www.cambridge-insitu.com/specs/Instruments/cpm.html.

Campanella, R.G. (1995). Guidelines for Geotechnical Design Using The Cone Penetrometer Test and CPT with Pore Pressure Measurement, Fifth edition, University of British Columbia, Vancouver, Canada.

Drnevich, V.P., Gorman, C.T., and Hopkins, T.C. (1974). Shear Strength of Cohesive Soils and Friction Sleeve Resistance, Proc. European Symposium on Penetration Testing, Stockholm, Vol. 2.2.

Fyffe, S., Reid, W.M., and Summers, J.B. (1985). "The Push-In Pressuremeter: 5 Years of Offshore Experience," The Pressuremeter and Its Marine Applications (2nd Int. Symp.), ASTM STP 950.

Handy, R.L. (1980). "Realism in Site Exploration: Past, Present, Future and Then Some – All Inclusive," Proceedings, Symposium on Site Exploration in Soft Ground Using Insitu Techniques, Report FHWA–TS– 80–202, Federal Highway Administration, Washington.

Hatanaka, M. and Uchida, A. (1996). "Empirical correlation between penetration resistance and effective friction of sandy soil," Soils & Foundations, Vol. 36 (4), 1-9, Japanese Geotechnical Society.

Imai, T. and Tonouchi, K. (1982). "Correlation of N-Value with S-Wave Velocity and Shear Modulus," Proceedings, 2nd European Symposium on Penetration Testing, Amsterdam, pp. 57-72.

Jamiolkowski, M., et al. (1985). "New Developments in Filed and Laboratory Testing of Soils," 11th ICSMFE, Vol. 1.2.

Kovacs, W.D., Salomone, L.A., and Yokel, F.Y. (1981). "Energy Measurement in The Standard Penetration Test," Building Science Series 135, U.S. Government Printing Office, Washington, D.C.

Kulhawy, F.H. and Mayne, P.W. (1990). "Manual on Estimating Soil Properties for Foundation Design," Report EL-6800, EPRI, Final Report.

Ladd, C.C. and Foote, R. (1974). "New Design Procedure for Stability of Soft Clays" Journal of the Geotechnical Engineering Division, ASCE, Vol. 100, No. GT 7, July.

Liao, S.S. and Withman, R.V. (1986). "Overburden Correction Factors for Sand," Journal of the Geotechnical Engineering Division, Vol. 112, No. 3, March.

Marchetti, S. (1980). "In Situ Tests by Flat Dilatometer," Journal of the Geotechnical Engineering Division, ASCE, Vol. 106 GT 3, March.

Marchetti, S., Monaco, P., Totani, G., and Calabrese, M. (2001). "The Flat Dilatometer Test (DMT) in Soil Investigations," A Report by the ISSMGE Committee TC16, Proceedings IN SITU 2001, International Conference on In Situ Measurement of Soil Properties, Bali, Indonesia.

Matlock, H. and Reese, L.C. (1960). "Generalized Solutions for Laterally Loaded Piles," Journal of Soil Mechanics and Foundation Division, ASCE, Vol. 86, SM 5, October.

Menard, L. (1963) "Calcu de la Force Portante des Foundations su la Base des Resultats de Essais-Prossiometriques" Sol-Soils, Vol.2, Nos 5 and 6.

Peck, R.B., Hanson, W.E., and Thornburn, T.H. (1974). Foundation Engineering, 2nd edition., John Wiley & Sons, New York.

Reid, W.M., St. John, H.D., Fyffe, S., and Rigden, W.J. (1982). "The Push-In Pressuremeter," Proceedings of the Symposium on the Pressuremeter and Its Marine Applications, Editions Technip, Paris.

Robertson, P.K. and Campanella, R.G. (1983). "Interpretation of Cone Penetration Tests: Parts1 and 2," Canadian Geotechnical Journal, Vol. 20.

Robertson, P.K., Hughes, J.M.O., Campanella, R.G., and Sy, A. (1984). "Design of Laterally Loaded Displacement Piles Using a Driven Pressuremeter: Analysis and Performance," STP 835. America Society for Testing Materials, Philadelphia.

Robertson, P.K., Davies M.P., and Campanella, R.G. (1989). "Design of Laterally Loaded Driven Piles Using the Flat Dilatometer," Geotechnical Testing Journal, Vol. 12, No. 1, March.

Roctest, Inc., "Standard Pencel Pressuremeter 2500 kPa Capacity Hallow and Solid Probes," Instruction Manual, E-931222.

Roctest, Inc., "Pressuremeter Model G-Am MENARD" http://www.roctest.com/roctelemac/product/product/g-am_menard.html .

Schmertmann, J.H. and Palacios, A. (1979). "Energy Dynamics of SPT," Journal of the Geotechnical Engineering Division, ASCE, Vol. 105 GT 8.

Schmertmann, J.H. (1986). "Suggested Method for Performing the Flat Dilatometer Test," Geotechnical Testing Journal, ASTM, Vol. 9, No. 2, pp. 93-101.

Schmertmann, J.H. (1979). "Statics of SPT," Journal of the Geotechnical Engineering Division, ASCE, Vol. 105 GT 5, May.

Schmertmann, J.H. (1978). "Guidelines for Cone Penetration Test: Performance and Design," FHWA-TS-209 (report), U.S. Dept. of Transportation.

Schmertmann, J.H. (1978). "Guidelines for Cone Penetration Test: Performance and Testing," FHWA-TS-209 (report), U.S. Dept. of Transportation.

Skempton, A.W. (1951) "The Bearing Capacity of Clays," Build. Res. Congress, London, British Institute of Civil Engineers, div I;180

Sowers, G.F. (1979). Introductory Soil Mechanics and Foundations: Geotechnical Engineering, 4th edition, Macmillan Publishing, New York.

Terzaghi, K. and Peck, R.B. (1948). Soil Mechanics in Engineering Practice, John Wiley & Sons, New York.

Townsend, F.C. and Anderson, J.B. (2001). "Evaluation of FEM Engineering Parameters from Insitu Tests – Final Report" FDOT BC-354.

Townsend, F.C., Anderson, J.B., and Grajales, B. (1999). “Insitu Testing for Evaluation of Lateral Load Capacity of Deep Foundations,” FDOT Final Report B-511.

US Army Corps of Engineers. (1995). “Geophysical Exploration for Engineering and Environmental Investigations,” Engineer Manual EM 1110-1-1802, August.

Vogelsang, D. (1995). Environmental Geophysics, A Practical Guide. Berlin, Springer-Verlag.

## Appendix A

## TESTING METHODS FOR PRESSUREMETER TEST (PMT)

### DEVICE

The PENCEL pressuremeter is more or less the commercial version of the pavement pressuremeter developed by Biraud and Shields (1979). Roctest, Inc. manufactures the unit in Canada and markets it worldwide. the device consists of; (1) a probe, (2) control unit, and (3) tubing as described below.

- Probe: The unit consists of a "Chinese lantern" inflatable pressuremeter 58–cm long and with a diameter of 3.2 cm. Quick connects are located on each end for pressurization and de-airing. The penetrating tip may or may not be equipped with a "steel ring friction reducer," which is a controversial influencing factor of this research. Typically, a friction reducer is placed in the rod string above the probe. These components are shown in Figure 1.
- Control/measuring unit: The UF control unit has been modernized by adding to the system a digital pressure gauge, which reads the changing values of pressure in PSI. This digital gage is an improvement over the analog dial gage and helps reading more precise values during test performance.
- Tubing/cabling.

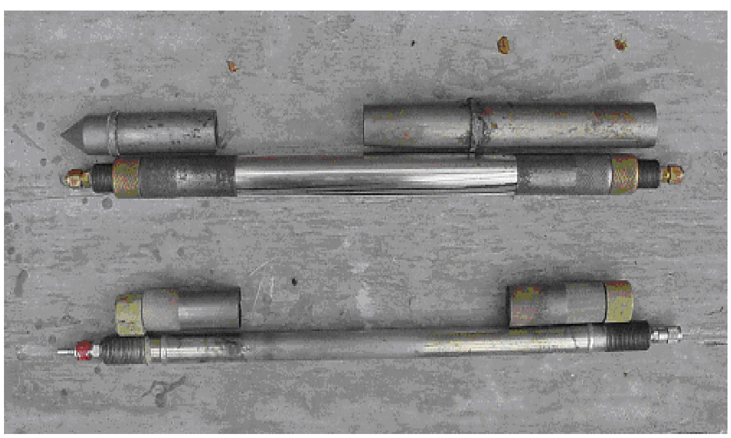

Figure 1. The PENCEL pressuremeter probe.

### TEST PROCEDURE

- The test is carried out by directly pushing the probe into the ground. Horizontal pressure is applied to the soil at the selected elevation by gradually inflating the probe until it reaches the capacity of the device. Applied pressure readings are recorded as increments of volume are applied, thus obtaining a relationship between the radial applied pressure and the resulting soil deformation. However, this radial pressure is affected by; (1) the resistance of the probe itself to expansion, (2) the expansion of the tubes connecting the probe with the pressure-volumeter, and (3) hydrostatic effects. All of these effects must be accounted for during data reduction.

## CALIBRATION OF EQUIPMENT

No ASTM standard exists for the PENCEL Pressuremeter test. Instead, the test and calibration methods are based on the information given on the manual Published by Briaud and Shields (1979). The following is a compilation of the information provided by the Standard Pencel Pressuremeter (CPMT) Instruction Manual, and our own experience performing these tests. New key elements must be added to the manual and followed in order to provide extended life span to key components of the equipment, and a better calibration curve during the process of data reduction.

There are two corrections to be applied to the field data:

- Pressure calibration. It determines the pressure correction necessary to nullify the inertia of the sheath. Inertia of the sheath is defined as the required pressure to dilate the probe to a specific volume when the probe is confined only by atmospheric pressure.
- Volume correction. It determines the volume correction caused by the parasitic expansion in the control system and in the tubing and probe. Such difference corresponds to that between the injected volume read in the meter and the real increase in volume of the probe.

### Pressure Correction

1. The entire system has to be completely saturated. See Filling and Saturating The Control Unit on ROCTEST manual for Cone PMT. The probe is placed vertically at ground level next to the apparatus. Place valves 3 and 4 in the "Test" position and inflate and deflate the probe five times by injecting 90cm$^3$. This is done to exercise the membrane.

2. The probe is then inflated to 90cm$^3$ at an injection speed of about 1/3 cm$^3$/second, which is equivalent to 1 crank turn in 9 seconds. The pressures are recorded for each step of 5 cm$^3$ injected.

3. The pressures that have been recorded are then corrected by taking into consideration the head of water between the pressure gauge and the center of the probe; the inertia curve is the plot of the corrected pressure versus the injected volume.

4. The inertia curve is required for interpretation of the test data and must be established for each new sheath mounted on a probe.

**Volume Correction**

5. Place valves 3 and 4 on “Test” position. Place the probe in a calibration tube. The calibration tube can be any thick wall metal tube with an inside diameter of about 34mm.

6. The manual recommends inflating the probe (in the tube) by injecting water at a rate of 1/3 $cm^3$/sec in increments of $5cm^3$. Record the pressure for each increment of $5cm^3$ injected. Continue with the same injection rate and keep record of the pressure at $5cm^3$ intervals up to 2000 kPa. However:

    - This procedure will provide a plot with just a few points for drawing the curve. To facilitate the plotting of this curve with more readings, we recommend recording values of volume based upon pressure once the gauge reached 250 kPa. The additional readings should be performed at pressure values of 2.5, 5, 10 15, and 20 kPa x 100. See example of readings at Table 1. This data is used to plot curve A or Control unit + tubing + Probe, shown at Figure 2.

7. Deflate the probe by bringing the volume counter back to zero

8. Disconnect the probe from the tubing

9. Progressively increase the pressure in the cylinder and in the tubing up to 2500 kPa, recording the pressure corresponding to each $cm^3$ injected. This data is used to plot curve B or Control unit + tubing, shown in Figure 2.

10. Bring back the volume counter to zero.

11. Using readings obtained during steps 2 and 5, trace curves A and B,

    - Trace a tangent to curve A, line C - D.
    - Add a horizontal line from C to E
    - Measure E – F
    - Set off distance E – F from point D to find a new point call G
    - Sketch a curve G – C
    - Transfer curve G – C – A to origin of graph and obtain the Volume Correction Curve, C as shown at Figure 2.

12. The probe can be connected to the tubing and the test may begin.

The calibration process must be applied again after finishing the test, and if the tubing or the probe sheaths are changed. Otherwise, calibrations should be repeated for each new job site or at regular intervals during a large test campaign.

Table 1. Example of proposed calibration method for Volume Correction curve.

| Volume Correction | | |
|---|---|---|
| cc | Kpa x 100 | PSI/30sec |
| 0 | | 0 |
| 5 | | 1.1 |
| 10 | | 2.6 |
| 15 | | 4.8 |
| 20 | | 9.2 |
| 25 | | 22.8 |
| 27.3 | 2.5 | 34.2 |
| 30.4 | 5 | 61.9 |
| 33.9 | 10 | 126.6 |
| 36.1 | 15 | 193.3 |
| 37.8 | 20 | 259.4 |
| 37 | 15 | 200.5 |
| 35.6 | 10 | 135 |
| 33.2 | 5 | 66.2 |
| 30.8 | 2.5 | 35.3 |
| 25 | | 9.5 |
| 20 | | 4.3 |
| 15 | | 2.1 |
| 10 | | 1 |
| 5 | | -0.3 |
| 0 | | -1.2 |

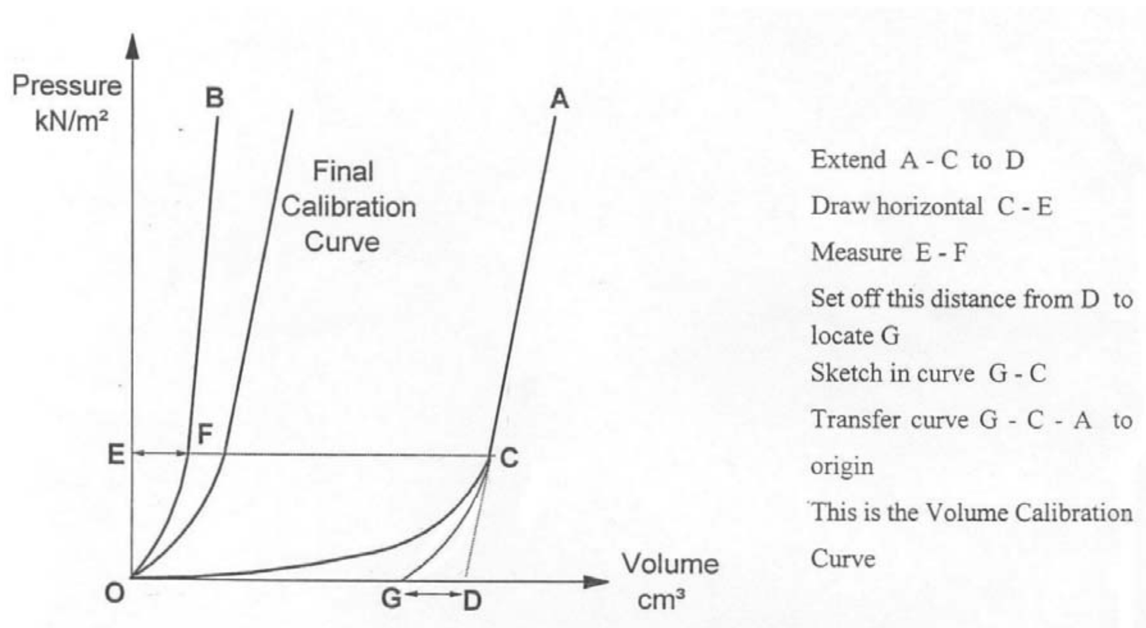


Figure 2. Figure show proceedings to plotting of calibration curve

**Probe Insertion**

The PENCEL probe is designed for insertion by pushing or light hammering. During the process of pushing the pressuremeter with a ram, especial attention must be given to the readings on the ram pressure gauge as well on the unit pressure gauge. These are great indicators of the potentially damaging stresses acting on the pressuremeter sheath through the soil layers. The operator most avoid abruptly increasing changes on unit pressure gauge; the values of the change in pressure may vary from – 12 PSI to 20 PSI during insertion on stiff soils. If the value goes over a value larger than 20 PSI the sheath must be receiving serious damage, and be close to yield.  The values of the pushing pressure on the ram gauge must be kept below 1000 PSI. A typical advancing rate in sands and clays should be 500 – 600 PSI. At the minimum sign of change on the probe pressure panel, insertion must stop, check that valves are in the right position "TEST" and handle of the piston has been rotated all the way to the deflate position. The correct position of actuators or valves at the control unit is shown at Figure 3.

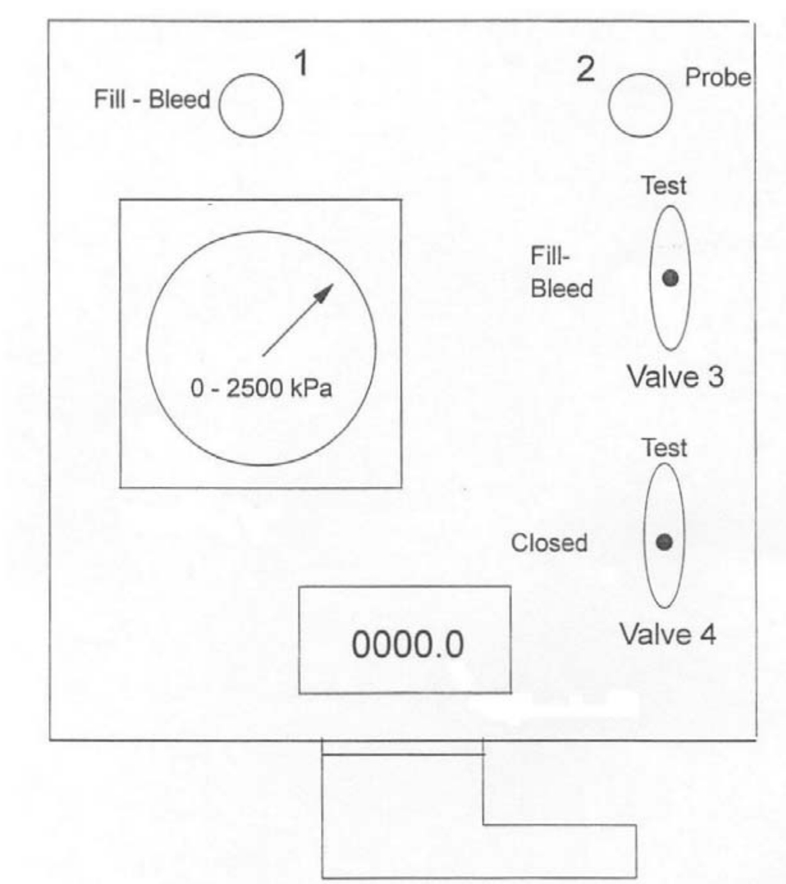


Figure 3.  Representation of control unit valves, during testing performance.

If this check is correct and same conditions persist, then the proper action is wait additional time to allow the suction in the piston cylinder inside the unit control to deflate further the probe. Do not attempt to retrieve the probe from the hole. The same conditions apply in either the  up or down directions.

After finishing each test at a certain depth, a good way to avoid damage to the sheath (Chinese lantern protecting the membrane) is by; after deflating the membrane, wait for the recommended recuperation or suction period of 7 to 10 minutes. Before continuing with penetration to a new testing depth, advance the probe one foot into the undisturbed soil below. This action will help to squeeze water out of the probe into the system, reducing the effect of friction during penetration.

**TEST EXECUTION**

Once the probe has been pushed to the desired test depth and valves Nos 3 and 4 are in TEST position, the testing can then be carried out in increments of equal volumes. The increment of increasing volume is 5 $cm^3$ and the corresponding pressure is noted 30 seconds after having injected the 5 $cm^3$. The maximum volume injected is 90 $cm^3$. A constant speed of injection should be maintained. Recommended speed is 1/3 $cm^3/s$ which is equivalent to 1 crank revolution in 9 seconds.

When the test is completed, prior to either removing the probe from the hole or advancing it to a lower level, the probe must be deflated by returning the water to the cylinder. Under no conditions should setting of the valves Nos. 3 and 4 be changed from the 'TEST" position, as the PENCEL does not have a release valve to deflate the probe, and the action of reversing the handle into the deflate position until volume counter reads 0000, is similar to the handling of a syringe, where the action is activating vacuum pressure on the system. If any of the valves is changed from test position, this will divert the suction on the system to the water container and will introduce more water in the circuit, inflating the probe. Probe inflation usually results in membrane destruction while advancing or retraction the probe.

**DATA REDUCTION**

The analysis of the pressuremeter data begins with the corrections for the volume and pressure. This is done merely by fitting the calibration curves obtained during pressure and volume calibration on a graph, following the procedure described in the previous section and adjusting a new curve, the Volume Correction Curve. (See Figure 2)

The first step to the interpretation will be to plot the raw pressuremeter curve (pressure vs. volume) as well as the corrected Volume correction curve. For each point on the raw curve there corresponds a point on the corrected curve with coordinates of corrected pressure and corrected volume. The corrected point is obtained by subtracting the volume correction and the pressure correction from the raw pressure and volume data. The corrected pressure must also include the hydrostatic pressure.

Volume corrected = Volume read – Volume Calibration
Pressure Corrected = Pressure read – Pressure Calibration + P Hydrostatic.

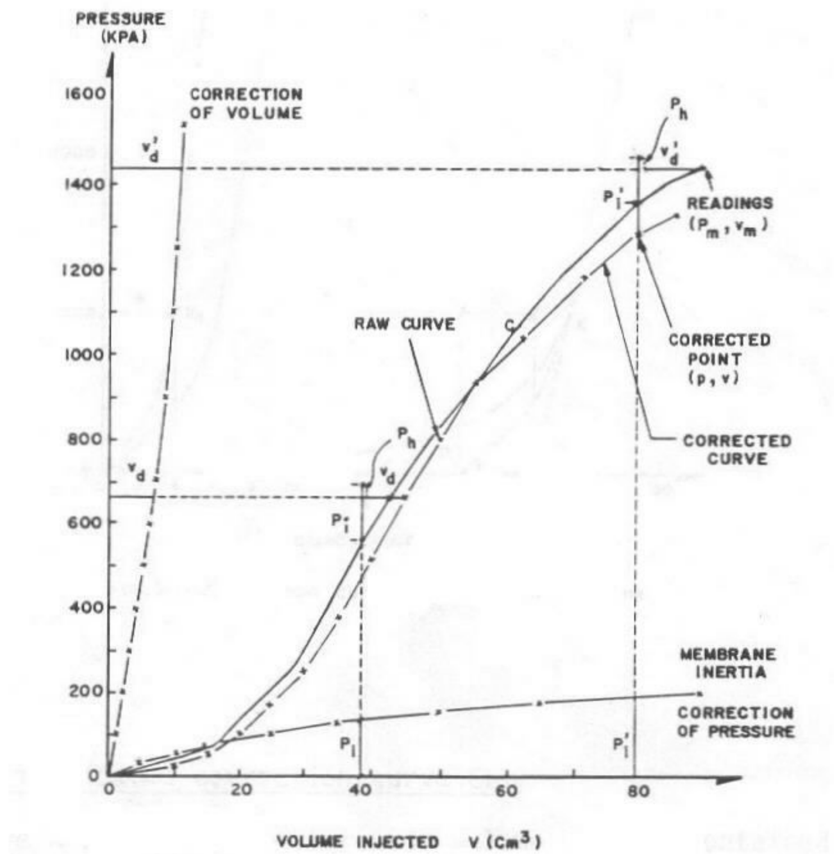


Figure 4. Example of how to correct the raw curve using pressure and volume correction curves.

**Hand Solution vs. Use of Computer to Aid Data Reduction**

The entire process of plotting the correction and raw curves, in order to obtain the soil properties and Pressuremeter Modulus from the PMT has two divergent methodologies. One of the methodologies requires the reduction of the data entirely by using a hand procedure, drawing the correction curves and raw data using French curves. The other method uses of a combination of hand plotting and computer programs or spreadsheets.

The hand method is more precise than the use of computers due to the fact that computers cannot obtain a single mathematical equation that fits the shape of calibration curves loading and reloading. Several approaches have been attempted by UF grad students, and consist of fitting several curves for each section of the correction curves. This procedure is more tedious but is closer to the hand procedure. See example on Figure 5 pressure correction curve.

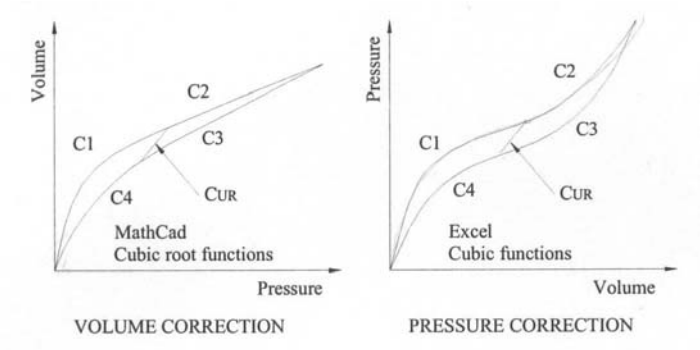


Figure 5. Example of the use of spreadsheets to obtain, the correction curves Anderson (2001).

Hand reduction of data results in a tedious and time consuming effort for everyday work. For this reason, Dr. Brian Anderson has developed excel spread-sheets that use macros to apply a 3 degree polynomial ‘best fit” equation to the calibration curves. A subsequent macro plots the corrected pressure – volume curve.

Once the corrected Pressure vs. Volume curve is plotted, two parameters inherent to the pressuremeter can be obtained. The values of limit pressure and pressuremeter modulus are obtained from the graph.

The PENCEL limit pressure is defined as the pressure required to double the probe volume, or more simple the maximum pressure during the test. On the other hand, the modulus could come from many potions of the curve. These moduli are referred to as initial modulus Ei, unload reload modulus EUR, and unload modulus EUL. Figure 6 shows these moduli and the limit pressure on an arbitrary pressuremeter test.

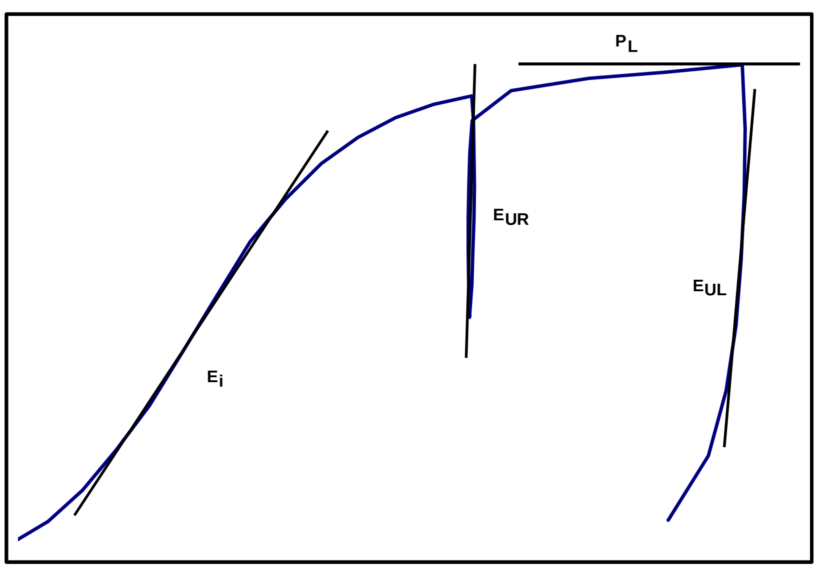


Figure 6. PENCEL Pressuremeter curve with Limit pressure and moduli denoted.

For calculation of the pressuremeter modulus the following expression, taken from Menard Method, is used.

$$E_{PMT} = 2(1+\mu)\left[V_c + \frac{V_o + V_f}{2}\right]\left[\frac{P_f - P_o}{V_f - V_o}\right]$$

Where:

μ = is Poisson's Ratio.

Vc is the initial volume of the pressuremeter

Vo and Po are the first point on the linear portion of the pressuremeter curve

$V_f$ and $P_f$ are the final points on the linear portion of the pressuremeter curve